1985

Metamorphism in the eastern Lac Seul region of the English River subprovince, Ontario

Steve J. Chipera
University of North Dakota

METAMORPHISM IN THE EASTERN LAC SEUL REGION OF THE ENGLISH RIVER SUBPROVINCE, ONTARIO

by
Steve J. Chipera

Bachelor of Science, University of Minnesota-Duluth, 1982

A Thesis

Submitted to the Graduate Faculty

of the

University of North Dakota

in partial fulfillment of the requirements

for the degree of

Master of Science

Grand Forks, North Dakota

May
1985

This thesis submitted by Steve J. Chipera in partial fulfillment of the requirements for the degree of Master of Science from the University of North Dakota is hereby approved by the Faculty Advisory Committee under whom the work has been done.

(Chairman)

This thesis meets the standards for appearance and conforms to the style and format requirements of the Graduate School of the University of North Dakota, and is hereby approved.

2/13/85

Dean of the Graduate School

Permission

Title Metamorphism in the Eastern Lac Seul-Region of the English River Subprovince, Ontario

Department Geology

Degree Master of Science

In presenting this thesis in partial fulfillment of the requirements for a graduate degree from the University of North Dakota, I agree that the Library of this University shall make it freely available for inspection. I further agree that permission for extensive copying for scholarly purposes may be granted by the professor who supervised my thesis work or, in his absence, by the Chairman of the Department or the Dean of the Graduate School. It is understood that any copying or publication or other use of this thesis or part thereof for financial gain shall not be allowed without my written permission. It is also understood that due recognition shall be given to me and the University of North Dakota in any scholarly use which may be made of any material in my thesis.

Signature Steve J. Chapin

Date January 25th 1985

TABLE OF CONTENTS

LIST OF ILLUSTRATIONS

Figure

LIST OF TABLES

Table

ACKNOWLEDGEMENTS

I wish to extend my deepest appreciation to the Mining and Minerals Resources Research Institute and the Graduate School of the University of North Dakota for the financial assistance they provided during this thesis. The logistical support provided by Don Janes and Ralph Huggins of the Ministry of Natural Resources proved to be invaluable. Immense gratitude is extended to Dexter Perkins III who invested his time, patience, guidance, and knowledge. Will Gosnold, Frank Karner, and Robert Stevenson also contributed valuable assistance and suggestions. Rod Baumann and Dexter Perkins are acknowledged for their assistance in the field. I also thank Rod Baumann, Scott Robinson, and Kevin Henke for many hours of stimulating, intellectual conversation. Most importantly, I wish to thank my future wife, Angela, for helping me through the hard times.

ABSTRACT

The English River subprovince of the Superior Province, Canada, is a linear, east-west trending high-grade metamorphic belt which extends from Lake Winnipeg in the west, to the James Bay lowlands in the east. It is composed of two prominent lithologic domains: a northern sedimentary gneiss-migmatite domain, and a southern plutonic domain. The northern domain consists primarily of alternating migmatized layers of garnet-biotite "wacke" and garnet-cordierite-biotite "pelitic" metasediments. The southern domain is composed mainly of intermediate granitic to trondhjemitic plutons. Bordering to the north and south are the lower grade Uchi and Wabigoon greenstone belts. Metamorphism and migmatization occurred during the Kenoran orogeny approximately 2.68 B.Y. ago.

By conducting a detailed geothermometry-geobarometry study, patterns of metamorphism were detected which further develop our understanding of the processes operating on the earth at this very early time in its history. Results from the application of geobarometers have shown that the pressures attained during metamorphism were constant throughout the 15000 Km^2 eastern Lac Seul region of the English River subprovince (5 +/- 1 Kbar). There is strong evidence from garnet-orthopyroxene barometry that pressures may have been constant over the rest of the subprovince as well.

Temperatures attained during metamorphism show a trend across the subprovince, depicting a "thermal anticline" whose axis runs approximately east-west parallel to the strike of the subprovince. Temperatures ranged from 600°C at the contact with the Uchi greenstone belt, 675°C for the garnet-cordierite "in" isograd, 700°C for the orthopyroxene "in" isograd, with maximum temperatures of around 750°C at the center of the subprovince.

Langford and Morin (1976), noting the similarity of the Superior Province to the Canadian Cordillera, propose a model of accreting island arcs for the Superior Province. The strong contrasts in lithologies and structure between the northern sedimentary and southern plutonic domains suggest that the southern domain could be an allochthonous terrain accreted onto the northern domain. Since geobarometry has shown that the sediments were buried to a depth of at least 20 kms, it is postulated that the southern domain was thrust onto the sediments. Erosion has cut obliquely through the thrust plane resulting in metasediments exposed in the north, and plutonics to the south.

The temperatures attained in the English River subprovince are several hundred degrees greater than can be explained by conductive heating alone. The contribution of a convective magmatic heat component must be invoked to explain the high temperatures. Block faulting and uplift with a magmatic heat source at the center of the block, combined with thermal diffusivity, explains both the high temperatures, and the "thermal anticline" of the English River subprovince.

INTRODUCTION

The English River subprovince of the Superior Province, Canada, is a linear, east-west trending high-grade metamorphic belt which extends from Lake Winnipeg in the west, to the James Bay lowlands in the east (Harris and Goodwin, 1976). It is composed of two prominent lithologic domains: a northern sedimentary gneiss-migmatite domain, and a southern plutonic domain (Beakhouse, 1977). The northern domain consists primarily of alternating migmatized layers of garnet-biotite "wacke" and garnet-cordierite-biotite "pelitic" metasediments. The southern domain is composed mainly of intermediate granitic to trondhjemitic plutons. Bordering to the north and south are the lower grade Uchi and Wabigoon greenstone belts (figure 1).

Metamorphism and migmatization occurred during the Kenoran orogeny approximately 2.68 B.Y. ago (Krogh et al., 1976). Grades of metamorphism vary from the upper-greenschist facies along the contact of English River subprovince and the bordering greenstone belts, to amphibolite facies with local occurrences of granulites at the center of the subprovince.

The rock types at the contact with the Uchi subprovince include phyllites, schists and basalts. These rock types then grade rapidly southward through biotite schists into migmatites with restite layers containing abundant garnet, cordierite, and biotite. The presence of migmatites is especially important because it suggests that extremely high heat flow was present at the time of their formation. If the depth of formation of these rocks can be approximated, it is possible to

Figure 1. Superior Province of Ontario. Stippeled belts are greenstone terrains, white belts are composed of high grade metamorphics and plutonics.

Enlargement of the English River subprovince shows the northern supracrustal domain, and the southern plutonic domain. The box depicts the study area.

(Modified from Breaks et al., 1978)

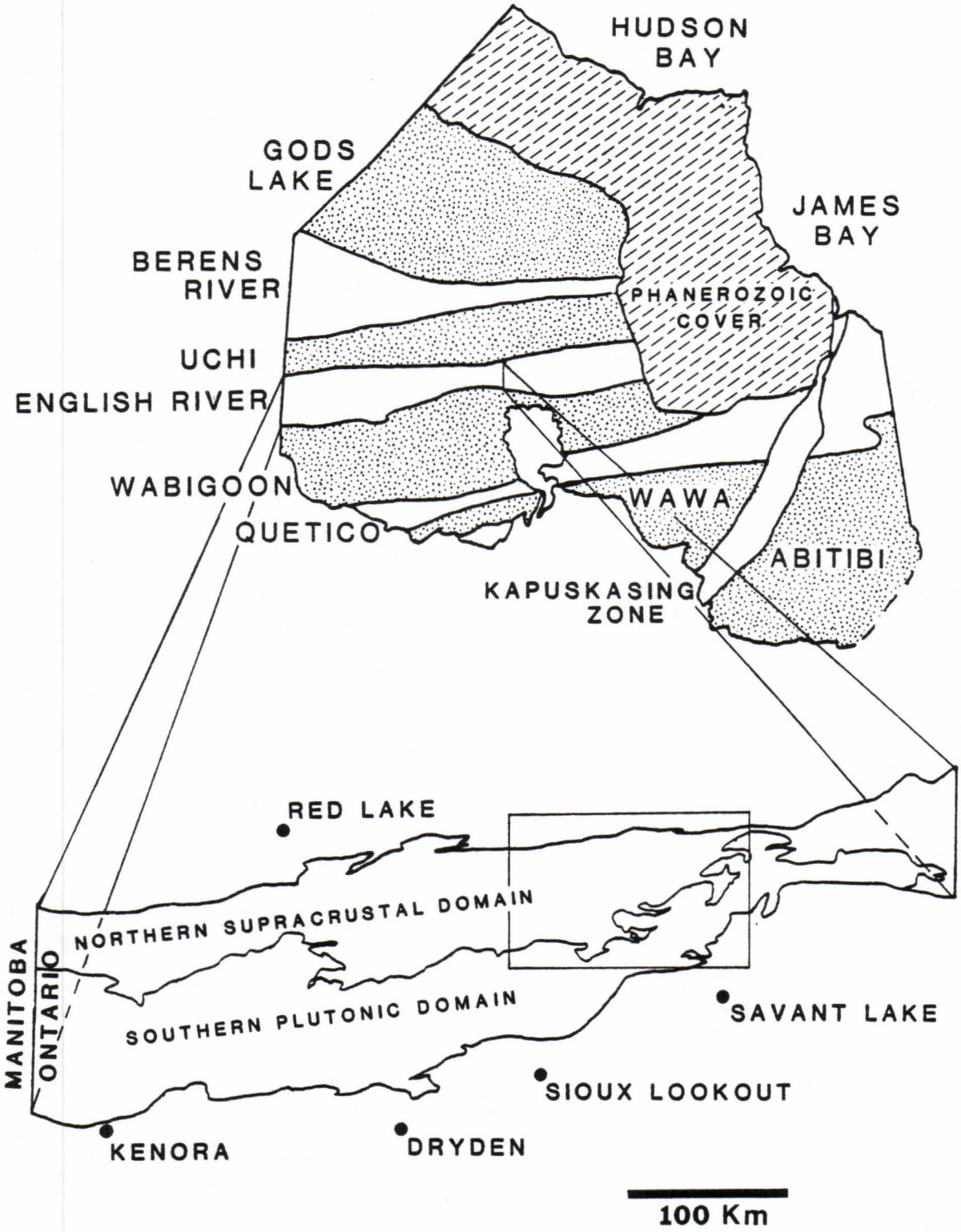
HUDSON BAY
GODS LAKE
JAMES BAY
BERENS RIVER
PHANEROZOIC COVER
UCHI
ENGLISH RIVER
WABIGOON
WAWA
QUETICO
ABITIBI
KAPUSKASING ZONE
RED LAKE
NORTHERN SUPRACRUSTAL DOMAIN
MANITOBA
ONTARIO
SOUTHERN PLUTONIC DOMAIN
SAVANT LAKE
SIOUX LOOKOUT
KENORA
DRYDEN
100 Km

determine whether metamorphism took place under conditions along a smooth geotherm, or if a tectonic or magmatic heat source was involved.

Langford and Morin (1976) propose that the major geological features of the western Superior Province (figure 1) are very similar to the younger rocks composing the Cordillera of western Canada, and thus postulate a model of accreting island arcs for the Superior Province. This is in direct contradiction to various workers, Goodwin (1981) for example, who believe that during the Archean, the earth was composed of thin, unstable plates until at least the Proterozoic.

If the tectonic processes were markedly different in the Archean than the Proterozoic and later rocks, then there should be some difference in the style of regional metamorphism. By applying careful geothermometry-geobarometry studies, patterns of metamorphism can be detected, which will further develop our understanding of the processes operating on the earth at this very early time in its history.

The area encompassed in this study is situated north-east of Sioux Lookout, Ontario, and extends from the lower edge of the Uchi subprovince at Lake St. Joseph, to the southern margin of the sedimentary domain (figure 2).

Since there is only one road traversing the study area, travel through the region was mainly undertaken by motorized boat and canoe. The numerous waterways provided excellent coverage of the region and access to 90 percent of the outcrop exposures. Approximately 500 samples were collected. 150 thin sections were cut for further study

Figure 2. Index map of the Eastern Lac Seul study area showing major lakes and all roads.

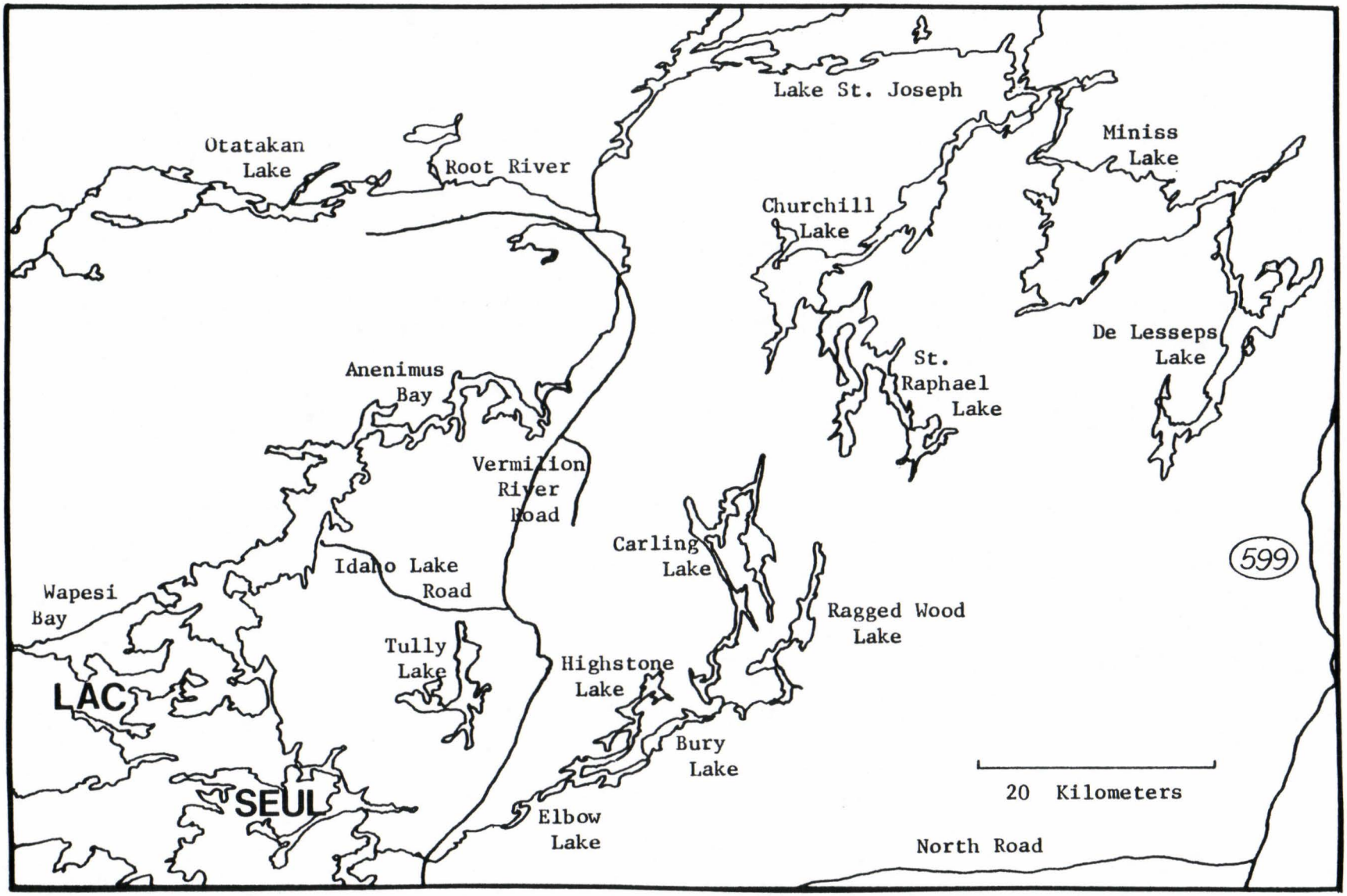
Lake St. Joseph
Otatakan Lake
Root River
Miniss Lake
Churchill Lake
De Lesseps Lake
St. Raphael Lake
Anenimus Bay
Vermilion River Road
Carling Lake
599
Idaho Lake Road
Wapesi Bay
Ragged Wood Lake
Tully Lake
Highstone Lake
LAC
Bury Lake
20 Kilometers
SEUL
Elbow Lake
North Road

using a petrographic microscope and a JEOL 35C scanning electron microscope/microprobe (SEM/Microprobe).

GENERAL ROCK DESCRIPTIONS

The greenschist and lower amphibolite facies rocks in the Lake St. Joseph area represent the only low- to medium-grade metamorphic rocks in this study. Typical rock types are conglomerates, basalts (with and without pillows), siltstones, banded iron formation, pyroclastic and/or ash-fall deposits, phyllites, schists, and graywacke sandstones. Shear zones and cataclastics are developed throughout the lower part of the lake. Crenulation cleavage is often well developed in the schists. A major deposit of iron formation, found on Eagle Island, extends west past Wolf and Fish islands until the magnetite beds become too thin and spaced out to be of economic interest.

Metamorphic grade sharply increases on the English River side of the Lake St. Joseph fault zone. The amphibolite facies rocks in this region grade into granulites farther south, and have been subdivided into several types: wacke sediments, pelitic sediments, and amphibolites (Breaks et al., 1978).

The wacke sediments have been labeled with the field term "salt and pepper sandstones" due to their equigranular nature in the coarse sand size range of light colored subhedral to anhedral plagioclase and quartz, and dark colored biotite. Though the biotite has a distinct preferred orientation, its low modal percentage leaves the rock with only a weakly foliated appearance. The typical assemblage is:

quartz, plagioclase, biotite, apatite, zircon, +/- garnet
+/- oxide, +/- sulphide

At higher grades, orthopyroxene often occurs in substantial amounts.

The pelitic sediments tend to have a high color index associated with abundant ferromagnesium minerals, show a strong foliation of biotite, and are often porphroblastic garnet-biotite +/- cordierite schists. They are generally more coarsely crystalline than the wacke sediments. Typical assemblages are:

quartz, plagioclase, biotite, garnet, apatite, zircon,
+/- oxide, +/- sulphide

quartz, plagioclase, biotite, garnet, apatite, zircon,
+/- oxide, +/- sulphide

quartz, plagioclase, biotite, cordierite, apatite, zircon,
+/- oxide, +/- sulphide, +/- Kspar, +/- sillimanite

Amphibolites can be distinquished by their dark black to green-black color, massive nature in outcrop, and their resistance to weathering. A typical assemblage is:

hornblende, plagioclase, apatite, +/- quartz, +/- oxide, +/- sulphide

Other minerals found associated with these rocks are biotite, epidote, sphene, and zircon, with orthopyroxene and clinopyroxene coexisting at granulite grades.

MINERAL DESCRIPTIONS

SILLIMANITE: Sillimanite. though not very common, is the only Al_2SiO_5 polymorph that was found in the English River part of the study area. Andalusite, not found during this study, has been reported at Soules Bay, Lake St. Joseph in the Uchi subprovince (Goodwin, 1965). Most of the metasediments in the English River subprovince are not extremely aluminous, (less sillimanite than biotite or quartz), and are at a grade where sillimanite is consumed with biotite and quartz to form more stable phases such as cordierite and garnet. When found, sillimanite may be of two types: coarsely matted clumps of needles, usually in the cores of cordierite (or occasionally plagioclase), or as fibrolite associated with biotite and perthite. Both types have been found in the same thin section. The fibrolite is interpreted to be the result of a second or retrograde metamorphic event for it is found only in the thin sections that contain secondary muscovite.

CORDIERITE: The cordierite found in these rocks show a limited range of composition from 0.65-0.75 Mg/Mg+Fe. It is occasionally gemmy-blue in color, and is often found forming large porphyroblastic clots in the leucosomes of the migmatites. H_2O and CO_2 analysis on sample VM2183 showed that this cordierite contains 1.25 wt percent H_2O and 0.95 wt percent CO_2. In thin section cordierite is easily distinquished by slightly higher relief than plagioclase, diagnostic pleochroic halos due to inclusions of zircon and/or apatite, polysynthetic twinning, and by the common occurrence of a yellow isotropic alteration pinite which surrounds the grain and works its way along fractures, giving the

cordierite a bubbly texture. In outcrop, cordierite is often hard to detect due to its close resemblence to quartz.

PLAGIOCLASE: Plagioclase shows a wide range in composition from An_{20} to An_{80} depending on the rock type and grade. It often does not show any twinning in thin section and is the most prevalent feldspar in these rocks.

ALKALI FELDSPAR: Alkali feldspar occurs in two forms: as microcline, or as stringy perthite. It is found mainly in the leucosome stringers associated with pelitic rocks just past the second sillimanite isograd, becoming quite rare at higher grades.

ORTHOPYROXENE: Orthopyroxene is predominantly hypersthene, often showing strong pink-green pleochroism in thin section. In the wacke rocks, it can be somewhat aluminous with up to 4 wt percent Al_2O_3. Chemically, it is homogenous, and does not show any exsolution.

GARNET: Garnet is mainly an iron rich almandine-pyrope solid solution with small amounts of grossular and spessartine. It often forms porphyroblasts up to 3 cm in size, and does not show any significant compositional zonation.

PROGRADE METAMORPHISM AND ISOGRADS

Low and Medium Grade Metamorphism

The only occurrences of low- and medium-grade metamorphic rocks noted during this study were from Lake St. Joseph, on the bordering edge of the Uchi subprovince. Pressures and temperatures may be constrained through mineralogical equilibria. Local occurrences of andalusite (eg Soules Bay, Lake St. Joseph; Goodwin, 1965) constrains pressures to less than 4 Kbars (Holdaway, 1971). The abundance of chlorite-muscovite-biotite assemblages suggests that temperatures were greater than 400°C, but the total absence of cordierite constrains temperatures to less than 500-550°C because chlorite + muscovite would break down to cordierite + biotite +/- Al_2SiO_5 ar such temperatures (Winkler, 1979). Restricted occurrences of staurolite, however, (Goodwin, 1965; Clifford, 1969; Breaks et al., 1978) suggest that locally, temperatures may have reached 525-550°C (Hoschek, 1969) (figure 3).

The Lake St. Joseph fault separates the Uchi subprovince to the north, from the English River subprovince. The fault zone also marks a sharp jump in metamorphism from the low-medium grade metamorphism of the Uchi subprovince to the medium-high grade metamorphism of the English River subprovice (figure 4).

Figure 3. Mineralogical phase equilibria:

KEY

Ab = Albite	AS = Al_2SiO_5
B = Biotite	Chl = Chlorite
Cord = Cordierite	Gt = Garnet
Ksp = K-Feldspar	Ms = Muscovite
OPX = Orthopyroxene	Q = Quartz
St = Staurolite	Stlp = Stilpnomelane
V = H_2O Vapor	

MINERALOGICAL REACTIONS:

Stlp + Mu = B + Mu	(Winkler, 1979)
Chl + Mu = St + B + Q + V	(Hoschek, 1969)
Chl + Mu = Cord + B + AS + Q	(Winkler, 1979)
Mu + St + Q = B + AS	(Hoschek, 1969)
Mu + Q = Ksp + AS	(Winkler, 1979)
Ab + Mu + Q + V = AS + Melt	(Winkler, 1979)
Ab + B + AS + Q + V = Cord + Gt + Melt (Wet)	(Grant, 1973)
Ab + B + AS + Q = Cord + Gt + Melt (Dry)	(Grant, 1973)
Granite Minimum Melt	(Winkler, 1979)
B + Gt = Ksp + Cord + OPX + Melt (dry)	(Grant, 1973)

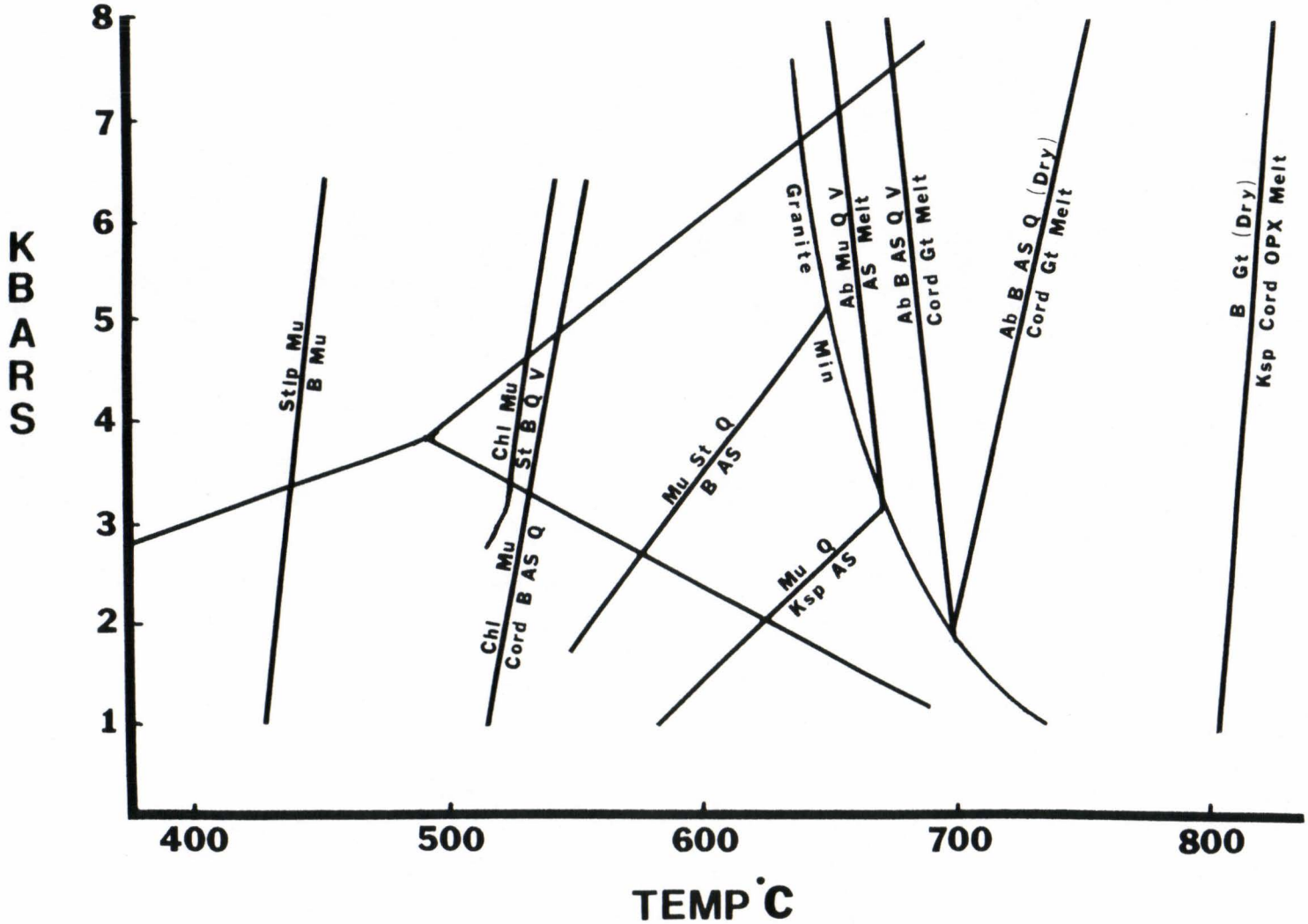
KBARS
8
7
6
5
4
3
2
1
400
500
600
700
800
TEMP °C
Stlp Mu
B Mu
Chl Mu
St B Q V
Chl Mu
Cord B AS Q
Mu St Q
B AS
Mu Q
Ksp AS
Granite
Ab Mu Q V
AS Melt
Ab B AS Q V
Cord Gt Melt
Ab B AS Q (Dry)
Cord Gt Melt
B Gt (Dry)
Ksp Cord OPX Melt

Figure 4. Isograds in the Eastern Lac Seul region.

KEY

- ○ Muscovite
- □ Chlorite
- ▲ Cordierite
- ◐ Cordierite with metastable sillimanite inclusions
- ● Orthopyroxene

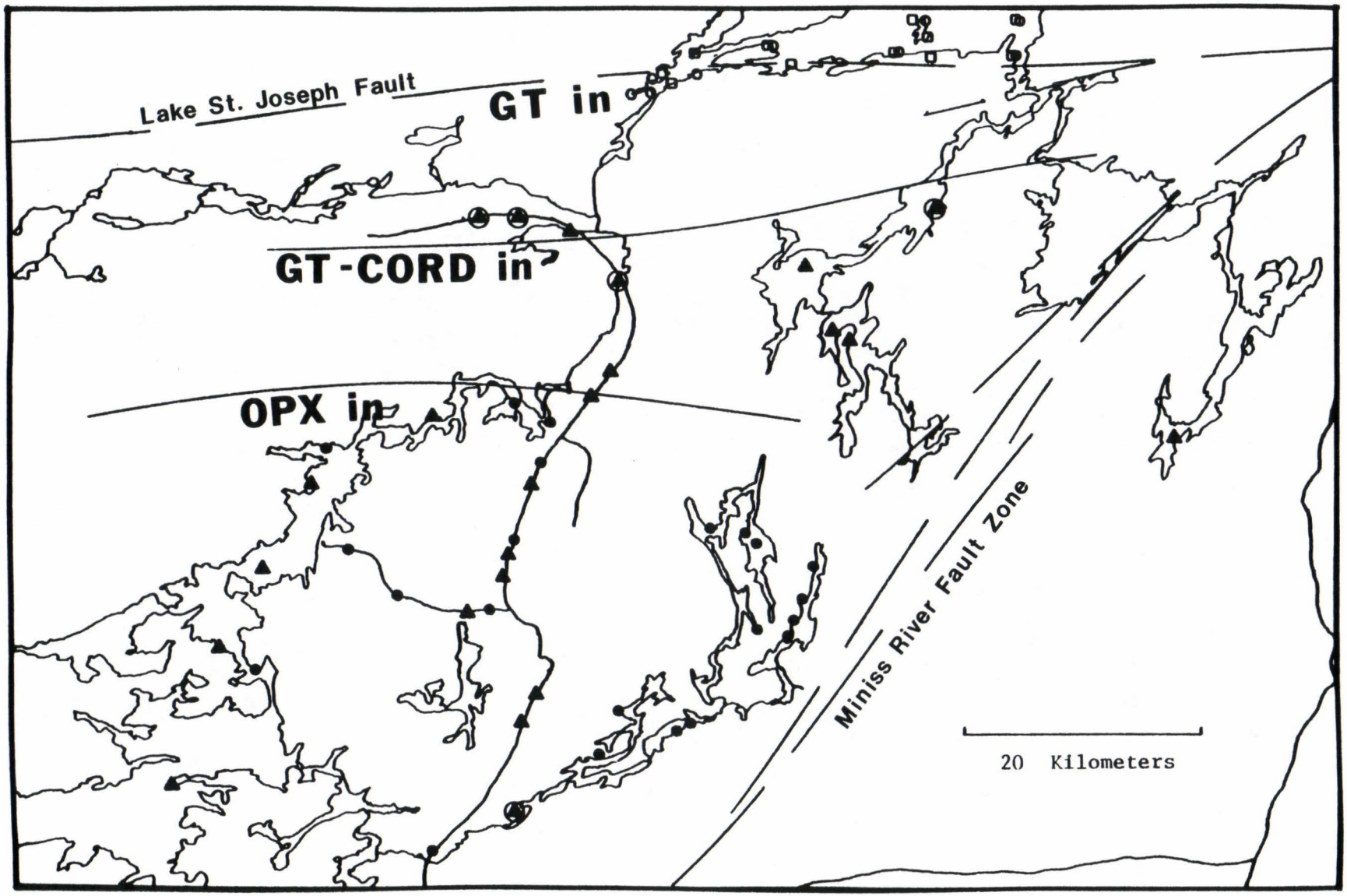
Lake St. Joseph Fault
GT in
GT-CORD in
OPX in
Miniss River Fault Zone
20 Kilometers

Transition from Medium to High-Grade Metamorphism

Winkler (1979) defines the transition from medium to high-grade metamorphism as the breakdown of muscovite in the presence of quartz which between the temperatures of 580-660°C, takes place along the reaction:

$$\text{muscovite} + \text{quartz} = \text{Kspar} + \text{sillimanite} + H_2O \qquad \text{(a)}$$

However, at sufficient H_2O pressures (greater than 3.5 Kbars), reaction (a) intersects the granite minimum melt curve to form the reaction:

$$\text{muscovite} + \text{quartz} + \text{plagioclase} + H_2O = \text{melt} + \text{sillimanite} \qquad \text{(b)}$$

The melt will be composed of K-feldspar, quartz, H_2O, and albite rich plagioclase components, with the restitic plagioclase increasing in anorthite (Winkler, 1979). In the English River subprovince, this reaction represents the onset of anatexis.

Significance of Coexisting Garnet-Cordierite

Various authors have noted the worldwide occurrence of coexisting garnet and cordierite (Wynne-Edwards and Hay, 1963; Harris, 1976; Bluemel and Schreyer, 1977). Several workers, e.g.(Thompson, 1976; Bluemel and Schreyer, 1977; Holdaway and Lee, 1977) attribute this to the reaction:

$$\text{biotite} + \text{sill} + \text{quartz} = \text{Kspar} + \text{garnet} + \text{cordierite} +/- H_2O \qquad \text{(c)}$$

There are, however, several problems with attributing coexisting garnet-cordierite of the English River subprovince to reaction (c). Natural garnet-cordierite pairs were found at lower temperatures than the temperatures at which reaction (c) takes place (Holdaway and Lee, 1977).

Hess (1969) noted that once partial melting does occur, K-feldspar is incorporated into the melt, and if plagioclase is also melted, any reaction involving the production of K-feldspar is coupled with the granite minimum melt reaction:

$$\text{Kspar} + \text{plagioclase} + \text{quartz} + H_2O = \text{melt} \qquad \text{(d)}$$

Thus, if anatexis occurs, we may add reaction (c) to reaction (d) to produce:

$$\text{bio} + \text{sill} + \text{qtz} + \text{Na-plag} = \text{gt} + \text{cord} + \text{melt} + \text{Ca-plag} \qquad \text{(e)}$$

Adopting the assumption from Grant (1973) that the liquids evolved in univariant reactions are initially more water rich than biotite, H_2O vapor can be added to the system to formulate his reaction:

$$\text{bio} + \text{sill} + \text{qtz} + \text{Na-plag} + H_2O = \text{gt} + \text{cord} + \text{melt} + \text{Ca-Plag} \qquad \text{(f)}$$

This system consists of the components FeO, MgO, SiO_2, Al_2O_3, CaO, Na_2O, K_2O, and H_2O for a total of 8 components, and since 8 phases are involved, reaction (f) maintains its continuous, divariant identity, sliding towards higher temperatures as the system becomes drier.

Evidence in the English River subprovince for reaction (f) is that sillimanite, when found, is usually isolated in the cores of cordierite,

oriented somewhat parallel to the local fabric in the rock. One may imagine a mat of sillimanite reacting with the biotite and quartz, forming cordierite which encased some of the sillimanite to prevent it from further reacting. A Churchill Lake sample containing both hercynite and sillimanite in a cordierite core, further suggests that sillimanite is metastable with respect to the rest of the thin section which contains abundant quartz (Hercynite reacts in the presence of quartz to form cordierite). At increasing grade, the cordierite will homogenize with the remnant sillimanite reacting to completion.

Hollister (1977) postulates for rocks from the Tertiary Khtada Lake metamorphic complex, British Columbia, an isothermal decompressional event resulting in the reaction:

biotite + sillimanite + garnet = cordierite (g)

This can be modeled by a region that moves isothermally from high pressures to low pressures and into the stability field of cordierite due to rapid uplift. He cites garnet zonation (Mn concentrating at the rim of the resorbing garnet) as evidence for his model. This model can not, however, be readily extended to the English River subprovince since the English River subprovince does not show the same textures (coronas of cordierite around garnet) as the Khtada Lake rocks, nor do the garnets show any significant zonation.

Granulites of the English River Subprovince

Granulites, here defined by the occurrence of hypersthene, may be more widespread in the English River subprovince than previously thought. Much of the subprovince has not been looked at in enough detail to locate all of the pockets of granulites. Hypersthene is found throughout the southern half of this study area in the regions of Ragged Wood, Carling, Bury, and Highstone lakes, Lac Seul, and along the Vermilion River and Idaho Lake roads. In addition, Skinner (1969) reports hypersthene in migmatites from Churchill, St. Raphael, and Miniss lakes, though no granulites were found in these lakes during this study. Granulites have not previously been reported in Ragged Wood or Carling Lakes. Recently R. M. Baumann, (personal communication), found granulites along the McKenzie Bay road (near Sawmill Bay) which travels east out of Ear Falls, Ontario (figure 5). Concerned mainly with the metasediments in this study, some hyperstene-bearing orthogneisses may have been overlooked.

Hypersthene was found in three separate rock types: orthogneisses, amphibolites, and wacke metasediments. Hypersthene, however, was not found in the more pelitic metasediments. The extra aluminum probably stabilized cordierite in its place.

De Waard (1965) proposes the following reaction for the formation of orthopyroxene;

hornblende + 2 biotite + 17 quartz = 15 opx + 4 Kspar + 2 plag (h)

Figure 5. Known granulite occurrences in the English River subprovince.

(Modified from Breaks et al., 1978)

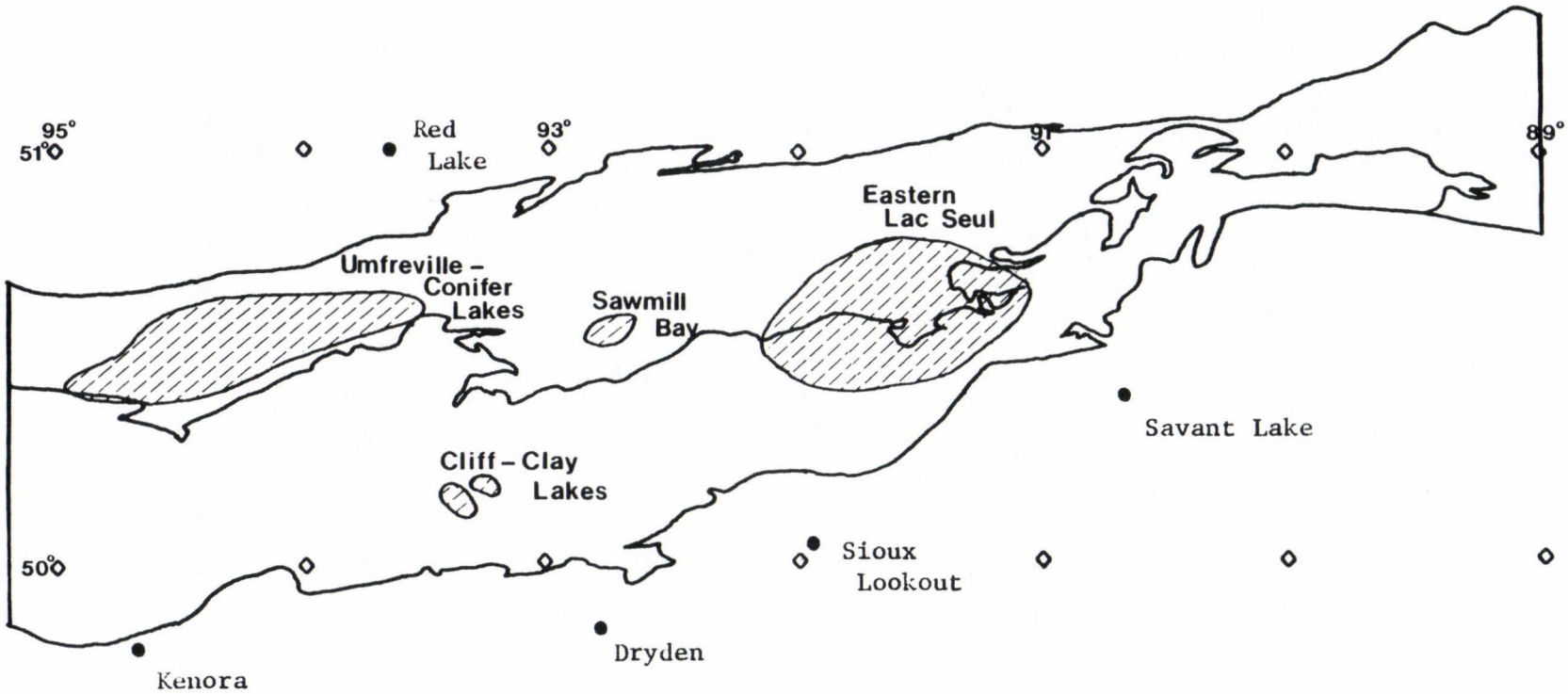
95°
51°
Red
Lake
93°
91°
89°
Eastern
Lac Seul
Umfreville -
Conifer
Lakes
Sawmill
Bay
Savant Lake
Cliff - Clay
Lakes
50°
Sioux
Lookout
Dryden
Kenora

with excess biotite producing almandine and excess hornblende producing clinopyroxene.

Winkler (1979) subdivides reaction (h) into two separate reactions:

$$\text{biotite} + \text{quartz} = \text{orthopyroxene} + \text{Kspar} + H_2O \qquad (i)$$

$$\text{hornblende} + \text{quartz} = \text{opx} + \text{cpx} + \text{plagioclase} + H_2O \qquad (j)$$

Reaction (i) would be relevant to the wacke metasediments, reaction (j) to the amphibolites, and reaction (h) to the orthogneisses. These are all continuous sliding reactions which depend not only on temperature and total pressure, but on water fugacity as well.

In reaction (i), K-feldspar and H_2O are on the product side of the reaction; adding the granite melt reaction (d) (Hess, 1969), creates the revised reaction:

$$\text{biotite} + \text{quartz} + \text{plagioclase} = \text{orthopyroxene} + \text{melt} \qquad (k)$$

Hess (1969) suggests that relatively Fe rich biotite reacts to yield hyperstene at some temperature near 700°C and at somewhat higher temperatures, biotite-garnet become incompatible and are replaced by cordierite-hypersthene.

Grant (1973) proposes the following reaction for the more pelitic metasediments:

$$\text{biotite} + \text{garnet} = \text{orthopyroxene} + \text{cordierite} + \text{Kspar} + \text{melt} \qquad (l)$$

Grant (1973), places this reaction at temperatures slightly greater than 800°C dry, though increased water fugacity decreases the reaction

temperatures. Cordierite and orthopyroxene were found together in only one sample. However, the cordierite is in a leucosome vein suggesting that the two phases are not of the same paragenesis and the high temperatures (800-850°C; Grant 1973) at which this reaction would occur were never attained.

Anatexis

In the layered sequences of wacke and pelitic sediments, leucosome stringers are often confined to the pelitic layers suggesting that the pelitic rocks are the first to melt. There is a distinct decrease in pelitic material in the regions of greater metamorphic grade due to the increased amount of melting. In the diatexite regions, it is quite common to find rafts of wacke metasediments floating in leucosome with patches of garnet +/- cordierite rich leucosome oriented subparallel to wacke xenoliths. These are interpreted as totally resorbed pelitic lenses with only the refractive, restite minerals remaining.

R. M. Baumann (personal communication; Baumann et al., 1984) is currently investigating the origin of the leucosome. Though there is much evidence for in situ melting, there is just as much evidence for injection. Some areas composed of diatexites contain far more leucosome than could be generated from in situ anatexis. Coupled with distinct cross cutting relationships, an intrusive origin is suggested for these rocks. Baumann suggests that the English River subprovince migmatites may have both an intrusive and an anatectic origin.

GEOTHERMOMETRY - GEOBAROMETRY

Obtaining Chemical Data

Chemical analyses of the minerals were obtained using a JEOL 35C scanning electron microscope equipped with a Li drifted silicon detector. Standard operating conditions were 15 KV and 1000 picoamps (beam current). Energy dispersive spectra were processed by a TN2000 (Tracor Northern) operating system and corrected using a Bence-Albee correction program. Natural garnets, biotites, feldspars, and pyroxenes were used as standards. Cordierite was analyzed using the pyroxene reference standards. Reproducibility of analyses were excellent; +/- 2% (of the amount present) for all major elements except Na (+/- 3%).

For each mineral of interest, 1 to 2 analyses on 4 to 5 grains scattered throughout each thin section were obtained and averaged together for application in the geothermometers-barometers used in this study. Counting times of either 60 or 100 seconds were used. Chi-square values were typically in the range of 0.60-3.00 indicating a good fit between the specimen and the reference standard. All microprobe analyses are given in Appendix C.

Mineral Zonation

Garnet, cordierite, and plagioclase were checked for zonation by running microprobe traverses across the grain, using a 200 second counting time per point. Except for slight retrogression of garnet rims

in contact with biotite, no significant compositional zoning was found in any of the phases. Tracy et al. (1976) found retrograde zoning in garnets from high-grade rocks from west-central Massachusetts. Garnets of that study were nearly homogeneous, except when they were in direct contact with biotite or cordierite which produced a substantial decrease in Mg/Fe in the garnet rim. In low and medium grade terrains, garnet often shows prograde zonation (Tracy et al., 1976). However, under high grade metamorphism, garnet becomes less refractory and homogenizes (Woodsworth, 1977). If any zonation is found, it is usually of retrograde origin (Tracy et al., 1976; Hollister, 1977; Edwards and Essene, 1981; Bohlen, 1983). In this study, only the cores of the mineral phases were probed to prevent the possibility of obtaining a retrograde rim composition.

For application of biotite-garnet K_D thermometers, Tracy et al. (1976) suggest that in cases where biotite is in far greater abundance than other Fe-Mg-Mn phases, the matrix biotite (not in contact with other Fe-Mg-Mn phases) will possess Fe/Mg ratios affected little by retogression. Furthermore they state that K_D's determined from garnet cores and matrix biotite should record the most correct estimate of prograde temperature. This is further substantiated by Edwards and Essene (1981) who found when applying the Thompson (1976) geothermometer to Adirondack samples, garnet and included biotite pairs produced temperatures up to 300°C lower than those obtained using matrix biotite-garnet pairs. Diffusion kinetics and closure temperature must be a function of distance between the two phases. Thus, probing matrix biotite and garnet cores should yield the highest effective closure compositions.

Biotite-Garnet Geothermometry

Many geothermometers are based upon the exchange of Fe and Mg between coexisting phases. The biotite-garnet geothermometer, in particular, has been widely applied since this is a common assemblage in many metamorphic and igneous rock types. Many calibrations of this geothermometer have been proposed. The more popular or more recent calibrations are by Thompson (1976), Goldman and Albee (1977), Ferry and Spear (1978), Perchuk and Lavrent'eva (1983), Ganguly and Saxena (1984), and Indares and Martignole (1985). These geothermometers have been applied to rocks from the eastern Lac Seul region in order to determine their accuaracy and precision, and also to gain insight into the thermal evolution of the Archean rocks exposed there.

Principles of Biotite-Garnet Geothermometry

The exchange of Mg and Fe between coexisting biotite and garnet is highly sensitive to temperature. With increasing temperature, biotite becomes more Fe-rich and garnet more Mg-rich as the following continuous exchange reaction occurs:

$$\text{Fe-garnet} + \text{Mg-biotite} = \text{Mg-garnet} + \text{Fe-biotite} \qquad \text{(m)}$$

At equilibrium, the Gibbs energy for the above reaction must be zero:

$$0 = \Delta G^{o} + RT\ln K$$

Though ΔG^{o} is a function of both pressure and temperature, the volume change of this reaction is small (0.057 cal/bar: Ferry and Spear, 1978) so that pressure has only a minor effect. Thus, reaction (m) is ideally suited as a geothermometer.

The equilibrium constant (K) for this reaction can be divided into an "ideal" term (equal to the distribution coefficient - K_D), and a "non-ideal" term which involves the activity coefficients (K_Y):

$$K = \frac{(XMg/XFe)gt}{(XMg/XFe)bio} * \frac{(YMg/YFe)gt}{(YMg/YFe)bio}$$

$$K = K_D * K_Y$$

Many studies have assumed ideal mixing in the phases. Activity coefficients and thus K_Y are then equal to 1. The equilibrium constant (K) then becomes equal to the distribution equilibrium coefficient (K_D). This assumption may not introduce serious errors, and may be justified if:

(1) The deviations from ideality in garnet and biotite are small, or

(2) The deviations from ideality in garnet and biotite tend to cancel out.

Several studies, including most recently, Ganguly and Saxena (1984), have derived activity models for garnet that show substantial deviations from ideality so that condition (1) above cannot be justified. Ganguly and Saxena formulated a biotite-garnet geothermometer assuming ideal mixing in biotite but complex, nonideal mixing in garnet. Such an approach, however, is inconsistent with both justifications (1) and (2) above, and may only be correct if biotite solutions behave much more ideally than garnet.

The various calibrations of reaction (m), all derived in different ways, produce large discrepancies when applied to identical biotite-garnet pairs (figure 6; table 1). The Thompson (1976) thermometer was calibrated by correlating K_D values of natural biotite-garnet assemblages against estimated temperatures based on experimental phase equilibria. Goldman and Albee (1977) related the biotite-garnet compositions to temperatures derived by quartz-magnetite oxygen isotope thermometry. Ferry and Spear (1978) experimentally calibrated the thermometer based upon experiments in systems with Fe/Fe+Mg held at 90%. Perchuk and Lavrent'eva (1983) also experimentally calibrated the thermometer, but in systems that averaged around 60 Fe/Fe+Mg. Ganguly and Saxena (1984), invoking ideal mixing in biotite but nonideal mixing in garnet, fit a thermodynamic model to the experimental data of Ferry and Spear (1978).

Bohlen and Essene (1980) point out that the partitioning of cations between coexisting phases may depend not only on temperature, but on bulk composition citing the $Mg\text{-}Fe^{+2}$ exchange between olivine and orthopyroxene as a prime example. Goldman and Albee (1977) statistically investigated the compositional effects on $\ln K_D$ due to Ca and Mn in garnet, and Ti and Al^{VI} in biotite. Increasing Ca and Mn in garnet and Al^{VI} in biotite has the effect of decreasing temperatures whereas increasing Ti in biotite increases the temperatures obtained using this calibration. Ferry (1980) found that although the Goldman and Albee calibration qualitatively corrects for compositional effects, it may occasionally overcompensate for them. More recently, Indares and Martignole (1985) combined the experimental data of Ferry and Spear with

Figure 6. Comparison of various Garnet-Biotite geothermometers: lnK vs temperature.

(The 2-parameter solution model is represented for Goldman and Albee, 1977)

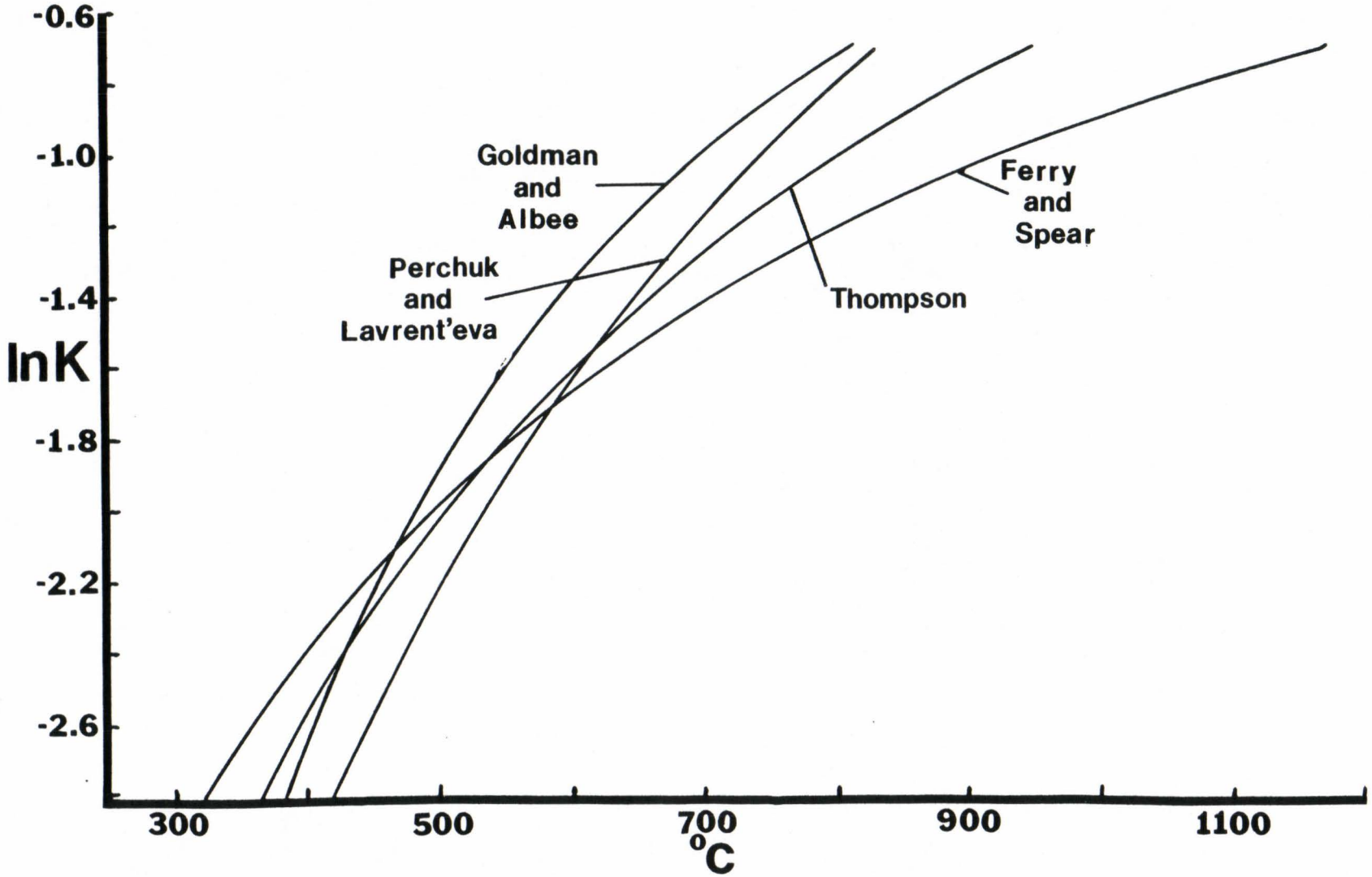
-0.6
-1.0
-1.4
-1.8
-2.2
-2.6
lnK
300
500
700
900
1100
°C
Goldman and Albee
Perchuk and Lavrent'eva
Thompson
Ferry and Spear

TABLE 1

BIOTITE-GARNET EQUILIBRIA

Temperatures in Degrees C
at 5 Kbars

Sample	Gt Mg/Mg+Fe	Bio Mg/Mg+Fe	lnK	FS	PL	TH	GS	GA_1	GA_2	IM_1	IM_2
BL1083C	0.297	0.579	-1.18	814	696	733	656	643	644	687	690
BL1083E	0.190	0.428	-1.16	827	702	741	784	649	618	737	783
CH1183A	0.181	0.485	-1.45	686	637	646	678	580	635	619	689
CH1283A	0.268	0.541	-1.17	825	701	740	698	648	707	714	713
CH1483B	0.254	0.527	-1.19	812	695	732	692	642	692	705	692
CH1683	0.196	0.484	-1.35	731	659	677	692	602	631	647	689
CL1183A	0.291	0.527	-1.00	925	742	803	759	696	679	769	784
CL2283A	0.252	0.482	-1.02	915	738	797	801	692	662	763	803
DS1683	0.223	0.493	-1.22	793	687	719	729	633	680	692	730
DS2183B	0.214	0.493	-1.27	767	675	701	706	620	682	679	702
DS2483	0.171	0.486	-1.52	656	622	625	645	564	597	585	632
EB1083A	0.183	0.476	-1.40	704	646	659	646	589	547	595	595
HS1483C	0.227	0.522	-1.31	747	666	688	648	610	583	629	627
HS1583C	0.202	0.473	-1.27	771	677	704	740	622	621	660	726
ID1283	0.292	0.573	-1.18	816	697	734	664	644	692	700	691
ID1683A	0.331	0.567	-0.97	946	750	816	757	706	746	739	750
JS2583	0.113	0.364	-1.50	662	625	629	682	568	576	629	623
JS2983	0.149	0.481	-1.66	601	593	585	616	536	570	575	622
JS3883A	0.199	0.557	-1.62	616	601	596	613	544	619	565	648
LS17	0.189	0.445	-1.24	785	683	714	747	629	659	704	741
LS42	0.254	0.492	-1.04	899	731	787	768	684	708	749	743
LS51A	0.321	0.528	-0.86	1027	780	864	820	744	821	870	857
LS66A	0.278	0.543	-1.13	846	710	754	716	659	716	738	749
LS69	0.252	0.490	-1.05	894	730	784	770	682	713	797	797
LS76A	0.292	0.546	-1.07	883	725	777	734	676	740	771	780
LS78	0.249	0.491	-1.07	880	724	775	757	675	708	752	745
LS92B	0.378	0.584	-0.84	1047	787	876	803	753	868	885	884
MN1083B	0.295	0.523	-0.96	953	753	821	787	710	782	832	830
MN1883	0.325	0.568	-1.00	924	741	803	735	696	777	774	764
MN1983	0.243	0.498	-1.13	846	710	754	740	659	709	713	714
MN2183	0.289	0.576	-1.21	800	690	723	659	636	708	691	682
RF1283	0.330	0.565	-0.97	947	750	817	749	707	770	796	790
RF1483	0.304	0.529	-0.95	963	756	826	796	714	800	854	864
RF1883	0.290	0.539	-1.05	893	729	783	750	681	748	772	786
RF2183A	0.322	0.580	-1.07	883	725	777	705	676	748	754	750
RF2283	0.241	0.515	-1.21	801	690	724	690	637	665	695	683
RF2583A	0.276	0.531	-1.09	868	719	768	726	669	724	745	740

TABLE 1 CONTINUED

Sample	Gt Mg/Mg+Fe	Bio Mg/Mg+Fe	lnK	FS	PL	TH	GS	GA_1	GA_2	IM_1	IM_2
RW1283B	0.327	0.572	-1.01	918	739	799	732	693	747	788	794
RW2583	0.258	0.548	-1.25	779	680	709	659	626	604	654	669
VM1683	0.180	0.440	-1.27	766	675	701	746	620	678	681	731
VM2183	0.194	0.461	-1.27	769	676	703	735	621	677	667	711
VM2683A	0.245	0.528	-1.24	785	683	713	679	629	674	686	682
VM2783	0.239	0.513	-1.21	799	690	723	725	636	704	714	749
VM3583B	0.285	0.516	-0.98	938	747	811	769	702	742	803	788
VM3883B	0.290	0.540	-1.06	890	728	781	736	679	706	733	739
VM4383	0.295	0.532	-1.00	927	742	804	761	697	732	773	776
VM4983	0.250	0.548	-1.29	758	671	696	656	616	658	672	680
VR13A	0.207	0.486	-1.29	760	672	697	691	617	655	659	657
VR1583	0.229	0.513	-1.27	770	677	704	667	622	600	658	657

lnK = ln ((XMg/XFe)Gt / (XMg/XFe)Bio)
FS = Ferry and Spear (1978)
PL = Perchuk and Lavrent'eva (1983)
TH = Thompson (1976)
GS = Ganguly and Saxena (1984)
GA_1 = Goldman and Albee (1977) second parameter solution
GA_2 = Goldman and Albee (1977) fifth rank solution
IM_1 = Indares and Martignole (1985) using thermodynamic data only
IM_2 = Indares and Martignole (1985) using both thermodynamic and empirical data

data from some natural garnet-biotite occurrences to derive an empirical thermometer that corrected for dilutents in both biotite and garnet.

The goal of this section is to take each of the above calibrations, and apply them to 49 samples from the eastern Lac Seul region of the English River subprovince (figure 7) in order to evaluate which of them produce the most accurate and precise results. Accuracy will be evaluated by comparing temperatures to experimental phase equilibria, and precision by conducting a least-squares regression (trend surface analysis) to determine how well the 49 temperatures fit to a regional temperature surface across the study area.

Evaluation of the Geothermometers

The evaluation of the geothermometers is based upon trend surface analysis which is based on the least-squares criterion of fitting polynomial functions to areally distributed data. The sources of variation can then be subdivided into two components; that of regional nature (the regression), and that of residuals or deviations from the regional component (local variation). Increasing the degree of the polynomial function will increase the "goodness of fit" by describing a more complicated regional surface. The statistical significance for each degree of regression in a trend compared to the next lower degree equation may be tested by performing an analysis of variance using an F-test (table 2):

Figure 7. Location of samples used for Garnet-Biotite geothermometry.

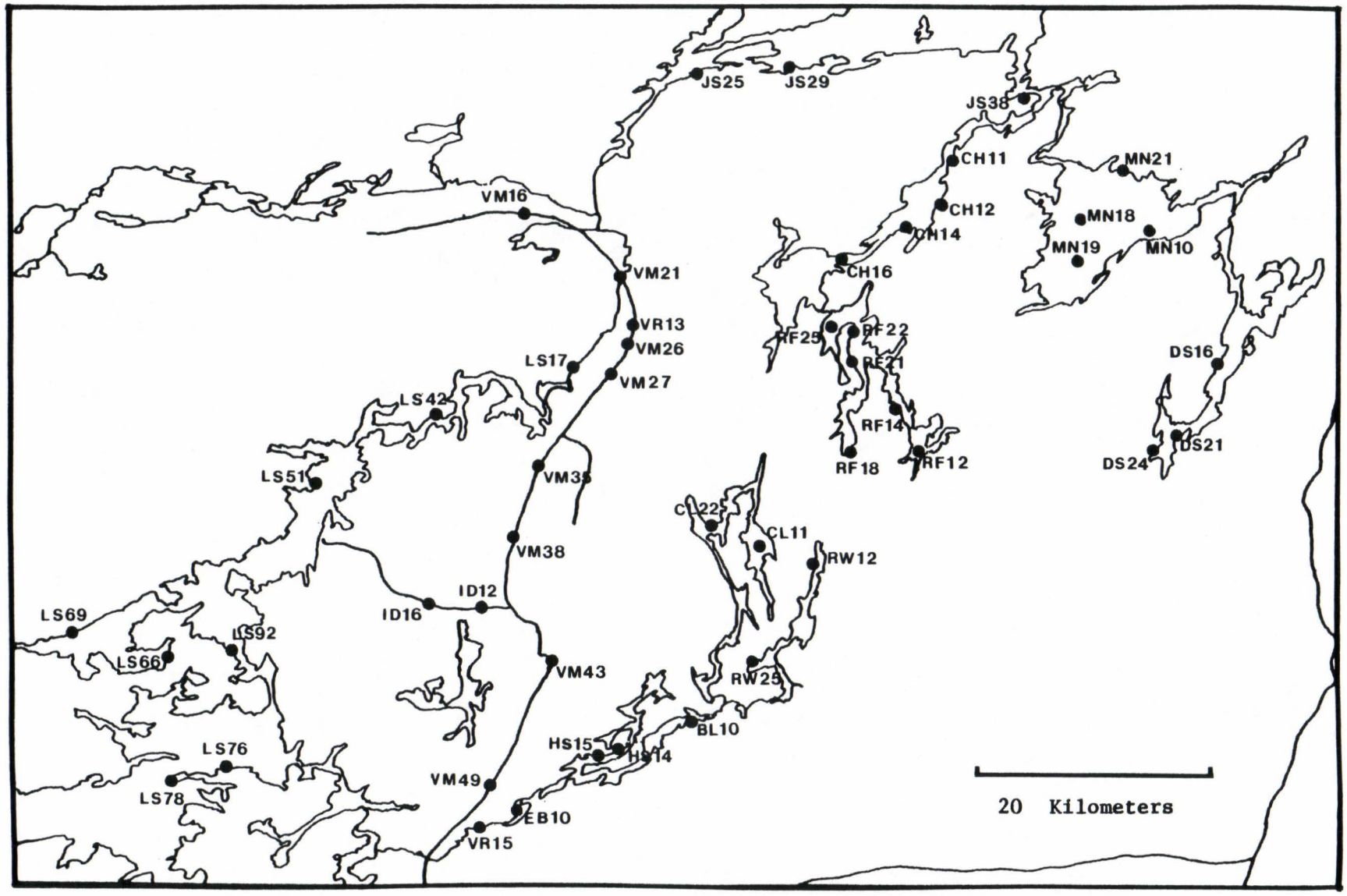
JS25
JS29
JS38
CH11
MN21
VM16
CH12
MN18
CH14
MN19
MN10
CH16
VM21
VR13
RF25
RF22
VM26
RF21
DS16
LS17
VM27
LS42
RF14
DS21
RF18
RF12
DS24
LS51
VM35
CL22
CL11
VM38
RW12
ID12
ID16
LS69
LS92
LS66
VM43
RW25
BL10
HS15
HS14
LS76
VM49
LS78
EB10
VR15
20 Kilometers

$$F \text{ ratio} = \frac{(SSR_n - SSR_{n-1}) / (DFR_n - DFR_{n-1})}{(SSD_n / DFD_n)}$$

(SSR = Sum of Squares Regression; SSD = Sum of Squares Deviation)
(DFR = Degrees Freedom Regression; DFD = Degrees freedom Deviation)
(n = Order of Equation)

If the computed F-ratio for a n'th degree polynomial regression exceeds the tabulated F-test value for the significance level desired (Davis, 1973), the extra terms that were added to increase the degree of the polynomial function do not produce a significantly better fit.

The precision of the various calibrations can be estimated by calculating the percentage of the total variation that is explained by each degree of trend (explained by the regression, table 2). The Thompson, Ferry and Spear, and Perchuk and Lavrent'eva thermometers, closely follow lnK with the 2nd, 3rd, 4th, 5th, and 6th degree trend surfaces explaining 58, 78, 85, 88, 91 percent of the variance respectively. The calibrations that attempt to incorporate effects of the diluting components (Goldman and Albee, Ganguly and Saxena, Indares and Martignole) yield surfaces which account for 5 to 30 % less of the variance -- more scatter and deviation from the trend.

The trend surface analysis (table 2) suggests that the higher (5th and 6th) degree surfaces are unnecessary to explain the regional variations in the data. Perturbations from the 4th degree surfaces are well within the precision of the thermometers.

It appears that until we fully understand the effects of impurities on the Fe-Mg exchange between biotite and garnet, the pure $\ln K_D$

TABLE 2

TREND SURFACE STATISTICS

Percent Varience Explained
by each Degree Trend Surface

First	Second	Third	Fourth	Fifth	Sixth
		lnK			
11.1	59.8*	79.0*	85.3*	88.4	91.3
		Thompson (1976)			
10.3	57.9*	77.3*	84.5*	87.5	90.7
		Goldman and Albee (1977) 5th rank			
3.0	57.6*	68.8	81.3*	82.8	86.4
		Ferry and Spear (1978)			
10.0	56.7*	76.4*	84.0*	87.1	90.5
		Perchuk and Lavrent'eva (1983)			
10.5	58.7*	78.0*	84.8*	87.8	91.1
		Ganguly and Saxena (1984)			
7.3	40.6*	56.8*	60.8	65.9	76.2
		Indares and Martignole (1985) model 1			
7.2	49.6*	70.7*	78.3	81.4	86.2
		Indares and Martignole (1985) model 2			
4.7	44.8*	60.8*	68.4	71.5	81.8

* Significant at the 95% level

thermometers will produce more precise and consistent values than the calibrations which attempt to incorporate impurities into the calculations. This hypothesis is further suported by biotite-garnet pairs that are located less than a kilometer apart, and have significantly different chemical compositions (i.e. BL1083C-BL1083E, HS1483C-HS1583C, VM2683A-VM2783; figure 7). Using one of the pure $\ln K_D$ thermometers generally produces the same temperatures in both samples. Using one of the thermometers which attempt to incorporate impurities, however, can produce temperatures with over 100°C difference between the two samples (table 1).

Comparison of the various trend surfaces (figures 8-10), shows that though the actual values of the contours do differ, the regional trend remains much the same regardless of the calibration used. Although it is rather difficult to assess which one of these geothermometers yields the most correct temperatures, they can be evaluated qualitatively by assuming that the thermometer should record peak metamorphic temperatures. The Goldman and Albee "two-parameter solution" thermometer appears to produce temperatures that are too low with respect to the prograde reactions which have taken place. In particular, muscovite breakdown, biotite-sillimanite forming garnet-cordierite, and the formation of orthopyroxene all suggest that temperatures ranged from 650 to 750°C (Grant, 1973; Thompson, 1976; Winkler, 1979). Ferry and Spear's thermometer appears to overestimate temperatures since cordierite and orthopyroxene have not been found forming a stable paragenises (Grant, 1973), nor have high temperature minerals such as sapphirine been reported. Though the remaining

Figure 8. Second degree trend surfaces for the Eastern Lac Seul region (figure 7):

KEY

lnK = natural log of the equilibrium constant
Thomp = Thompson (1976) geothermometer
F+S = Ferry and Spear (1978) geothermometer
G+A = Goldman and Albee (1977) 5th rank geothermometer
P+L = Perchuk and Lavrent'eva (1983) geothermometer
G+S = Ganguly and Saxena (1984) geothermometer
I+M1 = Indares and Martignole (1985) using thermodynamic data only
I+M2 = Indares and Martignole (1985) using both thermodynamic and emperical data

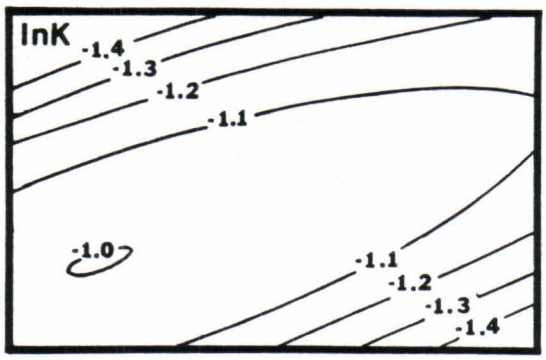
lnK
-1.4
-1.3
-1.2
-1.1
-1.0
-1.1
-1.2
-1.3
-1.4

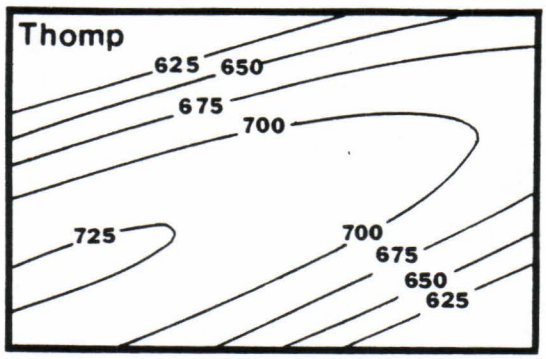
Thomp
625
650
675
700
725
700
675
650
625

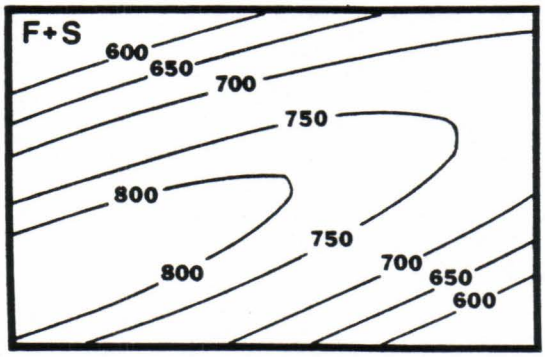
F+S
600
650
700
750
800
750
800
700
650
600

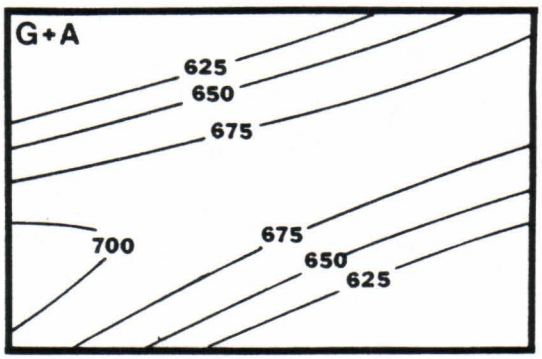
G+A
625
650
675
700
675
650
625

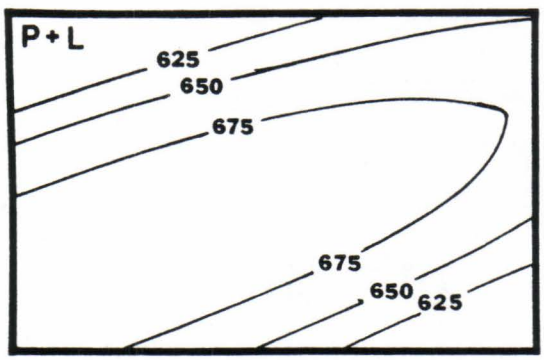
P+L
625
650
675
675
650
625

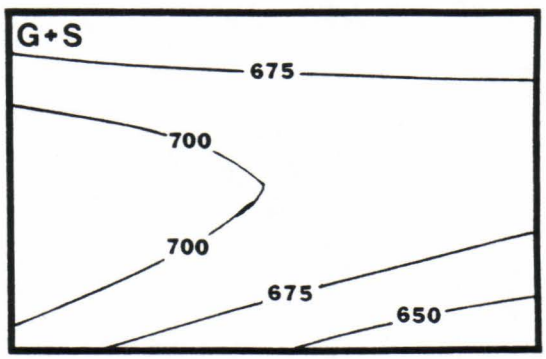
G+S
675
700
700
675
650

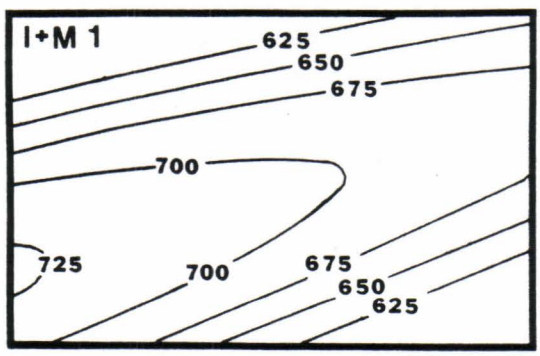
I+M 1
625
650
675
700
725
700
675
650
625

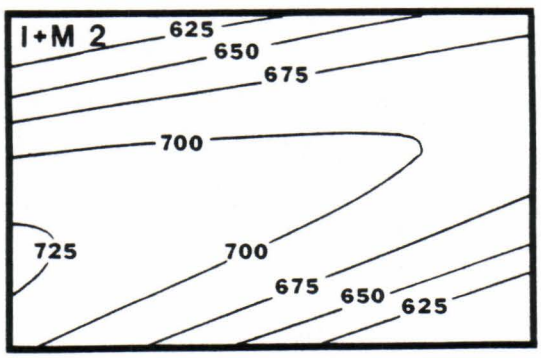
I+M 2
625
650
675
700
725
700
675
650
625

Figure 9. Third degree trend surfaces for the Eastern Lac Seul region (figure 7):

KEY

lnK = natural log of the equilibrium constant
Thomp = Thompson (1976) geothermometer
F+S = Ferry and Spear (1978) geothermometer
G+A = Goldman and Albee (1977) 5th rank geothermometer
P+L = Perchuk and Lavrent'eva (1983) geothermometer
G+S = Ganguly and Saxena (1984) geothermometer
I+M1 = Indares and Martignole (1985) using thermodynamic data only
I+M2 = Indares and Martignole (1985) using both thermodynamic and emperical data

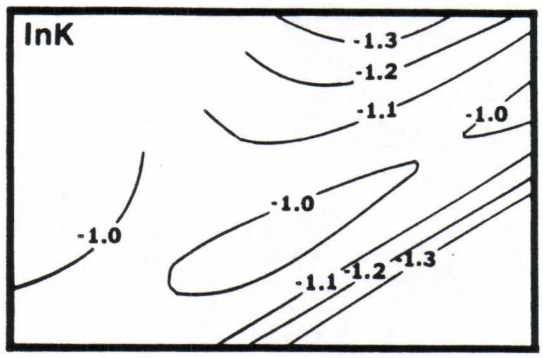
InK
-1.3
-1.2
-1.1
-1.0
-1.0
-1.0
-1.1
-1.2
-1.3

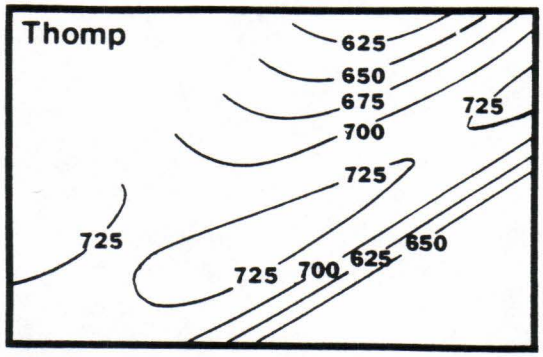
Thomp
625
650
675
700
725
725
725
725
700
625
650

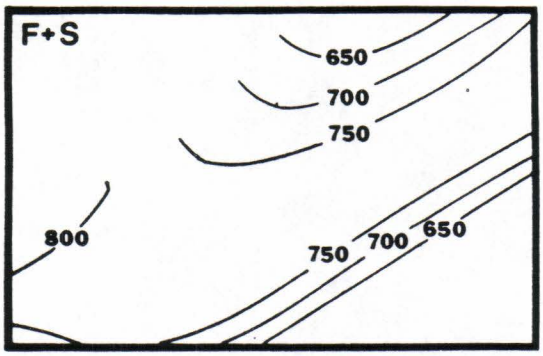
F+S
650
700
750
800
750
700
650

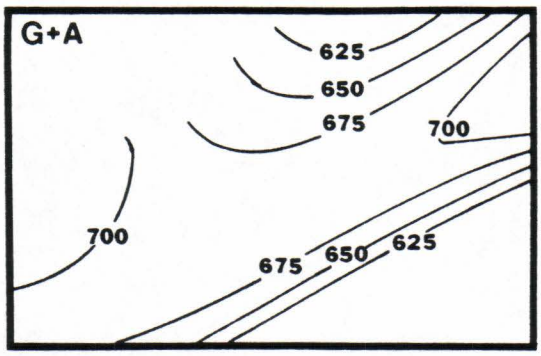
G+A
625
650
675
700
700
675
650
625

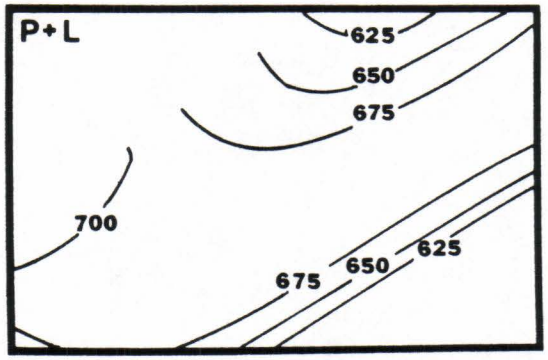
P+L
625
650
675
700
675
650
625

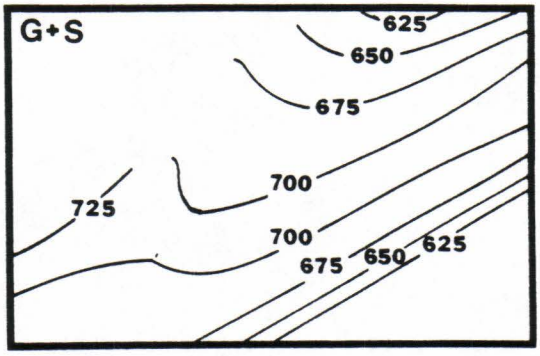
G+S
625
650
675
700
725
700
675
650
625

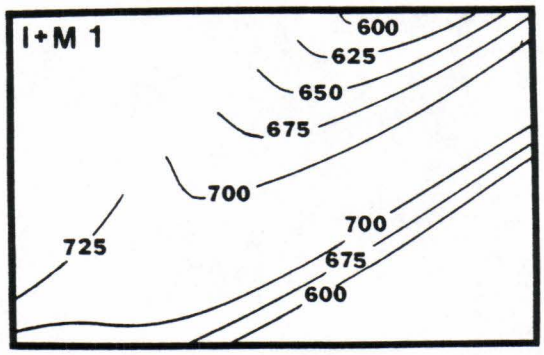
I+M 1
600
625
650
675
700
725
700
675
600

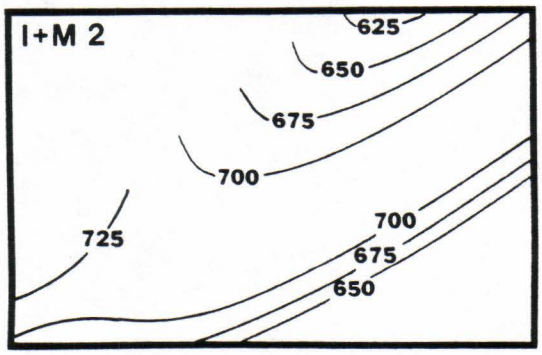
I+M 2
625
650
675
700
725
700
675
650

Figure 10. Fourth degree trend surfaces for the Eastern Lac Seul region (figure 7):

KEY

lnK = natural log of the equilibrium constant
Thomp = Thompson (1976) geothermometer
F+S = Ferry and Spear (1978) geothermometer
G+A = Goldman and Albee (1977) 5th rank geothermometer
P+L = Perchuk and Lavrent'eva (1983) geothermometer
G+S = Ganguly and Saxena (1984) geothermometer
I+M1 = Indares and Martignole (1985) using thermodynamic data only
I+M2 = Indares and Martignole (1985) using both thermodynamic and emperical data

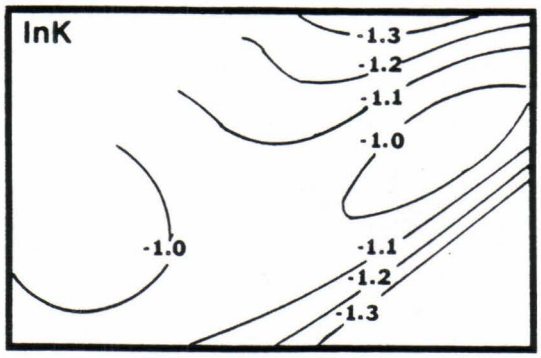
InK
-1.3
-1.2
-1.1
-1.0
-1.0
-1.1
-1.2
-1.3

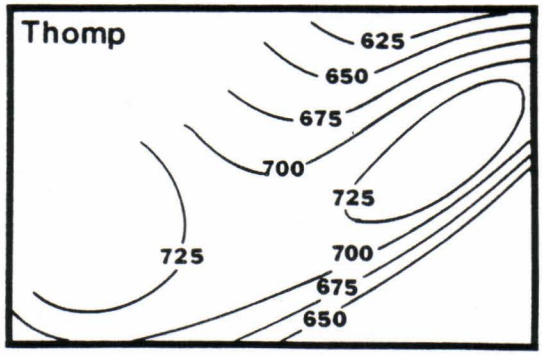
Thomp
625
650
675
700
725
725
700
675
650

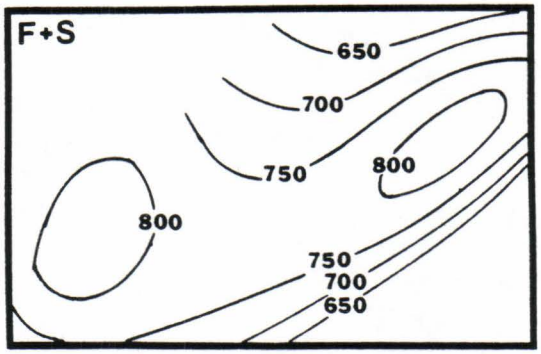
F+S
650
700
750
800
800
750
700
650

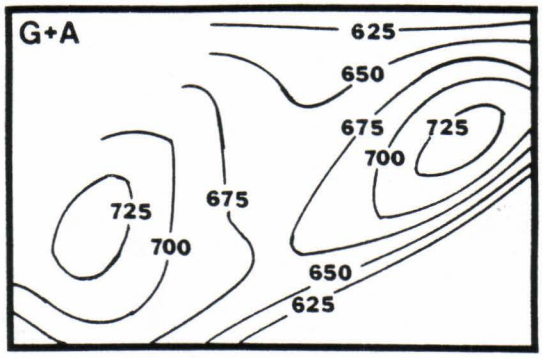
G+A
625
650
675
725
700
675
725
700
650
625

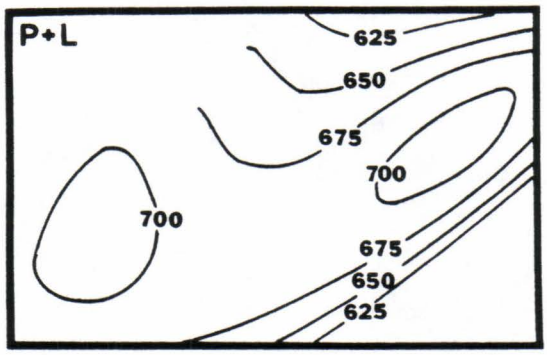
P+L
625
650
675
700
700
675
650
625

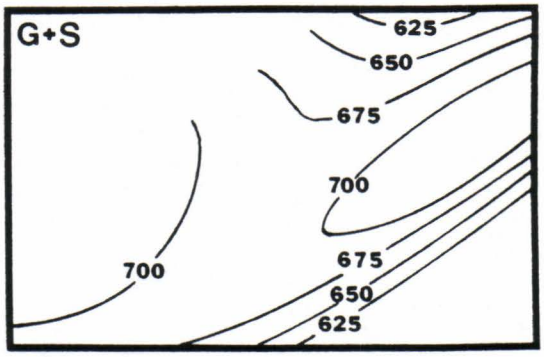
G+S
625
650
675
700
700
675
650
625

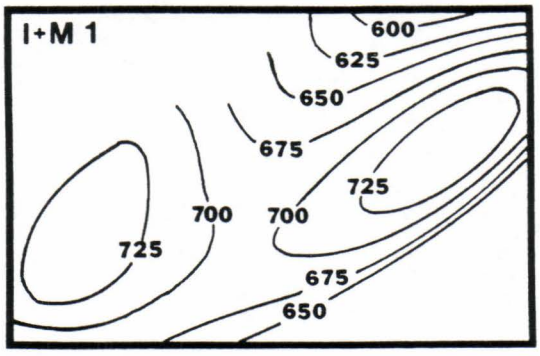
I+M 1
600
625
650
675
725
700
700
725
675
650

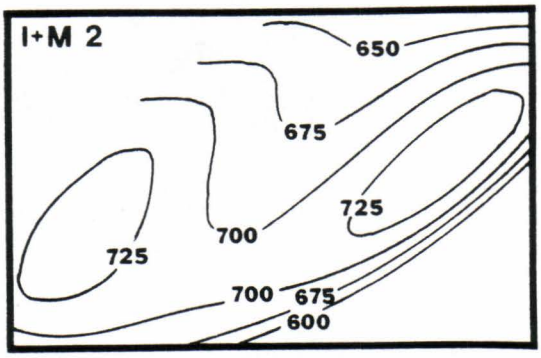
I+M 2
650
675
725
700
725
700
675
600

calibrations all produce geologically reasonable results (table 1), the Perchuk and Larvent'eva (1983) thermometer appears to produce the most reasonable and consistent results for the English River subprovince. The temperature values trend smoothly and correspond extremely well with experimental phase equilibria.

Results of Biotite-Garnet Geothermometry
For the English River Subprovince

The Eastern Lac Seul region of the English River subprovince can be envisioned as a "thermal anticline" (figure 11), whose axis extends locally along a latitude equivalent to Wapesi Bay - Carling Lake, and is then slightly contorted northeastwards by the Miniss River fault zone. Temperature falls off steadily on both sides of the axis. The isotherms are readily traceable northwards to the Lake St. Joseph fault, which coincides with the garnet-in isograd, but can be traced southwards only a short distance to the contact of the southern plutonic domain, where the lithologies are devoid of garnet. We find this same "thermal anticline" further west in the Western Lac Seul - Ear Falls region of the English River subprovince (Henke, 1984; R. M. Baumann, personal communication).

Based upon phase equilibria and the Perchuk and Lavrent'eva (1983) geothermometer, the metamorphic temperatures attained in the eastern Lac Seul region of the English River subprovince were approximately 600°C at the contact with the bordering Uchi subprovince. The garnet-cordierite "in" isograd occurs at about 675°C and the orthopyroxene "in" isograd at about 700°C. Maximum temperatures at the center of the granulite zone were about 750°C (figure 11).

Figure 11. Hand contoured isotherms for the Eastern Lac Seul region using the Perchuk and Lavrent'eva (1983) geothermometer.

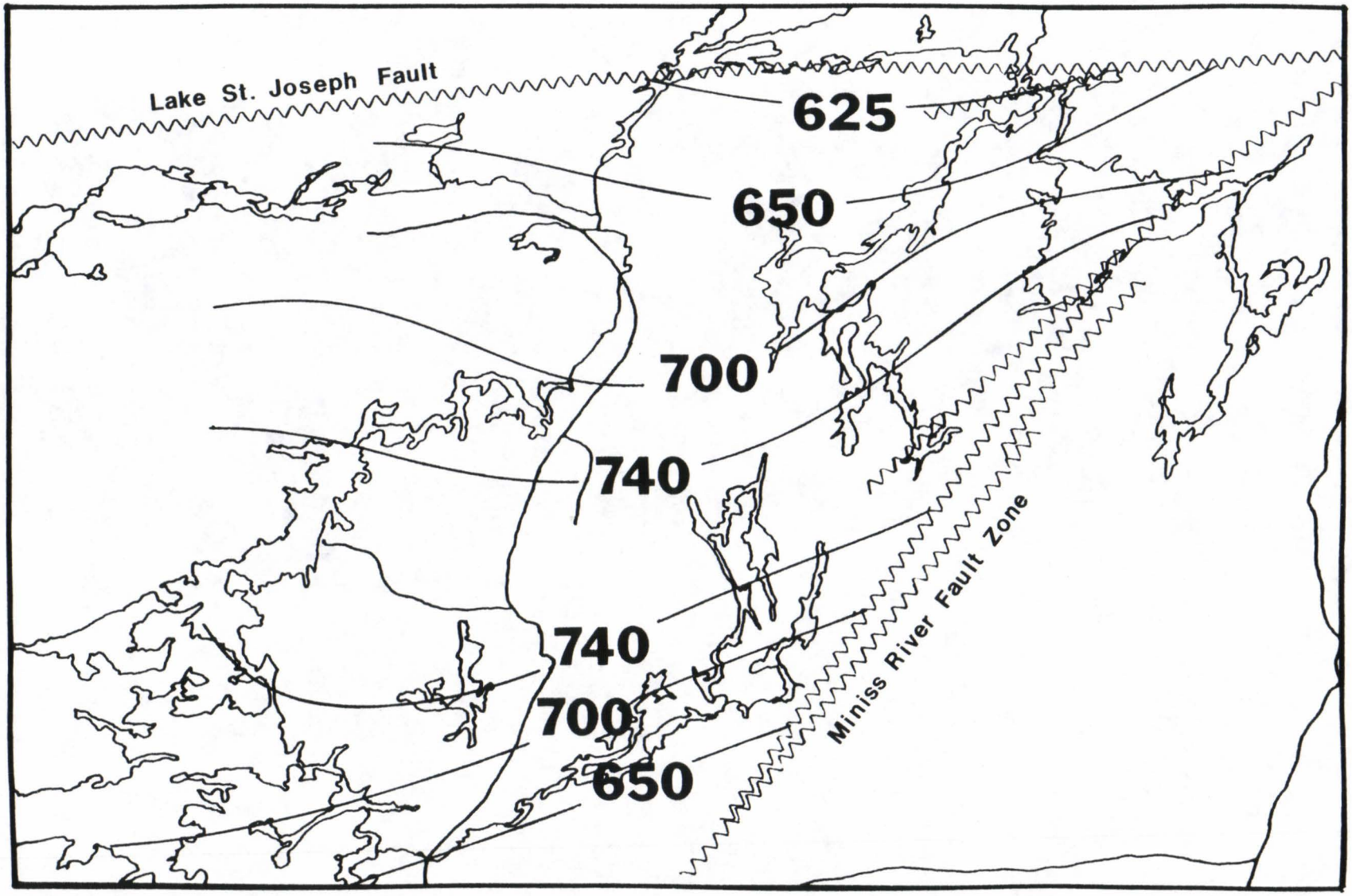
Lake St. Joseph Fault
625
650
700
740
740
700
650
Miniss River Fault Zone

The temperatures attained in the English River subprovince are far too great to be explained by conductive heating alone. Comparison with a modern day, basin and range geotherm, (Roy et al., 1972), suggests that a thermal perturbation in excess of 200-300°C had been imposed on an already steep geotherm. The contribution of a convective magmatic heat component must be invoked to explain the high temperatures (Chipera et al., 1984a). Modifying the thermal models of Wells (1980) and Thompson (1981), a model could be formulated that easily explains both the high temperatures and the observed thermal anticline.

Other Geothermometers

Garnet-Cordierite Geothermometry

Garnet-cordierite geothermometry is identical to garnet-biotite geothermometry though the degree of Fe-Mg distribution will be slightly different, and the effects of water in the cordierite have yet to be thoroughly evaluated (Newton and Wood, 1979; Martignole and Sisi, 1981). Results from the application of the Thompson (1976) and Perchuk and Lavrent'eva (1983) geothermometers are given in table 3.

Two-Pyroxene Geothermometers

The Wood and Banno (1973) and Wells (1977) two-pyroxene geothermometers were applied to three rocks from the eastern Lac Seul region (table 4). Though the two geothermometers are in close agreement, there are not enough samples to make more than a qualitative assessment of this geothermometer for the English River subprovince rocks.

TABLE 3

GARNET-CORDIERITE GEOTHERMOMETRY:
Results using 5 Kbars pressure
from the English River subprovince

Sample	Mg/(Mg+Fe) Garnet	Mg/(Mg+Fe) Cordierite	LnK	Perchuk Lavrent'eva (1983)	Thompson (1976)
CH1283A	0.268	0.690	-1.80	675	733
DS2183B	0.214	0.649	-1.92	642	692
EB1083A	0.183	0.682	-2.26	553	585
LS42	0.254	0.681	-1.83	666	722
LS51A	0.321	0.719	-1.69	712	779
LS78	0.249	0.679	-1.86	659	713
RF2283	0.241	0.694	-1.97	628	675
RF2583A	0.276	0.690	-1.77	687	748
RW1283B	0.327	0.729	-1.71	705	771
VM2183	0.194	0.620	-1.91	642	693
VM2683A	0.245	0.688	-1.92	641	692
VM3583B	0.285	0.683	-1.69	711	778
VM3883B	0.290	0.737	-1.93	639	689
VR13A	0.207	0.641	-1.92	640	690

TABLE 4

Two-Pyroxene Geothermometry:

SAMPLE	$Fe^{+2}/Fe^{+2}+Mg$ Cpx	$Fe^{+2}/Fe^{+2}+Mg$ Opx	Activities Cpx	Activities Opx	Wells temp°C	Wood-Banno temp°C
BL1183A	0.334	0.484	0.037	0.251	864	822
HS1183C	0.264	0.464	0.020	0.271	760	755
RW1683D	0.274	0.454	0.033	0.248	858	823

Two-Feldspar Geothermometry

Rocks from the English River subprovince are deficient in alkali-feldspar making the application of a two-feldspar geothermometer rather difficult. When the Stormer (1975) geothermometer was applied to microcline-plagioclase assemblages, low temperatures around 400-500°C were obtained. The microcline has probably reequilibrated and no longer represents peak metamorphic conditions.

Geobarometry

Garnet-Cordierite Geobarometry

In the last 15 to 20 years, there have been numerous publications concerning P-T calibration of garnet-cordierite reactions. A large amount of controversy and disagreement still exists because it has been discovered that the amount of water contained in cordierite has a considerable influence on its stability.

Three different calibrations of the reaction;

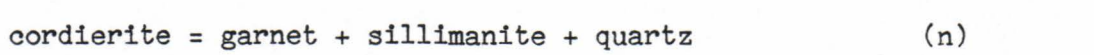

cordierite = garnet + sillimanite + quartz (n)

were applied to English River subprovince rocks. Since the rocks do not contain stable sillimanite, which is on the high pressure side of the reaction, these barometers will be recording maximum possible pressures.

When the Hutcheon et al. (1974) thermo/barometer was applied to English River subprovince rocks, "maximum" values of 500-700°C and 4-6

Kbars were obtained (table 5). The pressures correspond well with experimental phase equilibria and other geobarometers. The temperatures produced, however, are 50 to 200°C less than temperatures determined using biotite-garnet geothermometry.

Newton and Wood (1979) also investigated this assemblage as a potential geobarometer and derived a crude calibration. When applied to rocks from the English River subprovince, pressures came out to approximately 4.5 to 6.0 Kbars, though some inconsistancies were noted (table 6). The pressures determined from the cordierite isopleths were generally 1 Kbar greater than those determined from the garnet isopleths. Theoretically, both sets of isopleths should give the same pressures.

Martignole and Sisi (1981), reinvestigated this assemblage as a thermometer, barometer, and water-fugacity indicator. When their barometer was applied to rocks from the English River subprovince, more consistent results were obtained. Pressures varied from 4.5 to 6 and 6 to 8 Kbars, depending on how much water was assumed to exist in the cordierite (table 7). Three variables determine the pressure a rock will record using Martignole and Sisi's calibration: temperature, amount of water with which the cordierite equilibrated, and the mole fraction of Mg in garnet and cordierite. Assuming that pressure is constant and that the mole fraction Mg in the two phases is dependent only on temperature and water fugacity, the English River subprovince can be modeled as having rather high water pressure in the lower grade parts of the subprovince, with water fugacity decreasing with increasing

TABLE 5

GARNET-CORDIERITE-SILLIMANITE-QUARTZ THERMO-BAROMETER:
(HUTCHEON, FROESE, AND GORDON, 1974)
Results from the English River subprovince

SAMPLE	Bio-Gt Temp	Cord Mg/Mg+Fe	Garnet Mg/Mg+Fe	Hutcheon et al. Temp	Hutcheon et al. Kbars
CH1283A	700	0.690	0.268	618	4.9
DS2183B	675	0.649	0.214	558	4.2
EB1083A	650	0.682	0.183	408	3.5
LS42	730	0.681	0.240	599	4.9
LS51A	780	0.719	0.307	690	5.7
LS78	725	0.679	0.234	586	4.8
RF2283	690	0.694	0.241	530	4.4
RF2583A	720	0.690	0.276	641	5.1
RW1283B	740	0.729	0.327	677	5.5
VM2183	675	0.620	0.194	562	3.9
VM2683A	685	0.689	0.245	554	4.5
VM3583B	750	0.684	0.285	692	5.4
VM3883B	725	0.737	0.290	547	4.7
VR13A	675	0.641	0.207	555	4.2

TABLE 6

GARNET-CORDIERITE-SILLIMANITE-QUARTZ GEOBAROMETER:
(NEWTON AND WOOD, 1979)
Results from the English River subprovince

SAMPLE	Temp	Garnet Mg/Mg+Fe	Cord Mg/Mg+Fe	$P_{H_2O} = P_{total}$ Garnet Kbars	$P_{H_2O} = P_{total}$ Cord Kbars	$P_{H_2O} = 0$ Garnet Kbars	$P_{H_2O} = 0$ Cord Kbars
CH1283A	700	0.268	0.690	4.8	5.8	3.9	4.4
DS2183B	675	0.214	0.649	4.7	5.7	3.8	4.4
EB1083A	650	0.183	0.682	4.5	5.8	3.7	4.4
LS42	730	0.240	0.681	4.8	5.8	3.9	4.5
LS51A	780	0.307	0.719	5.2	5.9	4.3	4.9
LS78	725	0.234	0.679	4.8	5.8	3.8	4.4
RF2283	690	0.241	0.694	4.8	5.8	3.9	4.4
RF2583A	720	0.276	0.690	5.0	5.8	4.0	4.4
RW1283B	740	0.327	0.729	5.2	6.0	4.2	4.9
VM2183	675	0.194	0.620	4.5	5.6	3.5	4.3
VM2683A	685	0.245	0.689	4.8	5.8	3.9	4.4
VM3583B	750	0.285	0.684	4.9	5.8	4.0	4.6
VM3883B	725	0.290	0.737	5.0	6.0	4.0	4.8
VR13A	675	0.207	0.641	4.6	5.7	3.7	4.4

TABLE 7

GARNET-CORDIERITE-SILLIMANITE-QUARTZ GEOBAROMETER:
(MARTIGNOLE AND SISI, 1981)
Results from the English River subprovince

SAMPLE	Temp	Garnet Mg/Mg+Fe	Cord Mg/Mg+Fe	nH_2O = 0.8 Garnet Kbars	nH_2O = 0.8 Cord Kbars	nH_2O = 0.5 Garnet Kbars	nH_2O = 0.5 Cord Kbars	assuming P= 5 Kb nH_2O =	assuming P= 6 Kb nH_2O =
CH1283A	700	0.268	0.690	7.3	7.1	5.3	5.1	0.47	0.62
DS2183B	675	0.214	0.649	6.7	6.3	4.6	4.7	0.56	0.78
EB1083A	650	0.183	0.682	6.2	6.5	4.4	4.6	0.58	0.74
LS42	730	0.240	0.681	7.5	7.8	5.5	5.5	0.43	0.57
LS51A	780	0.307	0.719	8.6	8.8	6.2	6.3	0.36	0.48
LS78	725	0.234	0.679	7.5	7.7	5.1	5.2	0.48	0.60
RF2283	690	0.241	0.694	7.2	7.1	5.1	5.0	0.50	0.64
RF2583A	720	0.276	0.690	7.7	7.6	5.5	5.3	0.45	0.58
RW1283B	740	0.327	0.729	8.5	8.3	6.0	5.9	0.38	0.51
VM2183	675	0.194	0.620	6.4	6.2	4.4	4.5	0.58	0.75
VM2683A	685	0.245	0.689	7.1	6.8	5.0	4.9	0.50	0.66
VM3583B	750	0.285	0.684	8.1	8.0	5.6	5.5	0.44	0.55
VM3883B	725	0.290	0.737	7.8	8.3	5.5	5.8	0.41	0.54
VR13A	675	0.207	0.641	6.8	7.0	4.7	4.9	0.53	0.67

nH_2O = moles of water in cordierite

Figure 12. Moles of H_2O in cordierite using the Martignole and Sisi (1981) barometer-thermometer and water-fugacity indicator.

KEY

59/ nH_2O/100 nCordierite assuming a constant pressure of 5 Kbars

/66 nH_2O/100 nCordierite assuming a constant pressure of 6 Kbars

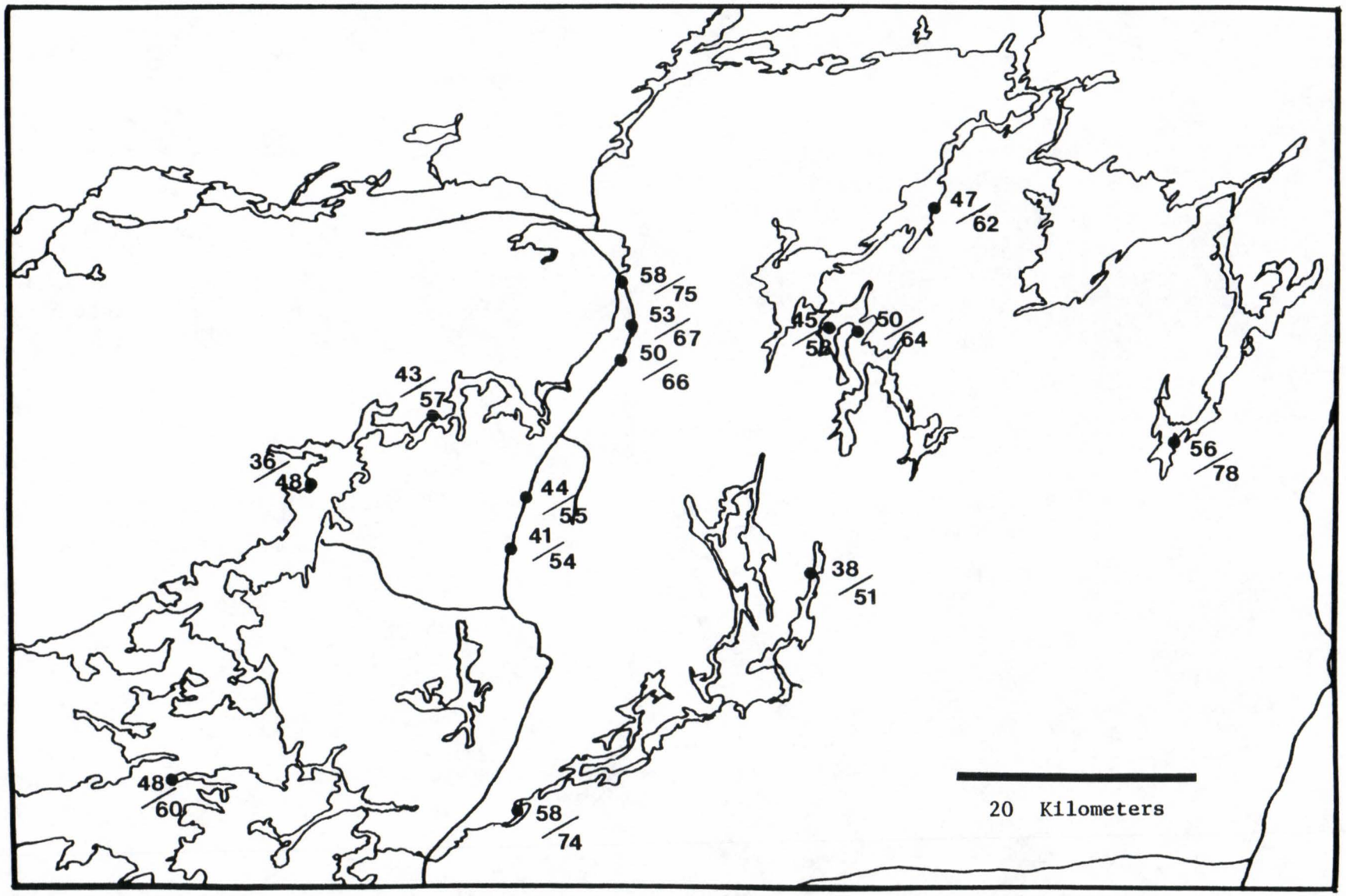
58
75
53
67
50
66
43
57
36
48
44
55
41
54
48
60
58
74
47
62
45
52
50
64
56
78
38
51
20 Kilometers

metamorphic grade (figure 12). Presumably, water was incorporated in the increased volume of melt. The Perkins and Chipera (1984) water fugacity indicator shows a similar trend.

Garnet-Plagioclase-Sillimanite-Quartz-Geobarometry

It has long been known that the assemblage garnet-plagioclase-sillimanite-quartz could be used to determine metamorphic pressures (Kretz, 1959). Ghent (1976) was the first person to present a usable geobarometer based on the reaction:

3 anorthite = grossular + 2 sillimanite + quartz (o)

Since then, there have been others who provide their own versions (Newton and Haselton, 1981; Perchuk et al., 1981; my own calibration presented in this thesis).

The English River subprovince provided few samples with the complete assemblage due to the low abundance of stable sillimanite; sillimanite is consumed with biotite and quartz to form garnet, cordierite, and melt. Since sillimanite is on the high pressure side of the reaction, the maximum possible pressures of equilibration are recorded. As a first approximation, however, one can assume that the rocks containing abundant garnet and cordierite are saturated with aluminum and are thus recording "actual" pressures.

Application of the Ghent (1976) barometer to the English River subprovince rocks yielded pressures of 5-6 Kbars for the samples that contain abundant cordierite and garnet (assumed to be aluminum

saturated), and 6-8 Kbars for the wacke rocks without cordierite (table 8). The highest pressures were associated with orthopyroxene bearing rocks, supporting an earlier hypothesis that orthopyroxene exists only in the less aluminous wacke, orthogneiss, and amphibolite rocks. Ghent uses a value of 1.276 (Orville, 1972) for the activity coefficient of anorthite. If the Newton (1983) activity model is used instead, pressures are reduced by a maximum of only 0.5 Kbars. Ghent also uses a value of W_{Al-Gr} = 1000 from Ganguly and Kennedy (1974), but suggests however, that a value of 750 may give better results. Decreasing W_{Al-Gr} to 750 reduced pressures 10%.

The Newton and Haselton (1981) barometer was applied using the partial molar volume expression from Newton (1983):

$$V\ (bar) = -58.7 + 45.5\ X_{gr}\quad (cm^3)$$

"Maximum" pressures ranging from 4 to 5 Kbars for the aluminous cordierite bearing rocks, and 6.0 to 7.5 Kbars for the less aluminous orthopyroxene bearing rocks (table 8). From Ganguly and Saxena (1984):

> "R. C. Newton (private comm.) has pointed out that the expression of P^o(Sill) given in Newton and Haselton (1981) is erroneous. The correct expression, derived by Edgar Froese, is P^o(Sill) = -1.17 + 0.0238 T(^{o}C), which yields P^o(Sill) in kbar."

This revised expression reduced the pressures obtained from the Newton-Haselton (1981) barometer by approximately 0.4 Kbars.

Perchuk et al. (1981) calibrate the assemblage garnet-sillimanite-quartz-plagioclase using the pressure formula from Aranovich and

TABLE 8

GARNET-PLAGIOCLASE-SILLIMANITE-QUARTZ GEOBAROMETRY:
ENGLISH RIVER SUBPROVINCE

SAMPLE	Temp	X_{an}	X_{gr}	Associated Key Mineral	lnK	Ghent (1976)	Newton Haselton (1981)	Perchuk et al (1981)	This Thesis
BL1083E	702	0.391	0.071	Opx	-6.6	8.9	7.2	7.8	7.5
CH1283A	700	0.240	0.023	Cord	-8.0	6.3	4.8	4.5	5.3
CL2283A	738	0.335	0.044	Opx	-7.3	8.1	6.5	6.9	6.8
DS2183B	675	0.222	0.023	Cord	-8.4	6.3	4.5	4.0	4.6
EB1083A	650	0.249	0.027	Cord	-8.6	6.1	4.2	3.7	4.1
HS1583C	677	0.471	0.092	Opx	-6.1	8.7	7.4	8.3	7.9
ID1683A	750	0.282	0.029	Opx	-7.3	7.1	5.9	6.2	6.8
JS2583	625	0.310	0.071	Sill	-6.7	8.6	6.4	6.5	6.5
LS42	732	0.242	0.023	Cord	-8.9	8.0	6.8	6.0	4.9
LS51A	780	0.262	0.022	Cord	-9.2	6.7	5.6	5.5	4.1
LS78	724	0.247	0.023	Cord	-9.5	6.4	4.9	4.5	3.3
RF2283	691	0.250	0.024	Cord	-8.4	6.1	4.5	4.2	4.7
RF2583A	719	0.248	0.022	Cord	-8.2	6.2	4.8	4.5	5.2
RW1283B	739	0.280	0.028	Opx	-7.4	7.0	5.7	6.0	6.7
VM1683	675	0.211	0.020	Cord	-9.0	5.9	4.0	3.2	3.7
VM2183	676	0.255	0.025	Cord	-8.9	6.0	4.0	3.8	3.9
VM2683A	683	0.258	0.025	Cord	-8.4	6.0	4.4	4.2	4.7
VM3583B	747	0.268	0.023	Cord	-8.3	6.3	4.9	4.8	5.4
VM3883B	728	0.334	0.030	Cord	-8.1	6.2	4.8	5.4	5.4
VR13A	672	0.247	0.023	Cord	-8.8	5.8	4.0	3.6	4.0

X_{an} = Ca/(Ca+Na+K) in Plag X_{gr} = Ca/(Ca+Fe+Mg+Mn) in Gt

$$\ln K = \ln((a_{gr})^3 / (a_{an})^3)$$

Podlesskii (1980). Applying their barometer to rocks from the English River subprovince produced "maximum" pressures between 3.5 to 5 Kbars for the aluminous cordierite bearing rocks, and 6 to 8 Kbars for the less aluminous orthopyroxene bearing rocks (table 8).

Recalibration of the

Garnet-Plagioclase-Sillimanite-Quartz Geobarometer

Though several good calibrations of the barometric assemblage garnet-plagioclase-sillimanite-quartz do exist, a recent activity model for garnet (Ganguly and Saxena, 1984) makes yet another calibration beneficial. Incorporating updated activity models in barometry-thermometry assembleges (old and new) tend to produce more accurate, consistent, and precise geothermometers-barometers.

Following the example of Newton and Haselton (1981), the experimental results of Goldsmith's (1980) end-member reaction;

3 anorthite = grossular + 2 kyanite + quartz (p)

were used. ΔG^{o}_{298} for reaction (p) was determined by taking a starting point on the reaction curve, (1245°C, and 26.45 Kbars), and applying equation (1):

$$0 = \Delta G_{rxn} = \Delta G^{o}_{298} + \int \Delta V dP - \int \Delta S dT \qquad (1)$$

Since sillimanite is present in rocks from the English River subprovince rather than kyanite, ΔG^{o}_{298} was calculated for the reaction

2 kyanite = 2 sillimanite (q)

in the same manner as reaction (p). A starting point of 501°C and 3.76 Kbars (the Holdaway (1971) aluminosilicate triple point) was used. By adding reaction (p) to reaction (q), the desired reaction (r) was obtained. Likewise, adding the ΔG's for reactions (p) and (q) together gave ΔG for reaction (r).

3 anorthite = grossular + 2 kyanite + quartz	9.84 KJ	(p)
2 kyanite = 2 sillimanite	6.66 KJ	(q)
3 Anorthite = Grossular + 2 Sillimanite + Quartz	16.50 KJ	(r)

Once ΔG^{o}_{298} had been calculated for reaction (r), the equation;

$$-RT\ln K = \Delta G^{o}_{298} + \int \Delta V dP - \int \Delta S dT \qquad (2)$$

was used to calculate lnK values in P-T space (figure 13). It can be seen that this barometer is relatively insensitive to temperature, with a slope of only 0.5-1.0 Kbars per 100°C.

High-temperature entropies were calculated by integrating C_p/T; heat capacity functions were stored as four term polynomials (cf. Holland, 1981). All relevant thermodynadic data can be found in table 9. Applying the best estimates for expansitivity and compressibility to the phases changed the calculated pressures by only 0.2 Kbars, so this term can be safely ignored.

The following activity models are used for application in this geobarometer. Newton's (1983) activity model for anorthite is preferred because, as pointed out by Haselton et al. (1983), it seems most consistent with other experimental and thermodynamic studies. The Ganguly and Saxena (1984) activity model for garnet is used because it

TABLE 9

Thermochemical Data:[a]

PHASE	FORMULA	S^o_{298}	V^o_{298}	a	b	c	d
ave-quartz	SiO_2	41.46	22.69	68.96861	4.70220	-0.33590	-22.00661
sillimanite	Al_2SiO_5	96.11	49.90	164.47147	33.57507	-0.00969	-46.06938
grossular	$Ca_3Al_2Si_3O_{12}$	269.12[b]	125.23[c]	545.02594	23.82557	-20.00407	-92.07404
anorthite	$CaAl_2Si_2O_8$	203.30	100.93[c]	277.50546	54.89608	-2.05850	-63.16164

$$C_p = a + bT\,10^{-3} + cT^{-\frac{1}{2}}\,10^2 + dT^{-2}\,10^5$$

a. All entropies and volumes are taken from Robie et al. (1978) unless otherwise specified. Units are J, cc, Kelvin.

b. Haselton and Westrum (1980)

c. Newton and Perkins (1982)

d. Holland (1981)

incorporates the latest thermochemical and mixing parameter data and takes into account the spessartine component in the garnet activity.

To use this geobarometer, first it is necessary to calculate the activities for anorthite and grossular, then calculate lnK:

$$\ln K = \ln \frac{(a_{gr})^3}{(a_{an})^3} \qquad (3)$$

Pressure is either read from figure 13, or calculated using the equation:

$$P = 2.65481 + 0.02067*T + 0.41699*\ln K + 0.00150*T*\ln K \qquad (4)$$

Pressure is in Kbars, temperature is in centigrade.

Equation (4) was derived from a third rank least squares analysis and will reproduce the lnK figure to within +/- 0.01 Kbar.

When this barometer was applied to rocks from the English River subprovince, it gave maximum pressures (lack of sillimanite) of around 3.7 to 5.0 Kbars for the cordierite bearing samples assumed to be saturated in aluminum, and 6.5 to 8.0 Kbars for the less aluminous orthopyroxene bearing assemblages (table 8).

In order to test and compare this calibration, a data base comprised of terrains throughout the world was drawn from the literature. A comparison of the pressures obtained using the four barometers: Ghent (1976), Newton and Haselton (1981), Perchuk et al. (1981), and the one proposed here, are given in tables 10 and 11. The temperature estimates of the individual authors were used in all calculations.

Figure 13. lnK plotted in pressure-temperature space for the reaction:

3 Anorthite = Grossular + 2 Sillimanite + Quartz

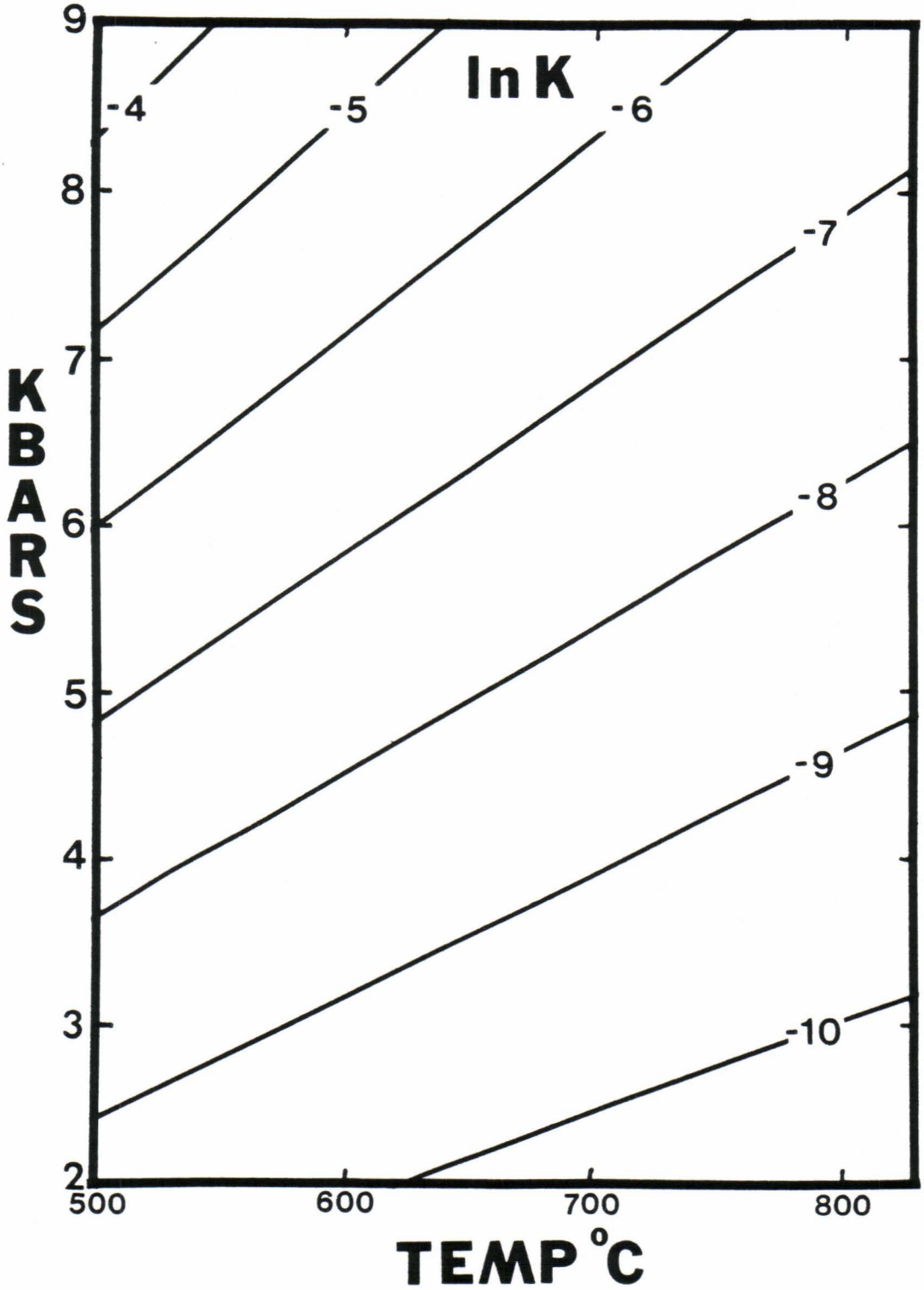
ln K
-4
-5
-6
-7
-8
-9
-10
KBARS
9
8
7
6
5
4
3
2
500
600
700
800
TEMP °C

TABLE 10

GARNET-PLAGIOCLASE-SILLIMANITE-QUARTZ GEOBAROMETRY
APPLIED TO TERRAINS THROUGHOUT THE WORLD:

SAMPLE	Temp	X_{an}	X_{gr}	X_{al}	X_{py}	lnK	Ghent (1976)	Newton Haselton et al (1981)	Perchuk (1981)	This Thesis
IVREA ZONE, ITALY Schmid and Wood (1976)										
SD 121	700	0.488	0.064	0.657	0.268	-6.6	7.4	6.4	7.6	7.4
TC 14	700	0.583	0.057	0.634	0.228	-7.5	6.2	5.3	6.5	6.1
SD 369F	700	0.436	0.056	0.676	0.245	-7.1	7.4	6.0	7.1	6.7
SD 798C	700	0.346	0.034	0.555	0.404	-6.6	6.3	5.3	6.7	7.4
SD 430E	700	0.402	0.043	0.611	0.333	-7.0	6.6	5.5	6.8	6.9
SD 1035	700	0.365	0.038	0.679	0.262	-7.8	6.5	5.0	5.8	5.7
OTTER LAKE, QUEBEC Perkins et al. (1982)										
C51	700	0.229	0.033	0.794	0.153	-7.7	8.0	6.2	5.3	5.8
DL 101	700	0.231	0.033	0.753	0.187	-7.4	8.0	6.3	5.6	6.2
Q 140	700	0.056	0.017	0.790	0.175	-4.2	11.4	11.1	7.2	10.9
DALY BAY, NORTHWEST TERRITORIES Hutcheon et al. (1974) plagioclase analysis from Newton and Haselton (1981)										
1	610	0.330	0.025	0.606	0.360	-7.8	4.1	2.8	4.0	4.8
2	650	0.308	0.036	0.659	0.291	-7.2	6.3	4.8	5.5	6.1
4	680	0.343	0.033	0.579	0.377	-7.0	5.9	4.8	6.1	6.7
HARA LAKE, SASKATCHEWAN Kays and Medaris (1976)										
K 359	700	0.180	0.028	0.792	0.171	-7.2	8.4	6.9	5.3	6.6
K 93	700	0.180	0.029	0.722	0.237	-6.4	8.5	7.3	6.1	7.8
K 376	700	0.300	0.031	0.759	0.186	-8.6	6.5	4.7	4.6	4.5
K 291	700	0.380	0.028	0.775	0.185	-9.6	5.0	3.2	3.6	3.0
ENDERBY LAND, ANTARCTICA Grew (1980)										
2045 C	900	0.364	0.026	0.511	0.454	-7.3	7.3	6.7	8.0	8.4
2083 C	900	0.546	0.035	0.444	0.512	-7.0	6.7	6.7	9.0	8.8
2083 E	900	0.513	0.038	0.462	0.491	-6.8	7.4	7.3	9.4	9.2

TABLE 10 CONTINUED

SAMPLE	Temp	X_{an}	X_{gr}	X_{al}	X_{py}	lnK	Ghent (1976)	Newton Haselton et al (1981)	Perchuk et al (1981)	This Thesis
					SOUTH CENTRAL MAINE Ferry (1980)					
388A	550	0.155	0.022	0.687	0.088	-8.6	5.6	3.5	2.4	3.4
663A	550	0.465	0.065	0.679	0.117	-8.0	5.5	3.5	4.7	4.1
666A	550	0.347	0.053	0.668	0.098	-8.3	5.8	3.3	4.3	3.7
674A	550	0.424	0.051	0.643	0.134	-8.6	4.9	2.8	4.1	3.4
675-4	550	0.242	0.031	0.649	0.110	-8.9	5.2	2.7	2.9	3.0
675-5	550	0.223	0.032	0.604	0.123	-8.3	5.7	3.3	3.4	3.7
905A	550	0.343	0.057	0.666	0.109	-7.9	6.1	3.7	4.6	4.2
925A	550	0.246	0.030	0.670	0.091	-9.2	5.1	2.5	2.7	2.6
969B	550	0.156	0.019	0.785	0.086	-9.2	5.1	3.0	1.6	2.5
1104-1	550	0.093	0.019	0.811	0.094	-7.2	7.1	5.5	2.9	5.1
					MT. MOOSILAUKE, NEW HAMPSHIRE Hodges and Spear (1982)					
78B	500	0.116	0.026	0.769	0.093	-7.2	6.6	4.6	2.8	4.6
80D	500	0.278	0.055	0.764	0.091	-7.9	6.0	3.3	3.7	3.8
90A	500	0.139	0.030	0.732	0.099	-7.3	6.4	4.2	3.0	4.5
92D	500	0.107	0.021	0.772	0.096	-7.5	6.1	4.2	2.3	4.2
145E	500	0.089	0.016	0.778	0.081	-7.9	5.8	4.0	1.7	3.8
146B	500	0.238	0.038	0.682	0.119	-8.3	5.3	2.7	3.0	3.3
146D	500	0.241	0.039	0.691	0.099	-8.5	5.3	2.7	3.0	3.1
					INARIJARVI COMPLEX, FINLAND Hormann et al. (1980) and Achermand (cited in Newton, 1983)					
119	750	0.470	0.028	0.592	0.374	-8.3	4.6	3.9	5.4	5.4
194	750	0.357	0.032	0.632	0.323	-7.6	6.5	5.3	6.2	6.4
160	750	0.334	0.029	0.603	0.358	-7.4	6.4	5.3	6.2	6.7
169	750	0.272	0.029	0.490	0.480	-5.7	7.4	6.8	7.9	9.4
161	750	0.281	0.024	0.649	0.319	-7.8	6.4	5.2	5.4	6.1
158	750	0.296	0.030	0.701	0.263	-7.8	7.1	5.7	5.8	6.1
89V	750	0.400	0.032	0.531	0.427	-7.0	6.0	5.2	6.9	7.3
93	750	0.392	0.037	0.642	0.298	-7.7	6.8	5.5	6.5	6.3
24	750	0.256	0.026	0.730	0.217	-8.2	7.2	5.6	5.1	5.6
177	750	0.517	0.036	0.576	0.374	-7.7	5.3	4.8	6.4	6.3
110	750	0.491	0.028	0.540	0.426	-7.9	4.4	4.0	5.8	5.9

TABLE 10 CONTINUED

SAMPLE	Temp	X_{an}	X_{gr}	X_{al}	X_{py}	lnK	Ghent (1976)	Newton Haselton et al (1981)	Perchuk et al (1981)	This Thesis
				BANGALORE REGION, INDIA Harris and Jayaram (1982)						
114	700	0.197	0.021	0.675	0.293	-7.2	6.8	5.7	5.0	6.6
110	700	0.294	0.037	0.747	0.196	-7.8	7.4	5.6	5.6	5.6
112	700	0.264	0.030	0.663	0.286	-7.3	6.9	5.5	5.6	6.4
104	700	0.277	0.025	0.639	0.324	-7.6	5.9	4.7	5.1	5.9
107	700	0.443	0.052	0.665	0.260	-7.2	7.0	5.7	6.8	6.5
				WEST CENTRAL MASSACHUSETTS Tracy et al. (1976)						
Q67X	550	0.230	0.058	0.778	0.131	-6.4	7.7	5.5	5.2	6.0
892U	550	0.270	0.039	0.669	0.116	-8.5	5.7	3.2	3.6	3.5
871	650	0.330	0.038	0.704	0.142	-8.6	6.3	4.1	4.6	4.0
869	650	0.310	0.046	0.687	0.130	-7.9	7.3	5.1	5.5	5.1
L11Y	650	0.400	0.054	0.643	0.175	-7.7	6.9	5.0	6.0	5.4
933A	650	0.230	0.030	0.732	0.171	-8.0	6.8	4.9	4.5	5.0
933B	650	0.280	0.043	0.724	0.186	-7.3	7.5	5.6	5.6	5.9
595C	650	0.320	0.051	0.592	0.179	-7.2	7.6	5.6	6.3	6.1
507B	650	0.160	0.036	0.765	0.162	-6.6	9.1	7.6	6.0	6.8
T10B	650	0.210	0.029	0.706	0.171	-7.7	7.1	5.3	4.6	5.3
T12A	675	0.280	0.035	0.756	0.176	-8.1	7.0	5.1	5.0	5.0
067D	675	0.230	0.026	0.756	0.166	-8.4	6.6	4.8	4.1	4.5
FW283	675	0.190	0.026	0.697	0.259	-6.8	7.4	6.2	5.3	6.9
FW122	675	0.270	0.034	0.696	0.242	-7.4	7.0	5.4	5.5	6.0
				SCOTTISH CALEDONIDES Ashworth and Chinner (1978)						
187C	750	0.390	0.039	0.725	0.222	-8.2	7.0	5.5	6.0	5.6
189C	750	0.350	0.039	0.722	0.223	-7.8	7.6	6.0	6.3	6.1
105570	700	0.540	0.054	0.649	0.254	-7.5	6.2	5.3	6.6	6.1
105568	700	0.270	0.021	0.762	0.176	-9.5	5.3	3.5	3.1	3.2
105716	700	0.280	0.029	0.731	0.185	-8.5	6.5	4.7	4.6	4.7
193C	700	0.290	0.028	0.748	0.116	-9.3	6.3	4.2	4.0	3.4
196C	700	0.250	0.029	0.750	0.118	-8.7	7.1	5.1	4.4	4.4

X_{gr} = Ca/(Ca+Fe+Mg+Mn) in Gt X_{al} = Fe/(Ca+Fe+Mg+Mn) in Gt

X_{py} = Mg/(Ca+Fe+Mg+Mn) in Gt X_{an} = Ca/(Ca+Na+K) in Plag

$$\ln K = \ln((a_{gr})^3 / (a_{an})^3)$$

TABLE 11

BAROMETRIC RESULTS
FOR VARIOUS TERRAINS THROUGHOUT THE WORLD
(in Kbars)

TERRAIN	Ghent (1976)	Newton Haselton (1981)	Perchuk et al (1981)	this thesis	original estimates
Ivrea Zone, Italy	6.7	5.6	6.8	6.7	8.7 - 9.2
Otter Lake, Quebec	9.1	7.9	6.0	7.6	5.3 - 6.6
Daly Bay, NWT	5.4	4.1	5.2	5.9	5.3 - 6.6
Hara Lake Saskatchewan	7.1	5.5	4.9	5.5	3.2 - 4.4
Enderby Land Antarctica	7.1	6.9	8.8	8.8	6-7 (9 max)
South-Central Maine	5.6	3.4	3.4	3.6	3.5 - 4.0
Mt. Moosilauke New Hampshire	5.9	3.7	2.8	3.9	3.5
Inarajarvi Finland	6.2	5.2	6.1	6.5	5.0 - 7.0
Bangalore Region India	6.8	5.4	5.6	6.2	4.5 - 5.0
West-Central Massachusetts	7.1	5.2	5.1	5.4	5.0 - 7.0
Caledonides Scotland	6.6	4.9	5.0	4.8	5.0 - 6.0

Though the four calibrations vary among the terrains as to which one produces the lowest, highest, and the largest range of values (table 10), the Ghent (1976) calibration generally gave the highest results, Newton and Haselton (1981) followed by the Perchuk et al. (1981) calibrations produced the lowest, and the calibration proposed here falls somewhere in between (table 11). Many of the terrains yield pressures consistent to +/- 1 Kbar, however, just as many show a range of +/- 2 Kbars, suggesting that when applying this assemblage as a barometer, enough samples are needed as to obtain a statistical average. The present calibration produces results close to the independent estimates of the various authors and agrees well with the New Hampshire rocks which are constrained by the Holdaway (1971) triple point, and for the Maine rocks which have both andalusite and sillimanite. The pressures obtained for Antarctica, Finland, and Scotland, where there are independent determinations from garnet-orthopyroxene-plagioclase-quartz geobarometry (Newton and Perkins, 1982; Bohlen et al., 1983; Perkins and Chipera, 1985), are in considerably better agreement than the other calibrations.

Garnet-Orthopyroxene Geobarometery

Five thin-sectioned samples were found to contain coexisting garnet-orthopyroxene fresh enough for application in the various garnet-orthopyroxene geobarometers. These five samples are scattered in the region of hornblende-granulite facies rocks located in Carling Lake, Bury Lake, Highstone Lake, Ragged Wood Lake, and on Idaho Lake road. In addition, R. M. Baumann provided sample MB8A from the McKenzie Bay

logging road east of Ear Falls, Ontario, and K. R. Henke provided sample G1A from the Cliff Lake granulite zone just off highway 105, and G63B from Wegg Lake in the Umfreville-Conifer Lake granulite zone, Ontario (figure 14).

Perkins and Newton (1981), Newton and Perkins (1982) calibrated the Mg end-member and Bohlen et al., (1983), calibrated the Fe end-member of the reaction:

plagioclase + orthopyroxene = garnet + quartz (s)

Subsequently, Chipera et al. (1984b) and Perkins and Chipera (1985) have recalibrated both the Fe and Mg end-members of the above reaction. The results for the English River subprovince using the various calibrations are listed in table 12. Figure 15 compares the pressures attained in the English River subprovince to those from other granulite terrains.

Harley and Green (1982) calibrated a garnet-orthopyroxene geobarometer based on aluminum solubility and exchange between coexisting garnet and orthopyroxene buffered by the reaction:

enstatite + Mg-Ts = pyrope (t)

This barometer is based on the preferential coordination of aluminum with temperature and pressure. Aluminum prefers octahedral coordination with increasing pressure, but tetrahedral coordination with increasing temperature (Boyd and England, 1964). Application of this barometer to English River subprovince rocks, produced pressures between 3 and 8 Kbars (table 13). The problem with this geobarometer is that it has a

Figure 14. Location of samples used for garnet-orthopyroxene geobarometry.

KEY

◆ BL1083B
○ CL2283A
● G1A
△ G63B
▲ HS1583C
◇ ID1683A
□ MB8A
■ RW1283B

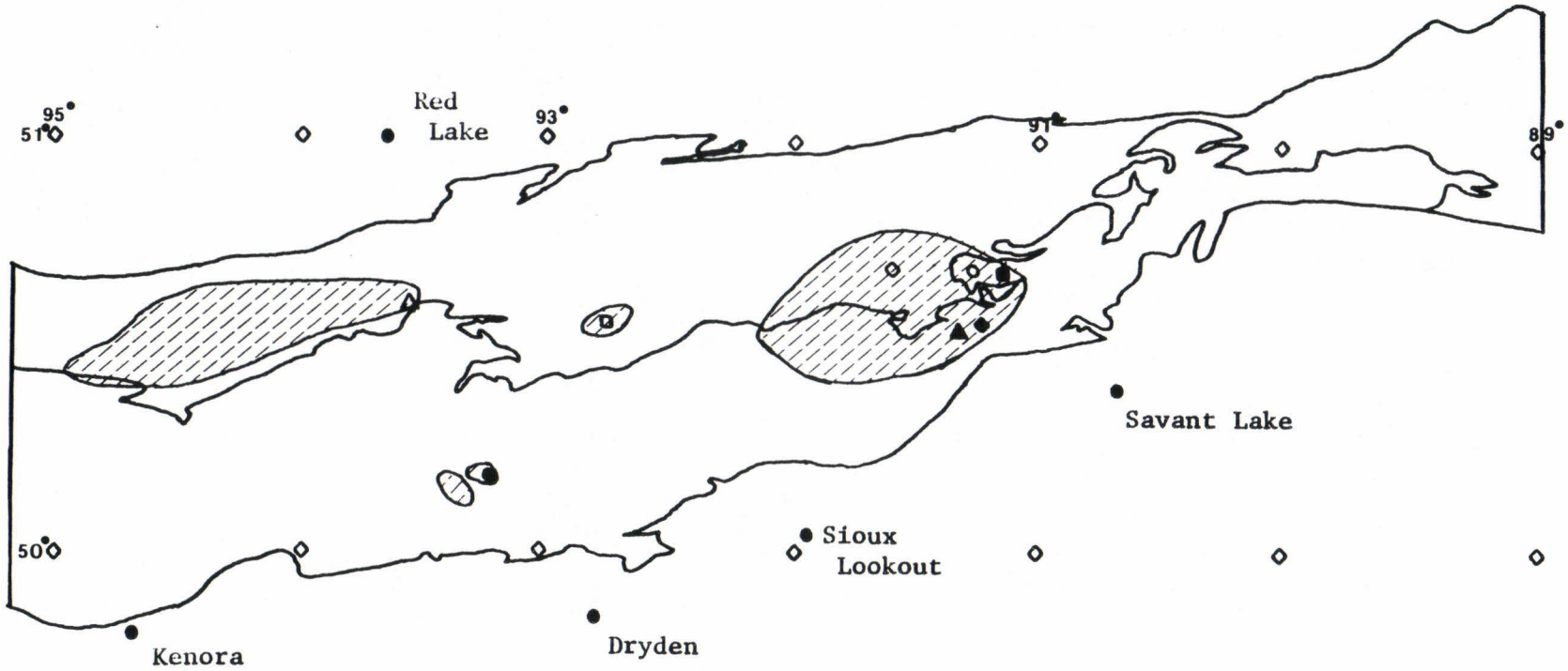
95
51
Red
Lake
93
91
89
Savant Lake
50
Sioux
Lookout
Kenora
Dryden

TABLE 12

GARNET-PLAGIOCLASE-ORTHOPYROXENE-QUARTZ GEOBAROMETRY:
Results from the English River subprovince

SAMPLE	X_{an}	X_{gr}	X_{py}	X_{al}	a_{en}	a_{fs}	Newton Perkins (1982)	Bohlen et al (1983)	Perkins Chipera (1985) MgRxn	Perkins Chipera (1985) FeRxn
BL1083E	0.391	0.075	0.176	0.749	0.231	0.211	3.8	6.4	4.7	5.4
CL2283A	0.335	0.046	0.240	0.714	0.258	0.162	4.5	6.5	4.0	5.2
HS1583C	0.471	0.100	0.182	0.719	0.271	0.170	4.1	6.8	5.0	6.4
ID1683B	0.282	0.030	0.322	0.649	0.297	0.140	5.5	6.3	3.8	5.1
RW1283B	0.281	0.029	0.317	0.653	0.285	0.138	5.5	6.6	3.9	5.2
G1A	0.359	0.089	0.200	0.720	0.204	0.222	6.1	6.9	6.0	5.3
G63B	0.565	0.054	0.271	0.658	0.324	0.127	3.9	5.5	4.4	6.0
MB8A	0.297	0.065	0.280	0.673	0.255	0.200	7.4	7.0	5.3	4.9

X_{gr} = Ca/(Ca+Fe+Mg+Mn) in Gt
X_{py} = Mg/(Ca+Fe+Mg+Mn) in Gt
X_{al} = Fe/(Ca+Fe+Mg+Mn) in Gt
X_{an} = Ca/(Ca+Na+K) in Plag

$a_{en} = M1_{Mg} * M2_{Mg}$ in Opx

$a_{fs} = M1_{Fe} * M2_{Fe}$ in Opx

Figure 15. Comparison of the pressures obtained for the English River Subprovince to other granulite terrains.

The plot compares the Fe-reaction pressures against the Mg-reaction pressures using the Perkins and Chipera (1985) geobarometers.

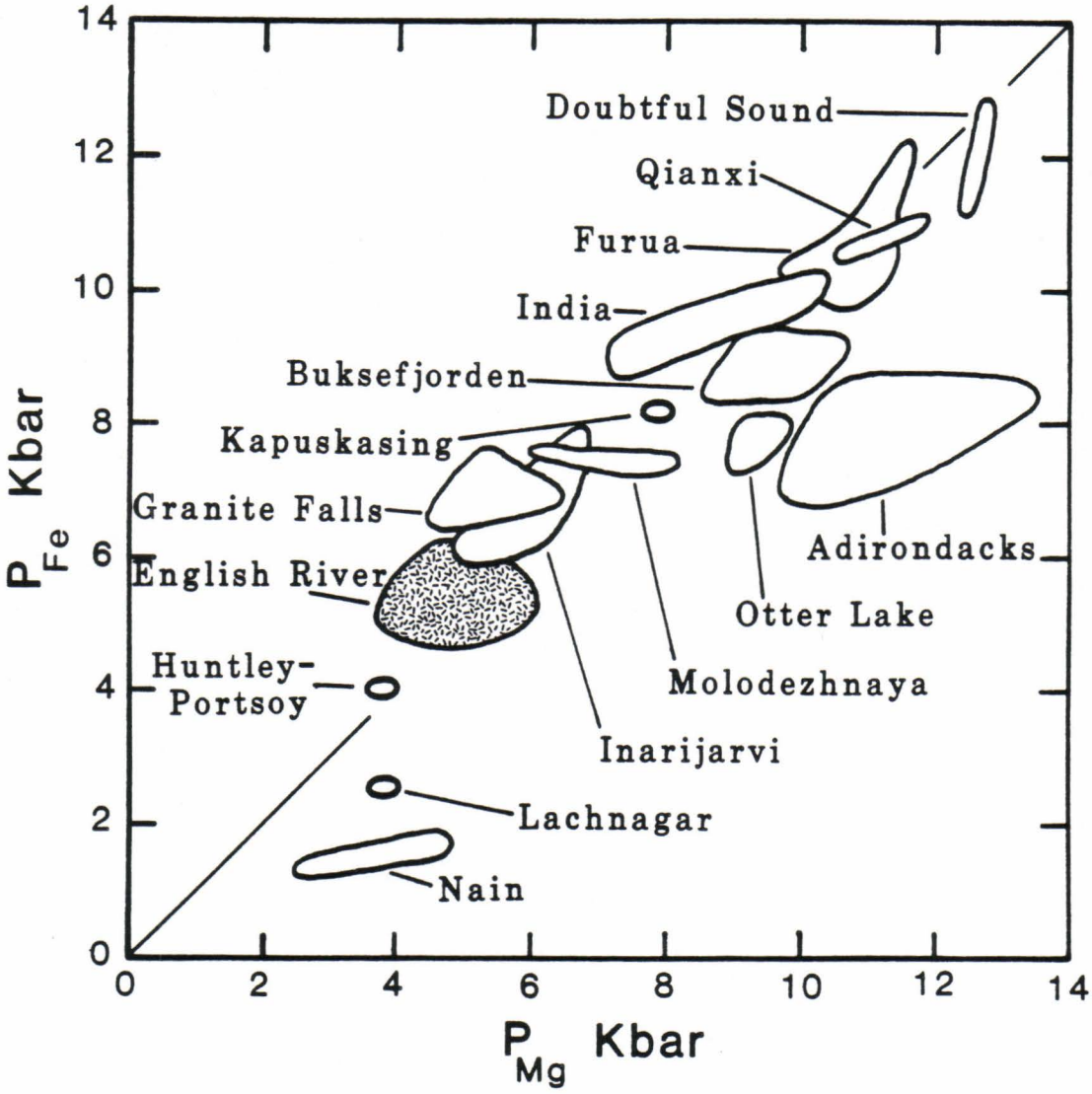
Doubtful Sound
Qianxi
Furua
India
Buksefjorden
Kapuskasing
Granite Falls
English River
Huntley-
Portsoy
Adirondacks
Otter Lake
Molodezhnaya
Inarijarvi
Lachnagar
Nain
P_{Fe} Kbar
P_{Mg} Kbar
0
2
4
6
8
10
12
14

TABLE 13

GARNET-OPX ALUMINUM EXCHANGE BAROMETER:
(HARLEY AND GREEN, 1982)
Results from the English River subprovince

SAMPLE	Garnet X_{gr}	Garnet X_{al}	Opx X_{fs}	Opx X_{Al}	Kbars at 600°C	Kbars at 700°C	Kbars at 800°C	Temp°C at 5 Kbars
BL1083E	0.071	0.713	0.489	0.031	3.4	8.4	13.4	635
CL2283A	0.044	0.684	0.469	0.084	-2.6	1.3	5.3	795
HS1583C	0.092	0.667	0.442	0.035	3.5	8.2	13.1	635
ID1683A	0.029	0.628	0.440	0.082	-1.9	2.1	6.1	775
RW1283B	0.028	0.636	0.445	0.095	-2.8	1.1	4.9	805
G1A	0.089	0.720	0.532	0.040	0.5	5.2	9.8	695
G63B	0.054	0.658	0.385	0.049	2.5	7.0	11.6	655
MB8A	0.065	0.673	0.486	0.031	3.5	8.5	13.5	635

X_{gr} = Ca/(Ca+Fe+Mg+Mn) in Gt
X_{al} = Fe/(Ce+Fe+Mg+Mn) in Gt
X_{fs} = Fe/(Fe+Mg) in Opx
X_{Al} = total Al/2 in Opx

large temperature dependance (+/- 50°C = +/- 2.5 Kbars). The limit on the accuracy of most K_D thermometers is around +/- 50°C. However, if pressure is known within +/-1 Kbar, the barometer could be run backwards to calculate temperature within 20°C, making the Harley and Green (1982) geobarometer a far better geothermometer than it does a barometer. To test this assumption, pressure verses temperature was plotted for the eight samples. Using a pressure of 5 Kbars, the samples gave temperatures which were closer to +/- 100°C than to +/- 20°C (table 13).

GEOPHYSICAL WORK CONDUCTED IN THE ENGLISH RIVER SUBPROVINCE

The University of Manitoba, in their Precambrian research program, conducted several regional seismic surveys across the English River subprovince. Hall and Hajnal (1969) interpret the seismological data as indicative of a two layer crust composed of a thickened upper crust and a thinner lower crust with an overall thinned total crust in the region of the English River subprovince and the bordering section of the Uchi subprovince (figure 16). This peculiar crustal structure beneath the English River subprovince has been related to a major early Precambrian sedimentary basin developed in a tectonic regime that produced sedimentation in conjunction with subsidence of the total crust and concomitant removal of material from the base of the lower crust (Beakhouse, 1977). Hall and Brisbin (1982) reinterpret the seismological data as indicative of a three layer crust with an upper, lower, and a seismically distinct mid-crustal layer. The seismic velocities in this middle layer suggest that it is either composed of intermediate to basic igneous rocks, or metamorphic rocks of the amphibolite facies.

Smithson and Brown (1977) and Smithson (1978) interpreting seismic reflection data from various terrains (eg. Wind River Mountains, Wyoming; Hardeman County, Texas; and the Ivrea zone in the southern Alps) state that conventional crustal models based on 2 to 4 continuous horizontal layers must be abandoned. They find instead, extensive lateral and vertical heterogeneity of the deep crust which is comparable to that indicated by surface geological field observations.

Figure 16. Seismically determined crustal struture under the English River subprovince and the bordering Uchi subprovince.

(Taken from Hall and Hajnal, 1969)

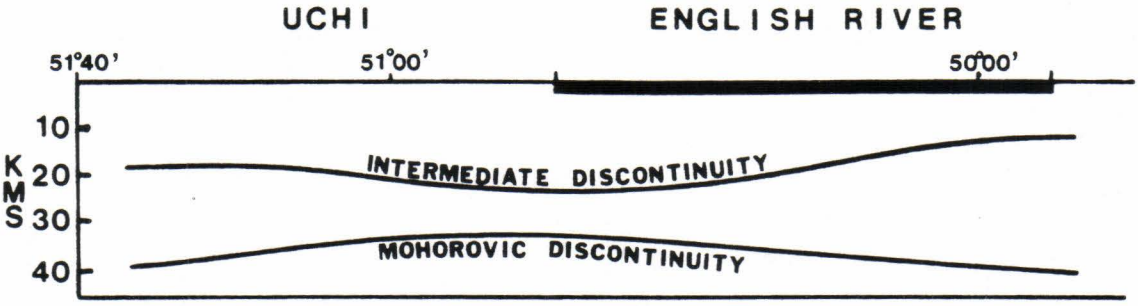
UCHI
ENGLISH RIVER
51°40'
51°00'
50°00'
10
20
30
40
KMS
INTERMEDIATE DISCONTINUITY
MOHOROVIC DISCONTINUITY

Gravity surveys were conducted over northwestern Ontario and adjoining Manitoba by the Gravity and Geodynamics Division, Earth Physics Branch of the Department of Energy, Mines and Resources, Canada. Significant positive bouguer gravity anomalies occur over the English River subprovince (figure 17). According to Beakhouse (1977), the effect of the relatively thick upper crust in the northern domain should produce a negative gravity anomaly, but this effect is apparently overwhelmed by the relatively thin total crust producing a positive gravity anomaly. Beakhouse also states that it is not yet clear why the high positive gravity anomaly does not include portions of the Uchi subprovince and that there is no satisfactory model to relate observed gravity anomalies and rock densities to the seismically determined crustal structure across the English River and Uchi subprovinces.

North-south gravity profiles across the English River subprovince are plotted in figure 18. These gravity profiles have been interpreted by forward modeling. Though not absolute solutions, modeling blocks of different dimensions and density contrasts can produce gravity profiles that are quite similar to the observed gravity profiles across the English River subprovince.

A best fit gravity profile (figure 19) was modeled using a lower crustal block having a density contrast of +0.40 g/cc (comparable to a thinner crust with an elevated mantle), and a surface crustal block composed of two separate blocks: a larger "sedimentary" block with a density contrast of -0.08 g/cc, and a smaller "tonalitic" block, corresponding to the southern domain, with a density contrast of -0.15

Figure 17. Bouguer gravity map of a section of the western Superior Province. Solid dark lines outline the English River subprovince.

(Modified from Manuscript Map No. 48090, (1981))
(Gravity and Geodynamics Division; Energy, Mines and Resources)

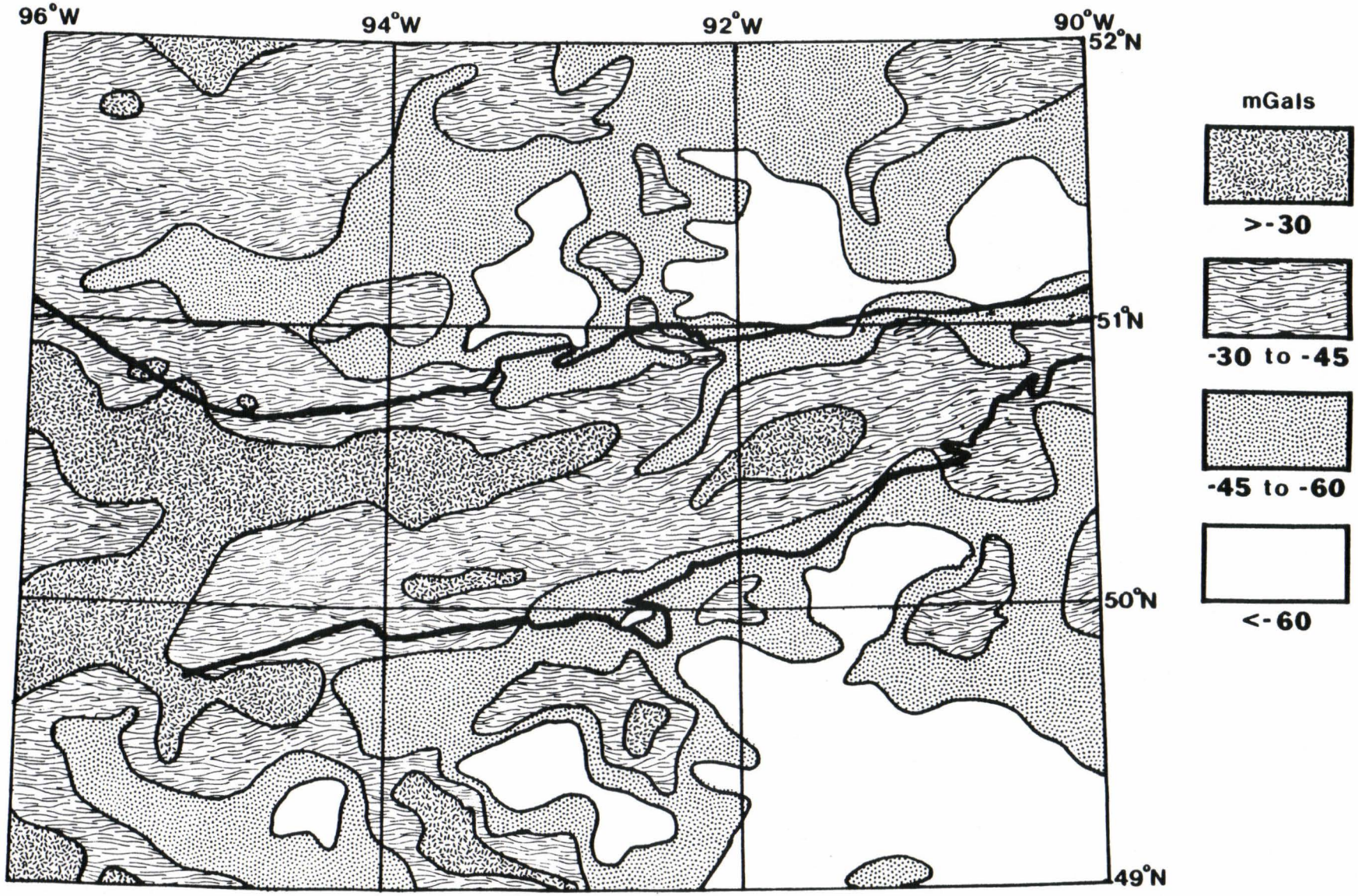
96°W
94°W
92°W
90°W
52°N
51°N
50°N
49°N
mGals
>-30
-30 to -45
-45 to -60
<-60

Figure 18. Bouguer gravity profiles across the English River subprovince.

KEY

A: Profile across 91°W
B: Profile across 92°W
C: Profile across 93°W
D: Profile across 94°W
E: Profile across 95°W

ERsp = English River subprovince

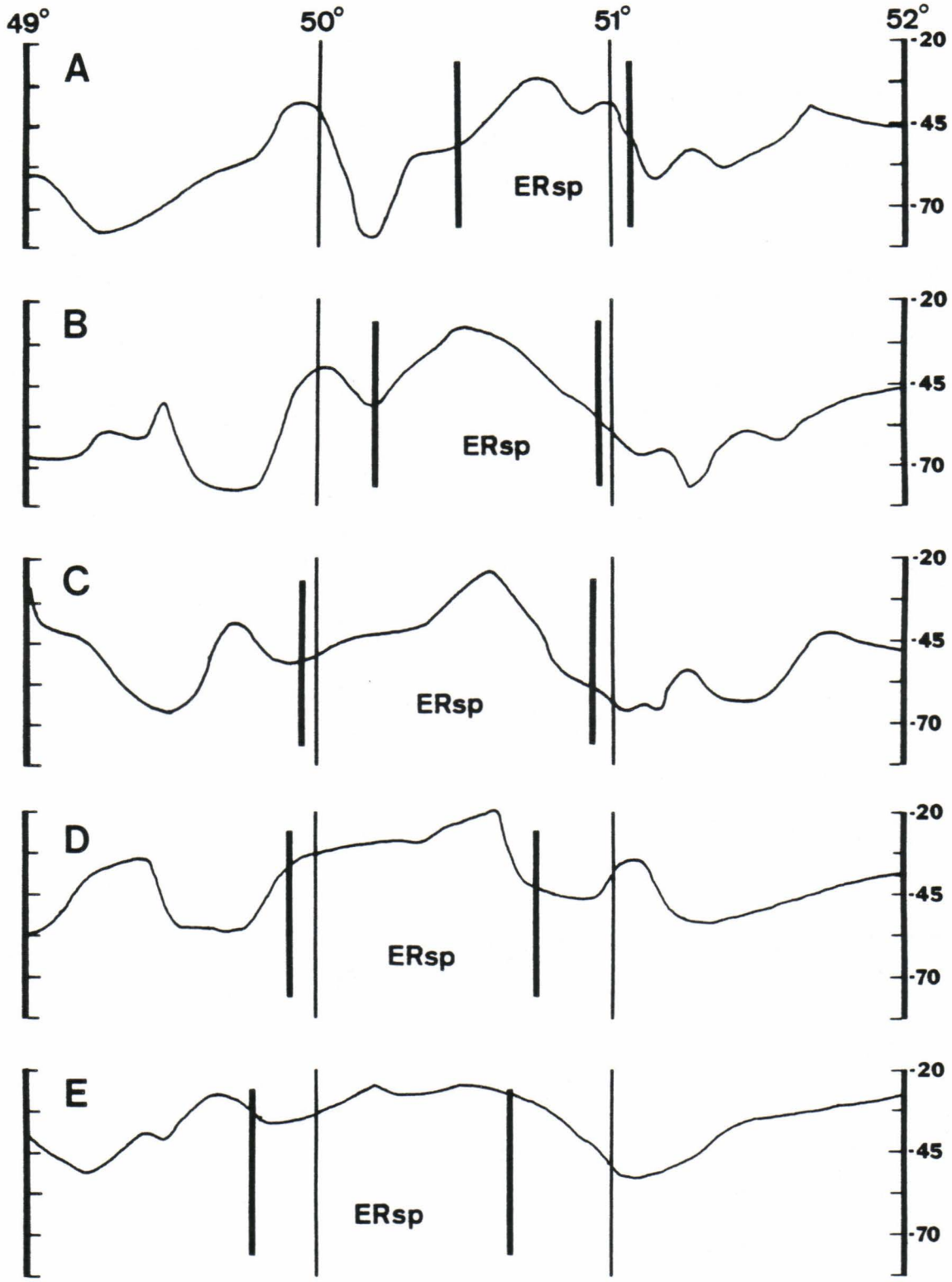
49°
50°
51°
52°
A
B
C
D
E
ERsp
-20
-45
-70

Figure 19. Modeled gravity profile.

A: Overlay of the observed gravity profile across 93°W and the modeled gravity profile.

B: Geological "block" model used to produce the modeled gravity profile assuming:

1: A thinner total crust (elevated mantle) with a density contrast of 0.40 g/cc.

2: A thick metasedimentary sequence at the surface with a density contrast of -0.08 g/cc.

3: A thin slab of tonalite (southern domain) with a density contrast of -0.15 g/cc.

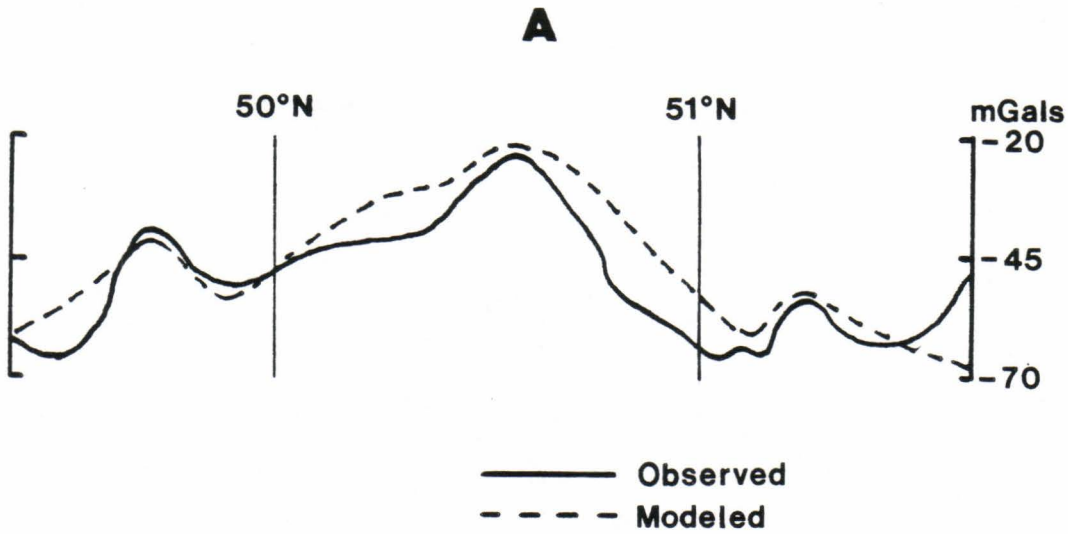
A
50°N
51°N
mGals
-20
-45
-70
Observed
Modeled

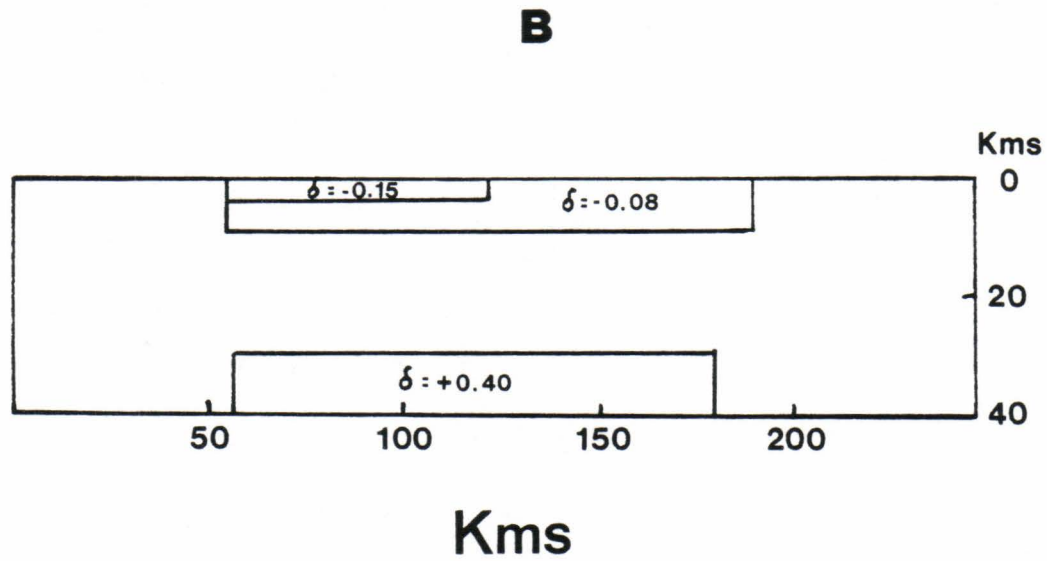
B
Kms
0
20
40
δ = -0.15
δ = -0.08
δ = +0.40
50
100
150
200
Kms

g/cc. Combining the anomalies produces a gravity profile that closely fits the observed gravity profile across the English River subprovince along 93°W. By slightly changing the dimensions and positions of the blocks, the other observed profiles were approximated.

The most extreme gravity highs (greater than -20 to -30 mGals) in the Ontario section of the English River subprovince correlate directly with known granulite occurrences; Umfreville-Conifer Lakes, Cliff-Clay Lakes, Eastern Lac Seul (Breaks et al., 1978), Sawmill Bay (Rod Baumann, personal comunication) (figures 17, 5), and Mojikit Lake-Ogoki Reservoir (Percival, 1983) granulite zones. The average densities for pyroxene-granulites, biotite-garnet gneisses, and trondhjemites from the eastern Lac Seul region are 2.98, 2.72, and 2.65 g/cc respectively (Urquhart, 1976). The granulites are significantly more dense than the amphibolite grade rocks on their flanks, possibly due to increased partial melting with the melt going out the "roof" leaving behind the more dense, refractive restite. Thus a positive local component would be added to the already positive regional component to produce the notably high anomalies over the granulite zones. Several large gravity highs occur in the Manitoba section of the English River subprovince, (greater than -25 mGals), and it is suggested that these zones may also contain granulites.

AN EVOLUTIONARY MODEL FOR THE ENGLISH RIVER SUBPROVINCE

Beakhouse (1977), noting locally preserved sedimentary structures such as graded bedding, together with the large extent and uniformity of the sedimentary units, suggests that the northern domain originated as an early Archean sedimentary basin which had most of its detritus deposited below wave base as turbidity flows. This basin could have been formed as an extensional feature, or on the continental margin as depicted by figure 20a.

Since these metasediments were once on the earth's surface, how did they become buried to a depth of at least 18 +/- 3 Kms? One viable mechanism proposed for these types of terrains is based on the model that the sediments were folded, turned on end, and compressed in a continent-continent type collision (Windley, 1977). A second possibility is that a relatively thick sliver of rock was thrust on top of the sediments (Oxburgh, 1972; Ashwal et al., 1983).

The theory of plate tectonics has progressed rapidly to the current theories of accretionary tectonics of allochthonous terrains. In recent years, accretionary tectonics has been called upon to explain numerous geologic regions from around the world; Dunage-Zone Newfoundland, Southwestern United States, Appalachians, North American Cordilleran, Barbados, Alaska, the South Kitakami Region of Japan (Coney et al., 1980; Churkin et al., 1982; Condie, 1982; Csejtey et al., 1982; Jones et al., 1982; Monger et al., 1982; Saito and Hashimoto, 1982; Speed and Larue, 1982; Williams and Hatcher, 1982; Karlstrom, 1983). Suspect accretionary terrains are identified on the basis of age dates,

structure, metamorphic and plutonic histories, mineral deposits, stratigraphy, paleontology, and paleomagnetism. Their boundaries are usually sharp structural junctions; marked discontinuities that cannot be explained by normal gradation in structural style (Williams and Hatcher, 1982). It may be possible to postulate processes of accretionary tectonics as far back as the Archean. Indeed, Langford and Morin (1976) noting the similarity of the alternating linear belts of the Superior Province to the Canadian cordillera, postulate a model of accreting island arcs for the Superior Province.

The English River subprovince is composed of two prominent lithological domains (Beakhouse, 1977) of differing ages. A granitoid gneiss from the southern plutonic domain yielded a U-Pb age date of 3.008 B.Y. (Krogh et al., 1976). Though Krogh et al. (1976) can not give specific information relevant to the time of sedimentation for the northern domain, they believe that the sediments were derived from a region having at least one source with a minimum age of 2.76 B.Y. Subsequent metamorphism and migmatization was dated at 2.68 B.Y.

The occurrence in the English River subprovince of two distinct domains, suggests the possibility of two distinct terrains. Taking this one step further, one could hypothesize that the southern plutonic domain was thrust on top of the northern sedimentary domain resulting in the 5 +/-1 Kbar pressures (approximately 18 +/-3 Kms burial depth) acquired during metamorphism (figure 20b). What is left today after significant erosion is the upper part of the sediments in the north, and the lower part of the plutonic thrust sheet to the south (figure 20c).

Figure 20. Hypothetical evolution of the English River subprovince.

A: Northern domain as a Precambrian sedimentary basin, southern domain as a separate terrain on a converging plate.

B: Detatchment and thrusting of the southern domain onto the sedimentary basin, resulting in the pressures attained during metamorphism.

C: Present configuration after considerable uplift and erosion. Erosion has cut through the paleo-thrust plane resulting with the sedimentary domain exposed in the north, and the plutonic domain exposed to the south.

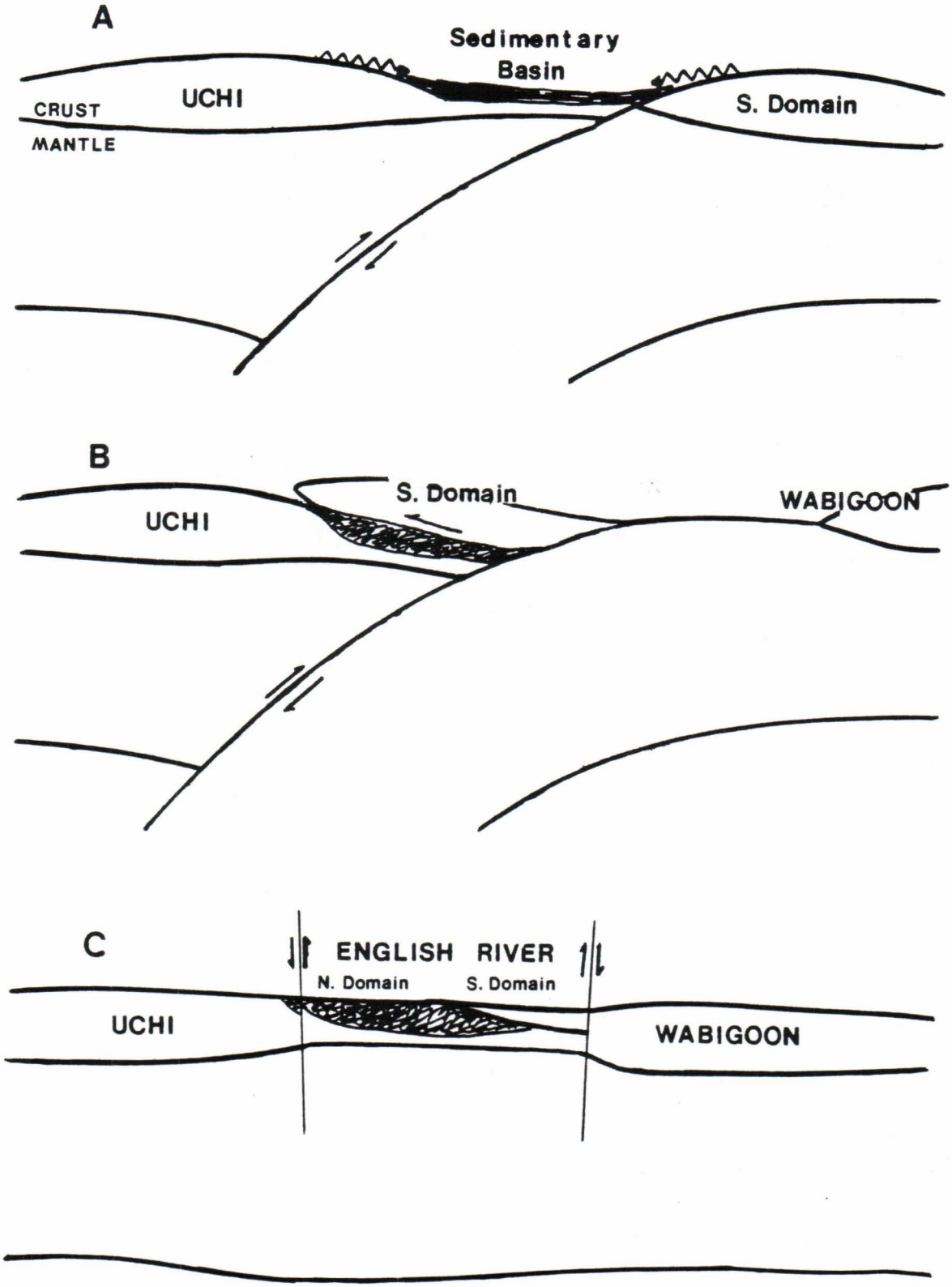
A
Sedimentary
Basin
UCHI
CRUST
MANTLE
S. Domain
B
S. Domain
WABIGOON
UCHI
C
ENGLISH RIVER
N. Domain
S. Domain
UCHI
WABIGOON

However, without more detailed geophysical surveys (both gravity and seismic), this hypothesis is rather difficult to prove.

Solid lithosphere could indeed overthrust soft sediments if the sediments were water saturated with enough pore fluid as to cushion the lithosphere. Seismic reflection data has shown this process to be occuring presently in the Barbados Ridge Complex (Westbrook and Smith, 1983). The hypothesis of the plutonic domain thrusting on to the sedimentary domain has the additional advantage in that it provides a pre-tectonic datum on which to hang an evolutionary model.

The thermal effects due to a thrust (Ashwal et al., 1983; Molnar et al., 1983), are shown in figure 21a using a calculated modern day basin and range geotherm. The initial geotherm would be that of a "saw-tooth". Relaxation of this geotherm could heat the sediments, originally at $0^{\circ}C$, to as much as $400^{\circ}C$. Though not the temperatures attained during metamorphism, it adds significantly to the quantity of heat required.

Since the crust was thickened by approximately 20 km, it would have sunk to isostatically compensate for the thrust sheet (figure 21b). The lower crust which has sunk farther down into the mantle, would warm up due to conductive heat and asthenosphere convection. With relaxation of the perturbed isotherms, the temperature in the lower crustal rocks could increase by as much as $100^{\circ}C$ which would initiate partial melting. The balance of the heat needed for metamorphism probably came up convectively in the form of magma generated from the anatexis of the lower crust. If this magma was emplaced as a pluton at a depth

Figure 21. Effects of a 20 Km thick thrust:

(Modified from Thompson, 1981)

A: Configuration of the crust with isotherms prior to the thrust.

B: Configuration of the crust with isotherms immediately after a 20 km thrust and 10 km's of isostatic sinking.

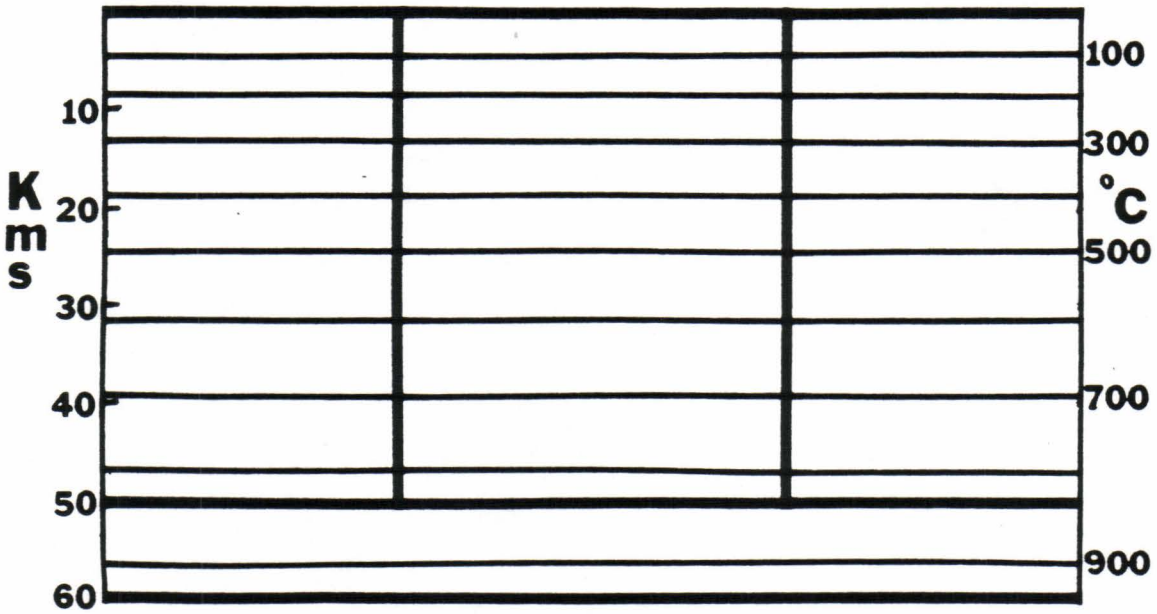
Kms
10
20
30
40
50
60
100
300
°C
500
700
900

A

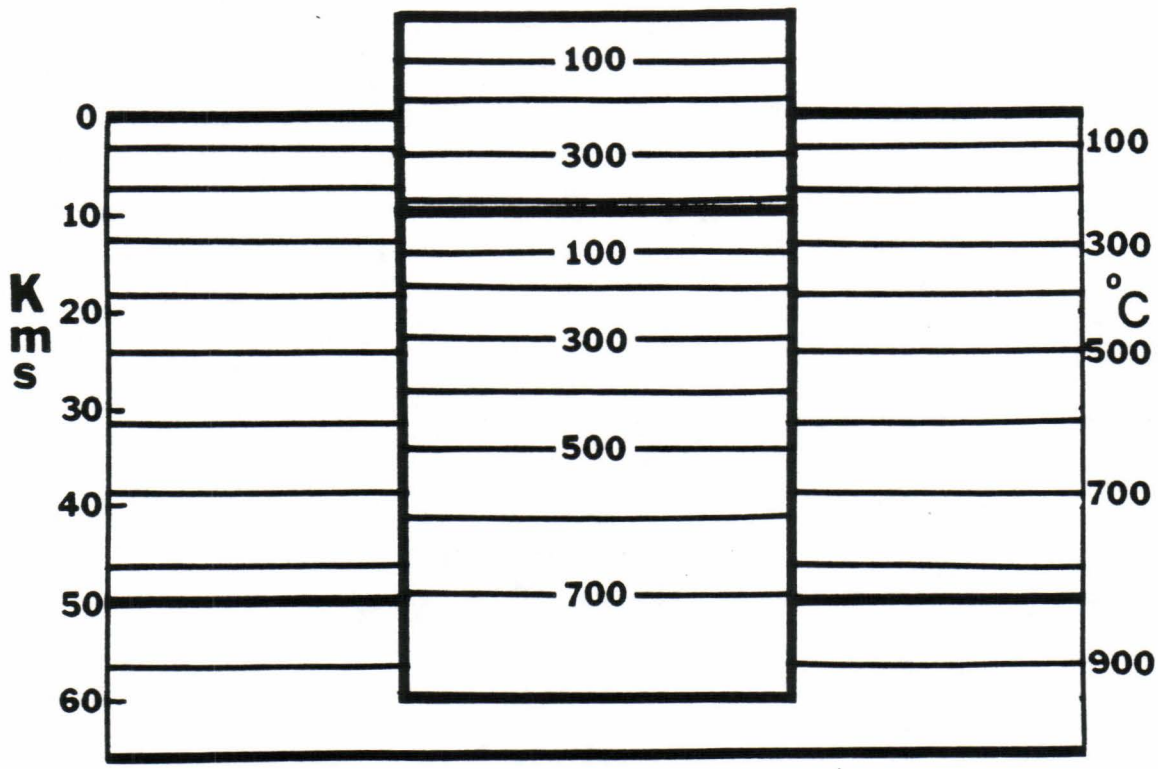
Kms
0
10
20
30
40
50
60
100
300
100
300
500
700
100
300
°C
500
700
900

B

comparable to other plutons, (Idaho batholith main group - 9 to 15 km, Swanberg and Blackwell, 1973; Boulder Batholith - 1 to 3 km, Hyndman, 1981; presently active pluton in the Cascades - 10 km, Blackwell and Steel, 1983) most remnants of its existance would now be eroded and gone.

If the above hypotheses are correct, the migmatite variety defined as inhomogeneous diatexite by Breaks et al. (1978) could be parts of the intrusive pluton with resorbed xenoliths of the metasedimentary country rock floating within it. Assuming that the southern plutonic domain was indeed thrust upon the sediments and that the present erosion level is close to the thrust plane, the overthrust plutonic sheet would have formed a stratigraphic trap where the upward migrating melt could collect and crystallize.

As England and Richardson (1977) have pointed out, uplift, erosion, and its associated thermal relaxation will play an important role in the thermal evolution of any metamorphic complex. The pressures of metamorphism for the English River subprovince were determined in this thesis to be 5 +/- 1 kbars. By noting that the Uchi subprovince contains pockets of andalusite and garnet bearing rocks in the eastern Lake St. Joseph region, pressures can be constrained to 3-4 kbars by the Holdaway (1971) aluminosilicate triple point, and the pressure required to stabilize garnet (Winkler, 1979). For the sake of argument, it was assumed that the pressures attained in the Wabigoon subprovince were approximately the same as for the Uchi subprovince. This shows a difference in metamorphism between the greenstone belts and the English

River subprovince of around 1.5 +/- 1.5 Kbars which translates to 5 +/- 5 Km's difference in burial depths, and since now at the same level, uplift. The thermal evolution incorporating a magmatic intrusion, uplift, and erosion, is depicted in figure 22.

The English River subprovince shows distinct evidence for block faulting. Wilson (1971) delineates the English River subprovince as a fault bound block on the basis of areomagnetic interpretation. Major bounding fault systems have also been mapped in the field (figure 23). Thompson's (1981) model of a magma body at the center of a large rising block (figure 22), explains the observed thermal anticline located at the center of the English River subprovince (figure 11). The center would have received the heat necessary for the observed high granulite temperatures. The edges, however, due to thermal relaxation would not have achieved the same high temperatures. Figure 24d depicts "fossil" isotherms after an amount of erosion comparable to that of the English River subprovince had occurred.

The initial pressure and thus the thickness of the thrust sheet can not be assessed since it is difficult to determine if peak metamorphic pressures and temperatures have been preserved. England and Richardson (1977) believe that rocks will reach final equilibrium on the temperature-pressure path at the maximum entropies of reactions. Since the exact reactions and the exact pressure-temperature path involved during metamorphism are unknown, the assumption is often made that the maximum entropy attained during metamorphism coincides with the maximum temperature. Thus the pressure recorded by a rock could coincide with the maximum temperature on any given P-T path (figure 24).

Figure 22. Thermal evolution incorporating a magmatic intrusion, uplift, and erosion.

(Modified from Thompson, 1981)

A: Pre-intrusive isotherms.

B: Isotherms soon after emplacement of a pluton at 20 km's depth.

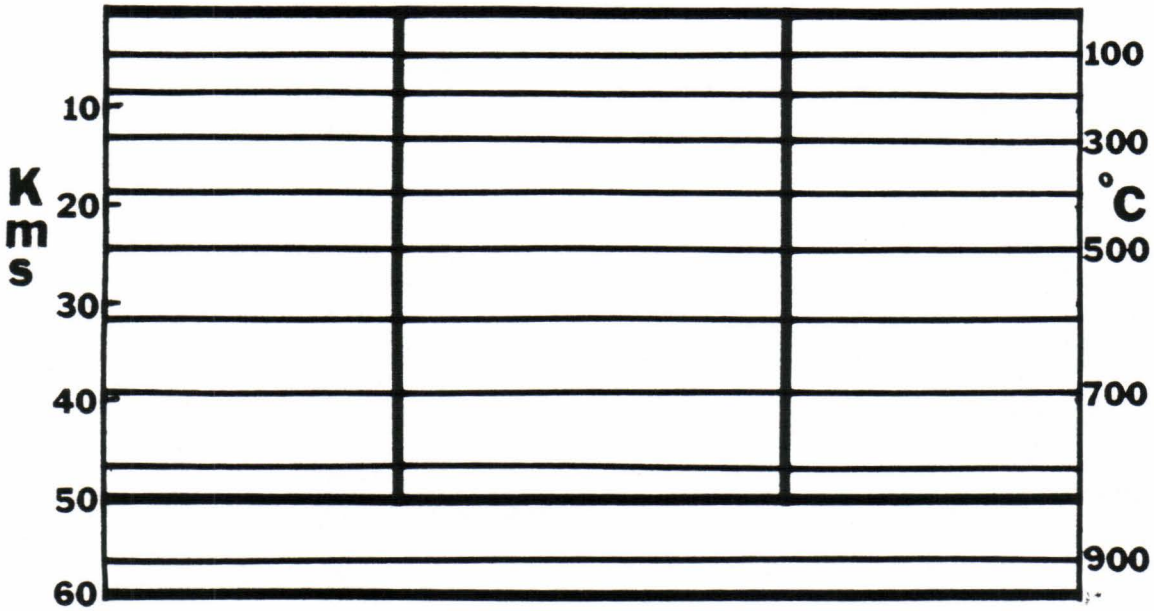
Kms
10
20
30
40
50
60
100
300
°C
500
700
900

A

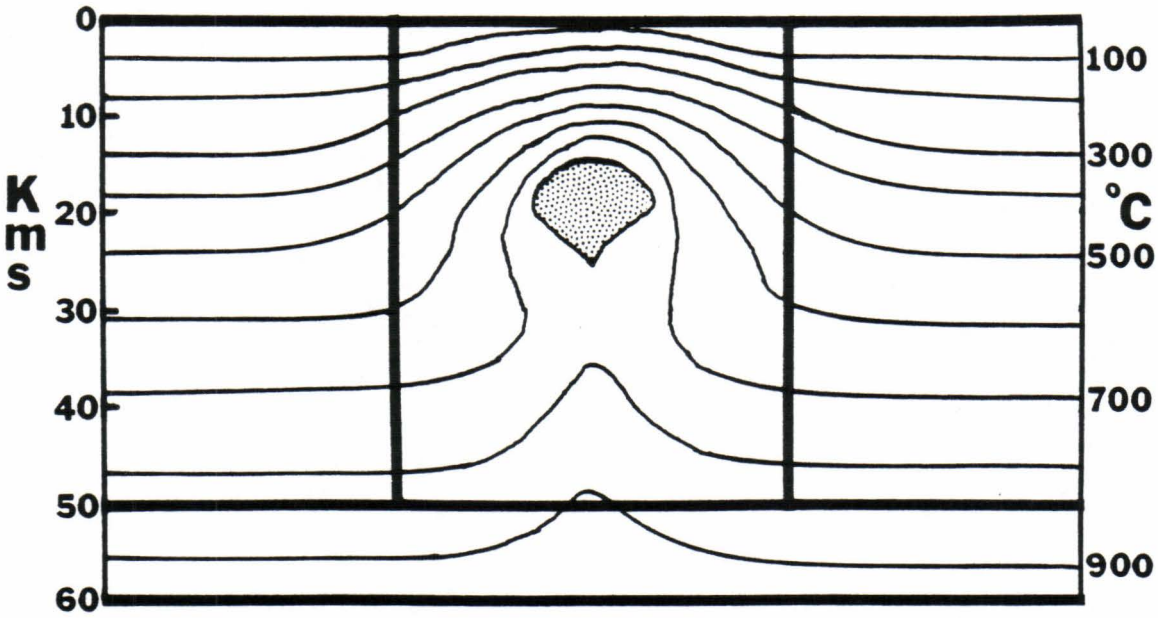
Kms
0
10
20
30
40
50
60
100
300
°C
500
700
900

B

Figure 22 continued.

C: Isotherms in response to both the cooling pluton and a 10 km uplift.

D: Hypothetical configuration of "fossil" metamorphic isotherms as would be asertained from geothermometry.

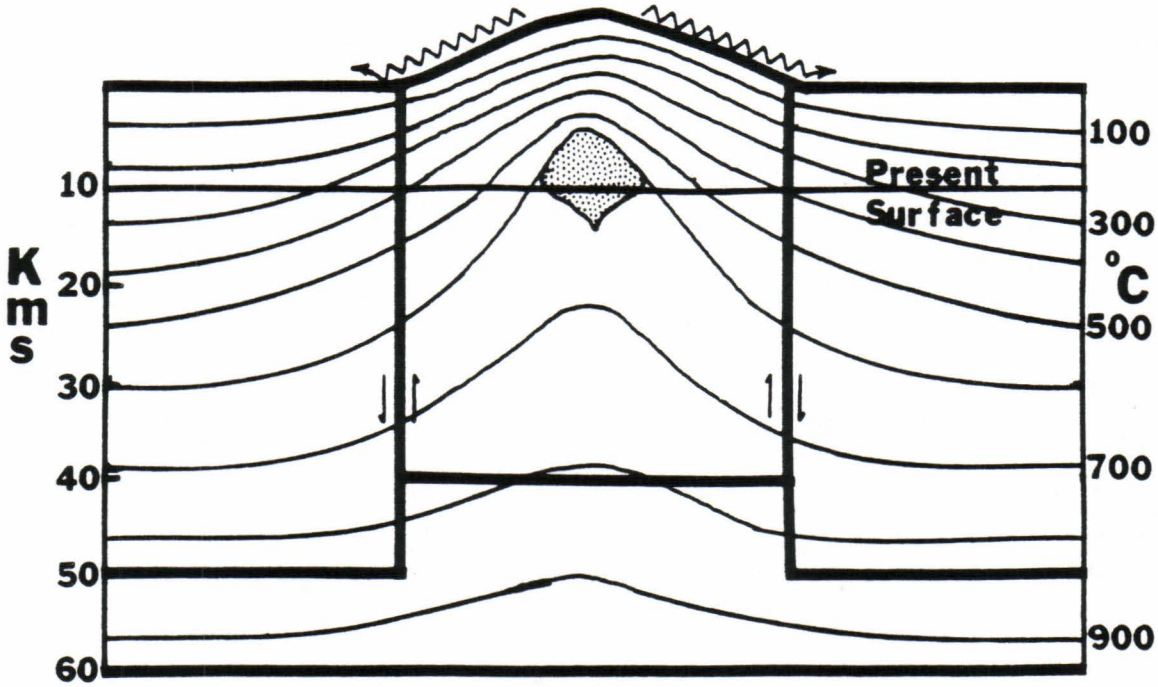
Present
Surface
Kms
10
20
30
40
50
60
100
300
°C
500
700
900

C

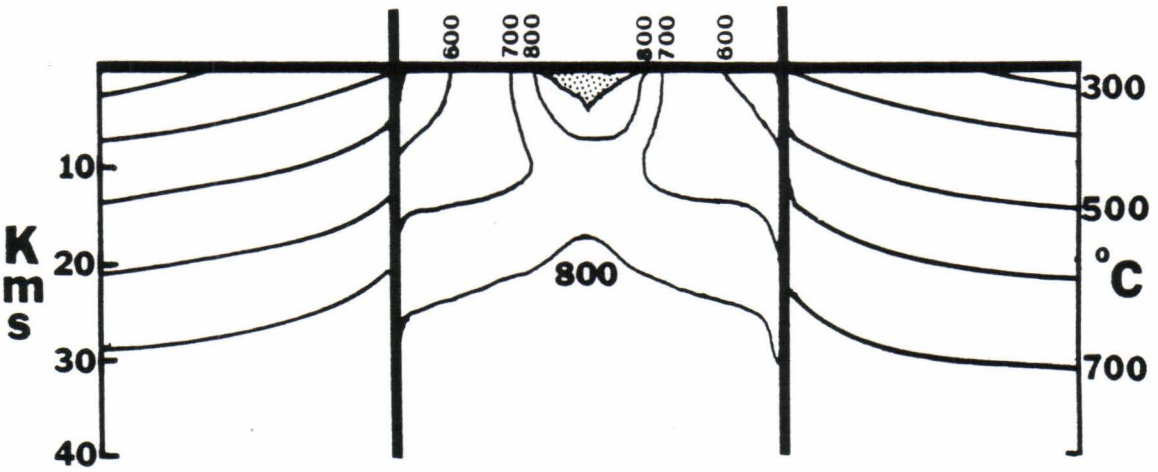
600
700
800
800
700
600
800
Kms
10
20
30
40
300
500
°C
700

D

Figure 23. Location of faults bounding the Ontario section of the English River subprovince.

(Modified from Breaks et al., 1978)

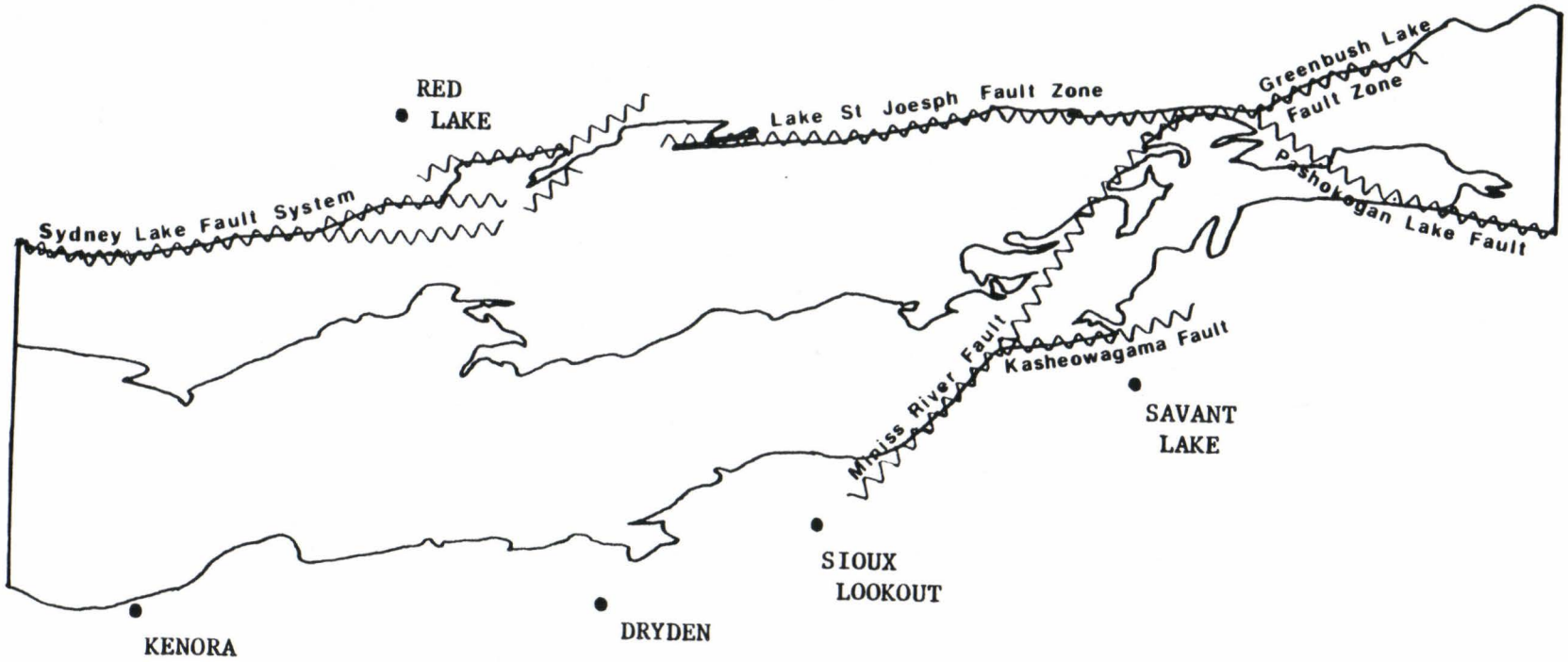
RED
LAKE
Sydney Lake Fault System
Lake St Joesph Fault Zone
Greenbush Lake
Fault Zone
Pashokogan Lake Fault
Mnaiss River Fault
Kasheowagama Fault
SAVANT
LAKE
SIOUX
LOOKOUT
DRYDEN
KENORA

Figure 24. A hypothetical pressure-temperature path invoking rapid burial with continued heating during uplift and erosion.

Hypothetical

P-T Path

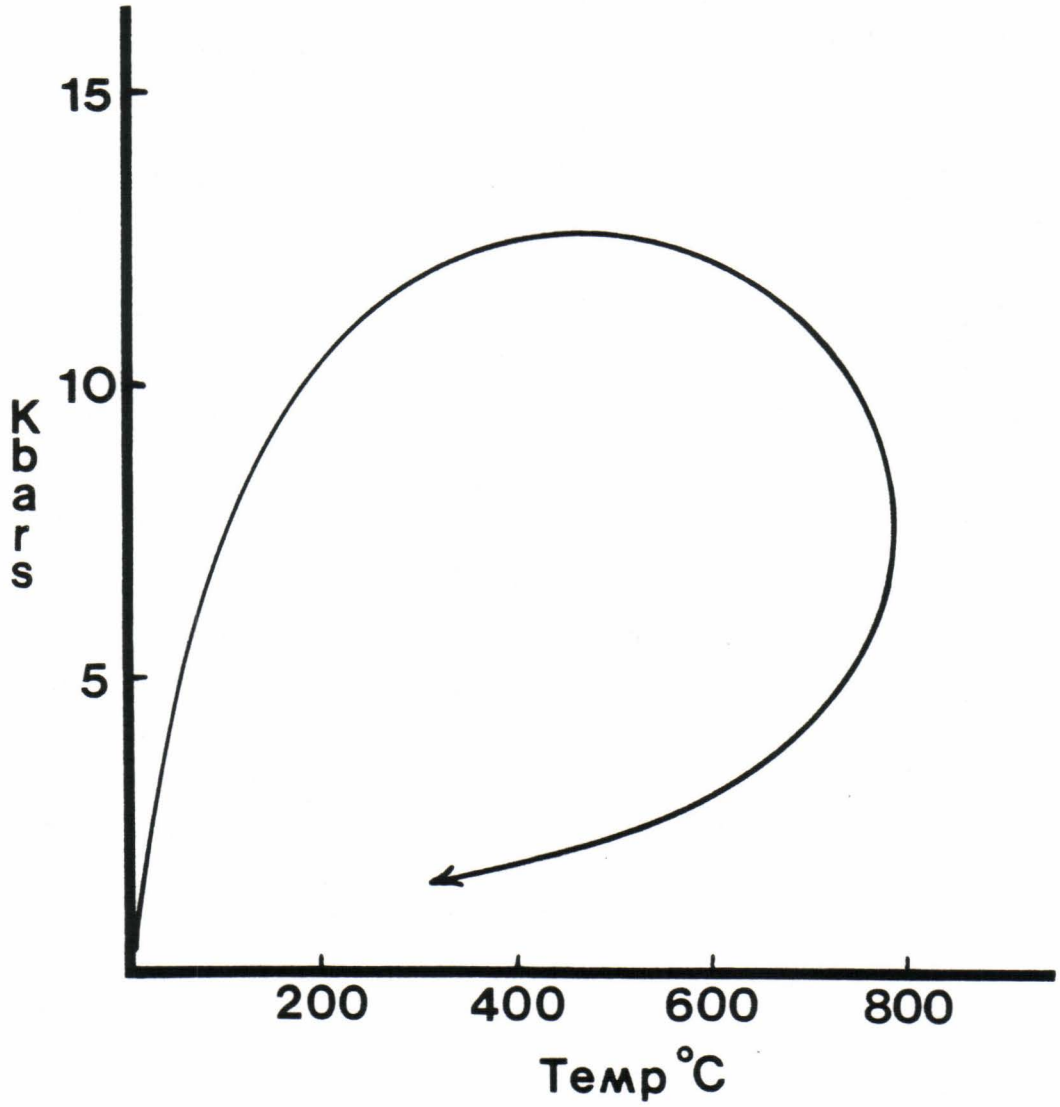

CONCLUSIONS

Results from geobarometry have shown that the pressures attained during metamorphism were relatively constant throughout the eastern Lac Seul region of the English River subprovince (5 +/- 1 Kbar). There is strong evidence from garnet-orthopyroxene barometry that pressures may also have been constant over much of the subprovince.

The temperatures attained during metamorphism show a trend across the eastern Lac Seul region, depicting a "thermal anticline". The axis extends approximately east-west parallel to the strike of the subprovince, and then is reorientated northeast-southwest in the region of the Miniss river fault zone. Temperature falls off rather symmetrically on both limbs of this thermal anticline with little regard to the presence of the southern plutonic domain. Contrary to the findings of Bohlen and Essene (1980), biotite-garnet geothermometry as used in this thesis, proved to be quite accurate, precise, and consistent. It provided good quantitative results for the thermal metamorphism in the eastern Lac Suel region of the English River subprovince.

Of the various biotite-garnet geothermometers, it was concluded that the experimentally calibrated Perchuk and Lavrent'eva (1983) geothermometer gave the most reasonable and consistent results. Imposing an ideal mixing model for biotite but a complicated mixing model for garnet may tend to overcorrect garnet activity producing significant scatter and error. Thus, the assumption of ideal mixing in both garnet and biotite appears to be valid on the basis that possible nonidealitys in biotite probably offsets the nonidealities in garnet.

The temperatures attained in the Eastern Lac Seul region were approximately 600°C at the border of the Uchi subprovince, 675°C for the garnet-cordierite "in" isograd, 700°C for the orthopyroxene "in" isograd, with maximum temperatures around 750°C.

Forward modeling of gravity has shown that the gravity profiles across the English River subprovince can possibly be attributed to a thinner total crust and a thick sequence of sediments in the immediate region of the English River subprovince. It is curious to note that all the granulite occurrences in the Ontario section of the English River subprovince are associated with a high gravity anomaly. Several such gravity highs occur in the Manitoba section and with future study, may also prove to have associated granulites.

Langford and Morin (1976), noting the similarity to the Canadian Cordillera, propose a model of accreting island arcs for the Superior Province. On the basis of the peculiar crustal structure, Beakhouse (1977) concludes that the northern domain originated as a major sedimentary basin. The strong contrasts in lithologies and structure between the northern sedimentary and southern plutonic domains suggest that the southern domain could be an allochthonous terrain accreted onto the northern domain. Inasmuch as geobarometry has shown that the sediments were buried to a depth of at least 20 kms, it is postulated that the southern domain was thrust onto the northern domain. Erosion has cut obliquely through the thrust plane resulting in metasediments exposed in the north and plutonics in the south. Irregularites from the thrust plane and erosional surface has resulted in fensters and klippes

which can explain the diffuse irregular contact of supracrustal metasediments and the intracrustal plutonics. Without detailed gravity and seismic geophysical studies, however, these hypothoses would be impossible to validate.

Isostatic compensation for the thrust sheet caused the whole crust to sink farther into the mantle resulting in partial melting of the lower crust. The intrusion of the melt into the upper regions (possibly trapped along the thrust plane) and thermal relaxation of the thrust perturbed geotherm, supplied the heat required for the thermal metamorphism.

Though there exist regions in the English River subprovince that show distinct in situ melting, the region at the center of the subprovince corresponding to the greatest temperatures, is composed of too much melt to have all been derived in situ. Either these huge bodies of leucosome represent melt due, to anatexis of slightly deeper sediments, squeezed upward to a "pressure low", or they could represent part of a magma body from a deeper source (lower crust?) that is in part responsible for the thermal metamorphism.

Block faulting and uplift with a magmatic heat source at the center of the block (Thompson, 1981) along with thermal diffusivity explains very well the observed thermal anticline of the English River subprovince.

The above arguments and hypotheses suggest that it was quite possible that plate tectonics was operating at a early time in the earth's history in a fashion quite similar to that of today.

APPENDICES

APPENDIX A
SAMPLE LOCALITIES

SAMPLE LOCALITIES

Universal Transverse Mercator Grid
Grid Zone Designation: 15U

BURY LAKE

BL1083	XF164891
BL1183	XF153887

CHURCHILL LAKE

CH1183	XG377355
CH1283	XG374327
CH1483	XG352310
CH1683	XG296283
CH2083	XG233250
CH2283	XG244294
CH2383	XG262288

CARLING LAKE

CL1083	XG219045
CL1183	XG219044
CL1483	XG210045
CL1783	XG224107
CL2283	XG182053
CL2483	XF219968
CL2583	XF213978

DE LESSEPS LAKE

DS1183	XG615298
DS1383	XG627245
DS1683	XG615193
DS1783	XG606176
DS1983	XG594146
DS2183	XG579134
DS2483	XG558118
DS2583	XG638224
DS2683	XG650226
DS2783	XG664235

ELBOW LAKE

EB1083	XF022816
EB1383	XF012807

HIGHSTONE LAKE

HS1183	XF106895
HS1483	XF094862
HS1583	XF085860

IDAHO LAKE ROAD

ID1083	WF994989
ID1283	WF980989
ID1683	WF924997
ID1983	WG895046
ID2083	WG891047

LAKE ST. JOSEPH

JS1083	XG362474
JS1383	XG373471
JS1483	XG366478
JS1683	XG357480
JS1783	XG104386
JS1983	XG131415
JS2183	XG135430
JS2283	XG113426
JS2383	XG148443
JS2483	XG163455
JS2583	XG178444
JS2783	XG232468
JS2983	XG248447
JS3183	XG334456
JS3283	XG369458
JS3483	XG433474
JS3583	XG442454
JS3683	XG450420
JS3883	XG456408
JS3983	XG425391

LAC SEUL

LS17	XG072185
LS25	XG044147
LS28	XG020154
LS32	WG966173
LS42	WG947150
LS49	WG849127
LS51	WG841095
LS61	WG764026
LS66	WF713940
LS67	WF685935
LS68	WF624946
LS69	WF628965
LS76	WF755847
LS78	WF716842
LS82	WG807022
LS85	WF769984
LS87	WF778963
LS88	WF789934
LS92	WF773957

MINISS LAKE

MN1083	XG564308
MN1283	XG537327
MN1883	XG481292
MN1983	XG485319
MN2183	XG524355
MN2483	XG562342
MN2583	XG596327
MN2783	XG623339

ST. RAPHAEL LAKE

RF1283	XG365117
RF1483	XG344152
RF1683	XG345212
RF1883	XG301122
RF1983	XG294138
RF2183	XG302193
RF2283	XG303215
RF2583	XG282218

RAGGED WOOD LAKE

RW1283	XG272029
RW1683	XF263994
RW1783	XF262992
RW1883	XF263991
RW2083	XF258981
RW2483	XF222942
RW2583	XF217938

VERMILION RIVER

VR1583	XF005803

VERMILION RIVER ROAD

VM1283	XG084298
VM1483	XG062306
VM1683	XG045314
VM1983	WG993312
VM2183	XG107269
VM2283	XG115238
VM2383	XG117226
VM2683	XG099205
VM2783	XG097203
VM3583	XG037098
VM3883	XG023052
VM4383	XF051946
VM4983	WF983826

VERMILION RIVER ROAD collected by K. R. Henke

VR13	XG114223
VR14	XG108214
VR17	XG092196
VR18	XG076178
VR20	XG072169
VR24	XG055122
VR30	XG037098
VR31	XG034092
VR33	XG011039
VR35	XG044028
VR40	WF977989
VR52	XF015980
VR57	XF036936
VR58	XF038932
VR65	XF934778
VR66	XF933776

Figure 25. Index map showing sample locations.

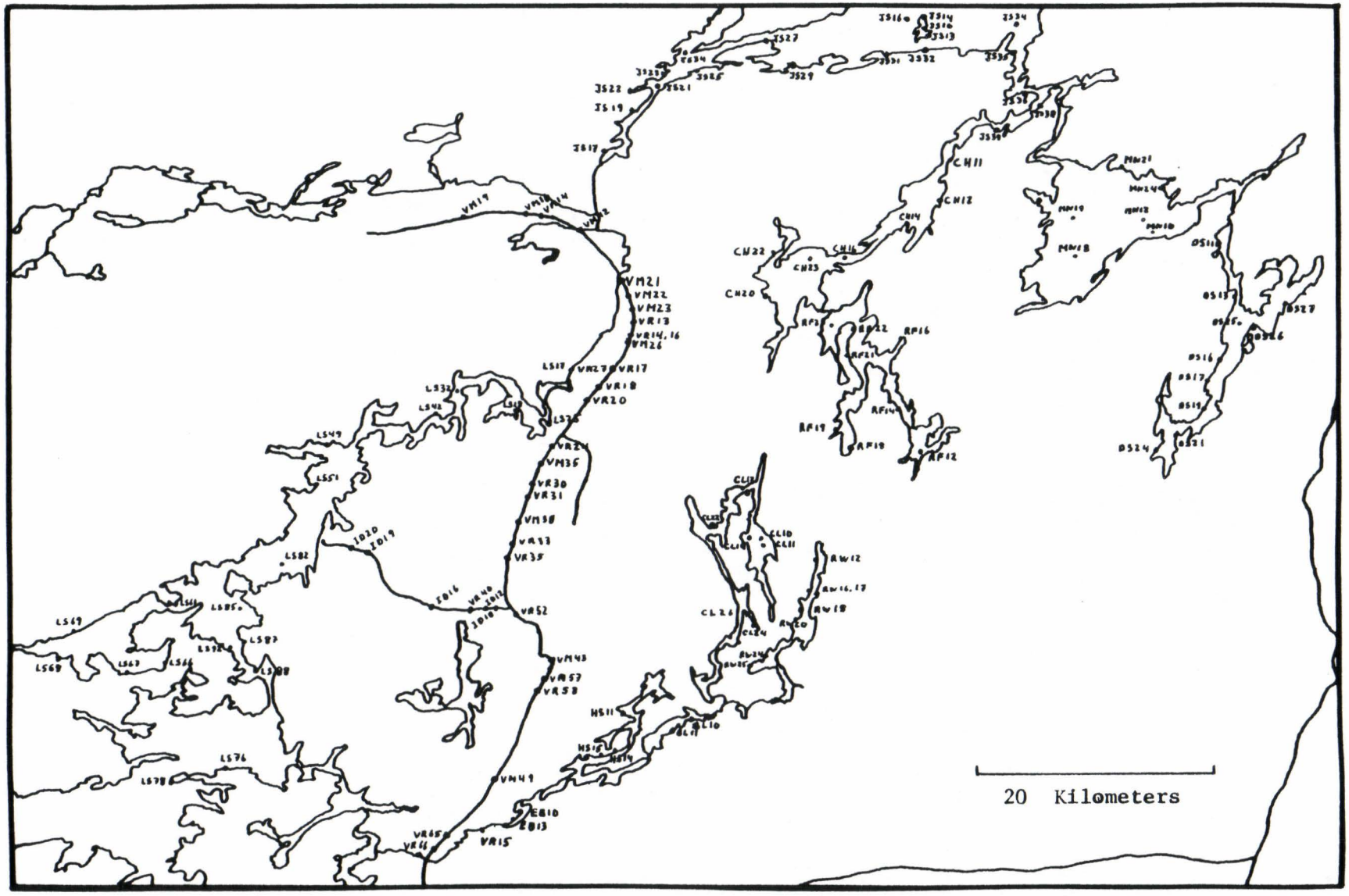
20 Kilometers

APPENDIX B

THIN SECTION MINERALOGY

APPENDIX B

THIN SECTION MINERALOGY:

MINERAL ABBREVIATIONS

Qtz	= quartz	Plag	= plagioclase
Kspar	= alkali feldspar	Perth	= perthite
Bio	= biotite	Gt	= garnet
Cord	= cordierite	Opx	= orthopyroxene
Cpx	= clinopyroxene	Sill	= sillimanite
Amph	= amphibole	Musc	= muscovite
Chlor	= chlorite	Apat	= apatite
Zirc	= zircon	Cumm	= cummingtonite
Tour	= tourmaline	Epid	= epidote
Cal	= calcite	Sph	= sphene
Her	= hercynite	Sta	= staurolite

KEY

X = present
V = present in a vein
T = trace amount
R = retrograde
2 = secondary
? = probably present
difficult to confirm

SAMPLE	Qtz	Plag	Kspar	Bio	Gtd	Opx	Cpx	Sill	Amph	Mul	Chl	Spl	Hcr	Apt	Zrc	Tur	Cmr	Epd	Cal	OTHERS	LITHOLOGY
BURY LAKE																					
BL1083C	.	X	.	X	.	.	.	.	X	.	.	.	.	.	.	.	X	.	.	Sph	Gt-Bio Schist
BL1083E	.	X	.	X	.	.	.	X	.	.	.	.	R	.	R	.	X	.	.		Gt-Granulite
BL1183Z	.	.	X	.	.	.	.	.	X	.	X	.	X	.	.	.	.	.	.		Amphibolite
CH1183A	.	X	.	X	.	.	.	.	.	.	.	.	.	.	.	.	.	.	.		Bio-Gt Wacke
CH1283A	.	X	.	X	.	X	.	X	.	.	.	X	.	R	.	R	.	X	.		Gt-Cord Pelite
CH1483B	.	X	.	X	.	X	.	?	.	.	.	.	.	.	X	.	X	.	.		Bio-Gt Semipelite
CH1683A	.	X	.	X	.	X	.	.	.	.	.	.	R	.	.	.	.	.	.		Bio-Gt Wacke
CH2083A	.	X	.	X	.	X	.	.	.	.	.	R	.	R	.	X	.	.	.		Bio-Gt Wacke
CH2283	.	X	.	X	.	.	.	.	.	.	.	.	.	X	.	X	.	.	.		Bio-Amph Schist
CH2383B	.	X	.	X	.	X	.	X	.	.	.	X	.	R	.	R	.	X	.	Her	Gt-Cord Pelite
CARLING LAKE																					
CL1083A	.	X	.	X	.	.	X	.	.	.	.	.	.	X	.	.	.	.	.	Sph	Wacke-Granulite
CL1183A	.	X	.	X	.	X	.	X	.	.	.	.	R	.	X	.	X	.	.	2	Gt-Granulite
CL1483B	.	.	X	.	.	X	.	.	X	?	.	.	.	.	X	.	.	.	.		Wacke-Granulite
CL1783B	.	X	.	X	.	.	.	.	.	.	.	.	.	.	X	.	.	.	.		Bio Wacke
CL2283A	.	X	.	X	.	X	.	X	.	.	.	.	.	.	X	.	.	.	.		Gt-Granulite
CL2483A	.	V	.	X	.	.	.	.	X	.	X	.	X	.	.	.	.	.	.	Sph	Opx-Amphibolite
CL2483C	.	X	.	X	.	.	.	X	.	.	.	.	.	.	X	.	X	.	.		Bio-Granulite
CL2583B	.	X	.	X	.	.	.	.	.	.	.	.	R	.	X	.	X	.	.		Amphibolite
DE LESSEPS LAKE																					
DS1183	.	.	X	.	.	X	.	.	.	.	.	X	.	R	.	X	.	X	.	2	Bio-Schist
DS1383	.	X	.	X	.	V	.	X	.	X	.	.	.	.	R	.	X	.	.		Bio-Gt Schist
DS1683	.	X	.	X	.	.	.	X	.	.	.	.	.	.	.	.	X	.	.		Bio-Gt Wacke
DS1783	.	X	.	X	.	X	.	.	.	.	.	.	.	.	X	.	.	.	.		Bio-Schist
DS1983B	.	T	.	X	.	T	.	V	.	X	.	.	.	X	.	R	.	X	.	R	Amphibolite
DS2183B	.	X	.	X	.	.	.	X	.	X	.	.	.	.	R	.	X	.	.		Gt-Cord Schist
DS2483	.	X	.	X	.	.	.	X	.	.	.	.	.	.	.	.	X	.	.		Bio-Gt Wacke
DS2583A	.	T	.	.	.	X	.	.	.	X	.	.	.	X	.	.	.	T	.		Amphibolite
DS2583C	.	X	.	X	.	X	.	X	.	.	.	.	.	R	.	X	.	X	.		Bio-Wacke
DS2683B	.	V	.	X	.	.	.	.	.	.	.	X	.	R	.	X	.	X	.	2 2	Amphibolite
DS2783B	.	.	X	.	.	X	.	.	.	.	.	X	.	.	.	X	.	.	.		Hbl-Bio Schist

SAMPLE	Qtz	Plag	Ksp	Perth	Biot	Gard	Cord	Opx	Cpx	Sill	Amph	Musc	Chl	Hcr	Apat	Zirc	Tcm	Cpx	Rdl	Epid	OTHERS	LITHOLOGY
ELBOW LAKE																						
EB1083A	.	X	.	X	.	V	.	V	.	X	.	X	.	X	.	.	.	X	.	X	.	Gt-Cord Schist
EB1383	.	X	.	X	.	X	.	X	.	X	.	.	.	.	.	.	.	X	.	.	.	Bio-Gt Schist
HIGHSTONE LAKE																						
HS1183A	.	X	.	X	.	.	.	X	.	.	.	X	.	.	.	.	R	.	X	.	X	Bio-Granulite
HS1183C	.	X	.	X	.	.	.	X	.	X	.	X	.	X	.	.	.	.	.	.	.	Opx-Amphibolite
HS1483C	.	X	.	X	.	.	.	X	.	X	.	.	.	.	.	R	.	R	.	X	.	Bio-Gt Pelite
HS1583C	.	X	.	X	.	.	.	X	.	X	.	X	.	.	.	R	.	.	X	.	.	Gt-Granulite
IDAHO LAKE ROAD																						
ID1083A	.	X	.	X	.	X	.	.	.	X	.	.	.	.	.	.	X	.	X	.	.	Charnokite
ID1283A	.	.	X	.	X	.	.	.	.	.	.	.	.	R	.	R	.	X	.	.	2	Charnokite
ID1283C	.	X	.	.	.	X	.	X	.	.	.	.	.	.	.	.	.	X	.	.	.	Bio-Gt Pelite
ID1683A	.	X	.	.	.	X	.	X	.	X	.	.	.	.	.	R	.	.	X	.	.	Gt-Granulite
ID1683B	.	X	.	.	.	X	.	.	.	X	.	.	.	X	.	R	.	X	.	.	.	Opx-Amphibolite
ID1983C	.	.	X	.	.	X	.	.	.	X	.	.	.	X	.	.	.	.	.	.	.	Opx-Amphibolite
ID2083A	.	.	X	.	.	X	.	.	.	.	.	.	.	X	.	.	.	X	.	.	.	Amphibolite
LAC SEUL																						
LS17	.	X	.	.	.	X	.	X	.	.	.	.	.	.	.	R	.	R	.	X	.	Bio-Gt Wacke
LS25C	.	X	.	.	.	X	.	X	.	X	.	.	.	.	.	.	X	.	X	.	.	Gt-Granulite
LS28	.	X	.	.	.	X	.	.	.	X	.	.	.	.	.	.	X	.	X	.	.	Charnokite
LS32A	.	X	.	.	.	X	.	X	.	.	.	.	.	.	.	R	.	X	.	X	.	Gt-Orthogniess
LS42	.	.	X	.	X	.	X	.	X	.	.	.	.	R	.	.	.	X	.	.	.	Gt-Cord Pelite
LS49A	.	X	.	.	.	X	.	X	.	X	.	.	.	R	.	R	.	X	.	X	.	Gt-Granulite
LS51A	.	X	.	X	.	X	.	X	.	X	.	.	.	.	.	.	.	X	.	.	.	Gt-Cord Pelite
LS61B	.	X	.	.	.	X	.	X	.	.	.	.	.	R	.	.	X	.	X	.	.	Gt-Bio Wacke
LS66A	.	X	.	X	.	X	.	X	.	X	.	.	.	.	.	.	X	.	X	.	.	Gt-Bio Pelite
LS67	.	X	.	X	.	.	.	X	.	.	.	.	.	.	.	.	.	X	.	.	.	Orthogneiss
LS68	.	X	.	.	.	T	.	.	.	.	.	.	X	.	.	.	.	.	.	.	.	Amphibolite
LS69	.	X	.	.	.	X	.	X	.	.	.	.	.	.	.	.	X	.	X	.	.	Gt-Bio Pelite
LS76A	.	X	.	.	.	X	.	X	.	.	.	.	.	.	.	.	.	X	.	.	.	Gt-Bio Wacke
LS78	.	X	.	X	.	X	.	X	.	X	.	.	.	R	.	.	X	.	X	.	.	Gt-Cord Pelite
LS82C	.	?	X	.	X	.	X	.	X	.	.	.	.	.	.	.	.	X	.	.	.	Gt-Cord Pelite
LS85A	.	X	.	X	.	X	.	X	.	.	.	.	.	R	.	R	.	X	.	.	.	Gt-Orthogneiss
LS87	.	X	.	.	.	X	.	T	.	.	.	.	.	R	.	.	X	.	.	.	R	Orthogneiss
LS88B	.	X	.	.	.	X	.	.	.	X	.	X	.	X	.	.	.	X	.	.	.	Charnokite
LS92B	.	.	X	.	X	.	X	.	X	.	.	.	.	.	.	R	.	X	.	.	.	Gt-Cord Pelite

SAMPLE	Qtz	Plag	KPsar	Bati	Gtho	Cotd	OGrx	Cpxl	Opl	Cim	Spl	Ahc	Mrt	hcm	Ulr	Aid	Zpl	Cio	Tu	Eo	pa	Cia	OTHERS	LITHOLOGY
LAKE ST. JOSEPH																								
JS1083C	.	X	.	X	.	X	.	.	.	.	.	.	.	X	.	X	.	.	.	.	X	.		Phylite
JS1383A	.	X	.	X	.	.	.	.	.	.	.	.	.	X	.	X	.	X	.	.	X	.		Phylite
JS1483	.	X	.	X	.	X	.	.	.	.	.	.	.	.	.	.	.	.	.	.	.	.		Arkosic Quartzite
JS1683B	.	X	.	X	.	.	.	.	.	.	.	.	.	X	.	X	.	.	.	.	X	.		Phylite
JS1783B	.	X	.	X	.	X	.	.	.	.	.	.	.	.	.	X	.	X	.	.	.	.		Arkosic Wacke
JS1983A	.	X	.	X	.	X	.	.	.	.	.	.	.	X	.	T	.	X	.	X	.	.		Bio-Schist
JS1983B	.	.	X	.	.	X	.	.	.	.	.	.	X	.	T	.	.	X	.	.	.	T	.	Meta Basalt
JS2183A	.	X	.	X	.	X	.	.	.	.	.	.	.	X	.	T	.	X	.	.	X	.	.	Bio-Musc Schist
JS2283B	.	X	.	X	.	.	.	.	.	.	.	.	.	X	.	R	.	X	.	.	X	.	.	Bio Schist
JS2383C	.	X	.	T	.	X	.	.	.	.	.	.	.	X	.	R	.	.	.	.	X	.	.	Sta Stauro Schist
JS2483	.	.	X	.	.	.	.	.	.	.	.	.	X	.	.	X	.	X	.	.	.	X	.	T. Sph Phylite
JS2583	.	X	.	X	.	X	.	.	.	.	.	.	X	.	.	X	.	R	.	.	.	X	.	.	Gt-Mica Schist
JS2783	.	X	.	X	.	.	.	.	.	.	.	.	.	X	.	X	.	.	.	.	X	.	.	Phylite
JS2983	.	X	.	X	.	X	.	.	.	.	.	.	.	.	X	.	X	.	X	.	.	X	.	Bio-Gt Schist
JS3183	.	X	.	X	.	.	.	.	.	.	.	.	.	X	.	X	.	X	.	.	X	.	.	Phylite
JS3283	.	X	.	.	.	X	.	.	.	.	.	.	X	.	R	.	X	.	.	.	X	.	X	Amphibolite
JS3483A	.	X	.	.	.	X	.	.	.	.	.	.	.	X	.	X	.	.	.	.	.	X	.	Bio-Wacke
JS3483C	.	.	X	.	.	X	.	.	.	.	.	.	X	.	.	R	.	.	.	.	X	.	X	Meta Basalt
JS3583A	.	X	.	.	.	.	.	.	.	.	.	.	.	X	.	X	.	.	.	.	.	.	.	Phylite
JS3683A	.	X	.	X	.	.	.	.	.	.	.	.	.	2	.	.	.	X	.	.	.	.	.	Bio-Wacke
JS3883A	.	X	.	X	.	X	.	.	.	.	.	.	.	.	.	X	.	X	.	.	.	.	.	Bio-Gt Wacke
JS3983	.	.	X	.	V	.	X	.	.	.	.	.	X	.	.	.	.	.	.	.	X	.	.	Bio-Hbl Schist
MINISS LAKE																								
MN1083B	.	X	.	X	.	X	.	X	.	.	.	.	.	.	.	.	.	X	.	.	.	.	.	Bio-Gt Pelite
MN1283B	.	X	.	X	.	V	.	X	.	X	.	.	.	.	.	.	.	X	.	X	.	.	X	. Bio-Gt Pelite
MN1883	.	X	.	X	.	.	.	X	.	X	.	.	.	.	.	.	.	X	.	.	.	.	.	Bio-Gt Pelite
MN1983	.	X	.	X	.	X	.	X	.	X	.	.	.	.	.	R	.	R	.	X	.	.	R	. Bio-Gt Wacke
MN2183	.	X	.	X	.	.	.	X	.	X	.	.	.	.	.	.	R	.	X	.	.	.	.	Bio-Gt Wacke
MN2483	.	X	.	X	.	.	.	X	.	X	.	.	.	.	.	.	.	X	.	X	.	.	T	. Bio-Gt Schist
MN2583	.	X	.	X	.	X	.	.	.	.	.	.	.	.	.	.	.	X	.	X	.	.	.	Bio-Wacke
MN2783	.	V	.	X	.	.	.	X	.	.	.	.	X	.	.	.	X	.	.	.	.	.	.	Amphibolite

SAMPLE	Qtz	Plag	KPar	Sericite	Biotite	Chlorite	Garnet	Opaque	Cordierite	Sillimanite	Muscovite	Hornblende	Chlorite	Apatite	Zircon	Tourmaline	Epidote	Carbonate	OTHERS	LITHOLOGY
ST. RAPHAEL LAKE																				
RF1283	.	X	.	X	.	.	X	X	.	.	.	.	.	R	.	.	X	.	.	Bio-Gt Pelite
RF1483	.	X	X	X	.	X	X	.	.	.	.	.	.	.	X	X	.	.	.	Bio-Gt Wacke
RF1683B	.	.	X	.	.	X	.	.	.	.	.	.	.	.	X	X	.	.	.	Bio-Schist
RF1883B	.	X	X	X	.	X	X	.	.	.	.	.	R	R	X	X	.	.	.	Bio-Gt Wacke
RF1983	.	X	X	.	.	X	X	?	.	.	.	.	R	R	X	.	.	.	.	Bio-Gt Pelite
RF2183A	.	X	X	X	.	X	X	.	.	.	.	.	R	R	X	X	.	.	R	2 Bio-Gt Pelite
RF2283	.	X	X	X	.	X	X	X	.	.	.	.	R	.	.	X	.	.	.	R Gt-Cord Pelite
RF2583A	.	X	X	X	.	X	X	X	.	.	.	.	.	.	.	X	.	.	.	. Gt-Cord Pelite
RAGGED WOOD LAKE																				
RW1283B	.	X	X	.	.	X	X	V	X	.	.	.	R	.	.	X	.	.	.	R Gt-Granulite
RW1683B	.	.	X	.	.	T	.	.	X	X	.	X	.	.	X	.	.	.	.	. Amphibolite
RW1783B	.	.	X	.	.	.	.	.	X	X	.	X	.	.	X	.	.	.	.	. Amphibolite
RW1883C	.	X	X	.	.	X	.	.	X	.	.	.	.	.	.	X	X	.	.	. Bio-Schist
RW2083	.	X	X	X	X	X	.	.	X	.	.	.	.	.	X	X	.	.	.	. Arkosic Quartzite
RW2483	.	X	X	.	.	T	.	.	.	X	.	T	.	.	X	.	.	.	.	. Sph Cpx-Wacke
RW2583	.	X	X	X	.	X	X	.	.	.	.	.	R	.	X	X	.	.	.	R Bio-Gt Schist
VERMILION RIVER ROAD																				
VM1283	.	X	X	X	.	X	.	X	.	.	X	.	2	R	.	X	.	.	.	. Bio-Cord Schist
VM1483A	.	X	X	X	X	X	.	X	.	.	.	.	R	R	.	X	.	.	.	. Bio-Cord Wacke
VM1683	.	X	X	X	X	X	X	X	.	.	X	.	.	.	.	X	.	.	.	. Gt-Cord Schist
VM1983	.	X	X	.	.	X	X	.	.	.	.	.	2	R	.	X	.	.	.	. Bio-Gt Wacke
VM2183	.	X	X	X	X	X	X	X	.	.	X	.	.	.	.	X	.	.	.	. Gt-Cord Pelite
VM2283A	.	X	X	.	.	X	X	.	.	.	.	.	R	.	.	X	.	.	.	R Bio-Gt Pelite
VM2383A	.	X	X	.	.	X	X	.	.	.	.	.	R	.	X	X	.	.	.	. Bio-Gt Pelite
VM2683A	.	X	X	.	.	X	X	X	.	.	.	.	.	.	.	X	.	.	.	. Gt-Cord Pelite
VM2783	.	X	X	.	.	X	X	.	.	.	.	.	.	.	X	X	.	.	.	. Bio-Gt Wacke
VM3583B	.	X	X	V	.	V	X	X	X	.	.	.	.	.	.	X	.	.	.	. Gt-Cord Pelite
VM3883	.	X	X	.	X	X	X	X	.	.	.	.	.	.	X	X	.	.	.	. Gt-Cord Pelite
VM4383B	.	X	X	.	.	X	X	.	.	.	.	.	.	.	.	.	.	.	.	. Bio-Gt Wacke
VM4983	.	X	X	.	.	X	X	.	.	.	.	.	.	.	X	.	.	.	.	. Bio-Gt Wacke
VERMILION RIVER																				
VR1583	.	X	X	.	.	X	X	.	.	.	.	.	.	.	X	.	.	.	.	. Bio-Gt Wacke

VERMILION RIVER ROAD
Collected by K. R. Henke

SAMPLE	Qtz	Plag	KPsar	Pert	BIot	Gtd	Cordx	OOpx	CPxl	Sill	Amph	Mscr	Chrt	AZpm	Tcrd	CTurm	Eudi	OPaq	CApl	OTHERS	LITHOLOGY
VR13A	.	X	.	X	.	X	.	X	.	.	.	.	.	R	.	R	.	X	.	.	Gt-Cord Pelite
VR14	.	X	.	X	.	.	X	.	X	.	.	.	.	.	.	.	.	X	.	.	Bio-Gt Wacke
VR16	.	X	.	X	.	.	.	X	.	.	.	.	.	R	.	.	.	X	.	.	Bio-Schist
VR17A	.	X	.	X	.	.	X	.	X	.	.	.	.	R	.	R	.	X	.	.	Bio-Schist
VR18B	.	X	.	X	.	X	.	X	.	X	.	.	.	.	.	R	.	X	.	.	Leucosome
VR20A	.	X	.	X	.	.	X	.	X	.	X	.	.	.	.	R	.	X	.	.	Leucosome
VR20B	.	X	.	X	.	.	X	.	X	.	.	.	.	.	.	.	X	X	.	.	Leucosome
VR24	.	X	.	X	.	X	.	X	.	.	X	.	.	.	.	.	X	X	.	.	Charnokite
VR30A	.	X	.	X	.	X	.	X	.	X	.	.	.	R	.	.	.	X	.	.	Leucosome
VR31B	.	X	.	X	.	.	X	.	.	.	X	.	.	R	.	X	.	X	.	R	Charnokite
VR33C	.	X	.	X	.	X	.	X	.	X	.	.	.	R	.	R	.	X	.	.	Leucosome
VR33D	.	X	.	X	.	X	.	X	.	X	.	.	.	R	.	R	.	.	.	.	Leucosome
VR35	.	X	.	X	.	.	X	.	X	.	.	.	.	.	.	.	.	X	.	.	Leucosome
VR40A	.	X	.	X	.	X	.	X	.	X	.	.	.	R	.	R	X	X	.	.	Leucosome
VR52	.	X	.	X	.	X	.	X	.	.	.	.	.	R	.	R	.	.	.	.	Bio-Gt Pelite
VR57	.	X	.	X	.	.	X	.	X	.	X	.	.	.	.	.	.	.	.	.	Gt-Cord Pelite
VR58A	.	X	.	X	.	.	X	.	X	.	.	.	.	.	.	R	.	X	.	.	Gt-Cord Pelite
VR65	.	X	.	X	.	.	.	X	.	.	.	.	X	R	.	R	X	X	.	.	Bio-Wacke
VR66A	.	X	.	X	.	.	X	.	.	X	.	.	X	.	.	.	.	.	.	.	Bio-Granulite

APPENDIX C

MIRCOPROBE ANALYSES

APPENDIX C

MICROPROBE ANALYSES

I Amphibole
II Biotite
III Cordierite
IV Feldspar
V Garnet
VI Pyroxene

X_{Mg} = Mg/Fe+Mg

X_{Fe} = Fe/Fe+Mg

* calculated as Fe^{+2}

MICROPROBE ANALYSES

AMPHIBOLES

	BL1183A Hbl	CH2283 Cumm	DS1183 Hbl	DS1183 Cumm	DS2583A Hbl	HS1183C Hbl	ID1683B Hbl
SiO_2	42.67	54.12	46.56	54.52	42.43	43.05	49.37
TiO_2	2.50	0.05	0.63	0.02	0.22	1.74	0.79
Al_2O_3	10.26	0.54	9.66	0.60	4.53	10.74	7.09
FeO	18.07	23.23	11.77	17.22	5.77	15.92	9.31
MnO	0.43	0.65	0.45	1.08	0.12	0.40	0.15
MgO	9.91	18.72	15.12	21.95	19.17	11.13	17.39
CaO	11.34	1.63	11.24	1.53	12.64	11.55	11.85
Na_2O	1.62	0.20	1.00	0.21	0.55	1.41	1.20
K_2O	1.26	0.02	0.22	0.00	0.24	1.09	0.41
Total	98.06	99.16	96.65	97.13	85.67	97.03	97.56

Normalized moles based on $(O_{22}(OH)_2)$

Si	6.456	7.823	6.818	7.837	6.924	6.498	7.078
Al^{IV}	1.544	0.092	1.182	0.102	0.871	1.502	0.922
Al^{VI}	0.286	0.000	0.485	0.000	0.000	0.408	0.276
Ti	0.284	0.005	0.069	0.002	0.027	0.197	0.085
Mg_*	2.235	4.034	3.301	4.704	4.664	2.504	3.717
Fe	2.286	2.808	1.441	2.070	0.788	2.009	1.116
Mn	0.055	0.080	0.056	0.131	0.017	0.051	0.018
Na	0.475	0.056	0.284	0.059	0.174	0.413	0.334
Ca	1.838	0.252	1.764	0.236	2.210	1.868	1.820
K	0.243	0.004	0.041	0.000	0.050	0.210	0.075
Total	15.704	15.155	15.441	15.140	15.725	15.661	15.442
X_{Mg}	0.494	0.590	0.696	0.694	0.856	0.555	0.769
X_{Fe}	0.506	0.410	0.304	0.306	0.144	0.445	0.231

MICROPROBE ANALYSES

AMPHIBOLES

	ID2083A Hbl	JS1983B Hbl	JS2483 Hbl	JS3283 Hbl	JS3483C Hbl	RW1683B Hbl	RW1883C Cumm
SiO_2	43.96	50.45	49.27	50.04	49.39	42.14	53.03
TiO_2	1.32	0.15	0.00	0.33	0.15	1.68	0.02
Al_2O_3	10.69	5.96	6.23	5.28	4.76	11.51	0.92
FeO	14.29	11.15	15.58	11.16	16.10	16.04	26.73
MnO	0.15	0.37	0.28	0.35	0.27	0.41	0.76
MgO	12.66	15.67	12.51	16.49	12.54	10.86	16.47
CaO	11.70	11.78	12.24	11.19	12.02	11.61	0.90
Na_2O	1.52	0.34	0.00	0.84	0.38	1.66	0.07
K_2O	0.76	0.14	0.24	0.30	0.12	1.04	0.02
Total	97.05	96.01	96.35	95.98	95.73	96.95	98.92

Normalized moles based on $(O_{22}(OH)_2)$

Si	6.555	7.358	7.323	7.325	7.418	6.384	7.803
Al^{IV}	1.445	0.642	0.677	0.675	0.582	1.616	0.160
Al^{VI}	0.433	0.382	0.415	0.236	0.261	0.439	0.000
Ti	0.148	0.016	0.000	0.036	0.017	0.191	0.002
Mg_*	2.814	3.407	2.772	3.599	2.808	2.453	3.613
Fe	1.782	1.360	1.937	1.366	2.022	2.032	3.289
Mn	0.019	0.046	0.035	0.043	0.034	0.053	0.095
Na	0.439	0.096	0.000	0.238	0.111	0.488	0.020
Ca	1.869	1.841	1.949	1.755	1.934	1.885	0.142
K	0.145	0.026	0.046	0.056	0.023	0.201	0.004
Total	15.650	15.175	15.154	15.330	15.210	15.741	15.127
X_{Mg}	0.612	0.715	0.589	0.725	0.581	0.547	0.523
X_{Fe}	0.388	0.285	0.411	0.275	0.419	0.453	0.477

APPENDIX C II

BIOTITES

MICROPROBE ANALYSES

BIOTITE

	BL1083C	BL1083E	CH1183A	CH1283A	CH1483B	CH1683	CL1183A
SiO_2	35.18	34.19	36.53	38.45	38.21	37.36	35.13
TiO_2	3.52	3.07	1.79	2.83	2.71	2.39	3.91
Al_2O_3	16.61	15.99	19.32	19.47	20.03	18.85	16.41
FeO	16.50	23.09	18.43	17.26	17.37	19.29	18.74
MnO	0.00	0.07	0.02	0.05	0.00	0.03	0.11
MgO	12.75	9.69	9.72	11.39	10.87	10.14	11.73
CaO	0.17	0.13	0.09	0.07	0.10	0.05	0.25
Na_2O	0.37	0.29	0.15	0.00	0.14	0.00	0.26
K_2O	9.65	8.61	8.77	9.00	9.13	8.94	9.58
Total	94.75	95.13	94.82	98.52	98.56	97.05	96.12

Normalized moles based on $(O_{10}(OH)_2)$

Si_{IV}	2.678	2.667	2.759	2.767	2.752	2.764	2.664
Al_{VI}	1.322	1.333	1.241	1.233	1.248	1.236	1.336
Al	0.168	0.138	0.478	0.419	0.453	0.408	0.131
Ti_*	0.201	0.180	0.102	0.153	0.147	0.133	0.223
Fe	1.050	1.507	1.164	1.039	1.046	1.194	1.189
Mn	0.000	0.005	0.001	0.003	0.000	0.002	0.007
Mg	1.447	1.127	1.094	1.222	1.167	1.118	1.326
Ca	0.014	0.011	0.007	0.005	0.008	0.004	0.020
Na	0.055	0.044	0.022	0.000	0.020	0.000	0.038
K	0.937	0.857	0.845	0.826	0.839	0.844	0.927
Total	7.872	7.868	7.713	7.667	7.680	7.703	7.862
X_{Mg}	0.579	0.428	0.485	0.541	0.527	0.484	0.527
X_{Fe}	0.421	0.572	0.515	0.459	0.473	0.516	0.473

MICROPROBE ANALYSES

BIOTITES

	CL2283A	DS1683	DS2183B	DS2483	EB1083A	HS1483C	HS1583C
SiO_2	34.25	37.51	37.42	37.46	34.16	34.20	34.76
TiO_2	4.05	2.74	2.18	2.23	3.18	3.45	4.05
Al_2O_3	15.80	18.88	20.41	19.85	17.53	17.08	15.98
FeO	20.48	18.77	18.07	18.96	19.26	18.08	20.65
MnO	0.05	0.11	0.02	0.03	0.11	0.06	0.13
MgO	10.69	10.24	9.84	10.05	9.83	11.06	10.40
CaO	0.19	0.07	0.07	0.08	0.12	0.15	0.12
Na_2O	0.25	0.00	0.00	0.00	0.17	0.07	0.16
K_2O	9.22	9.00	8.90	8.96	9.36	9.12	9.19
Total	94.98	97.32	96.91	97.62	93.72	93.27	95.44

Normalized moles based on $(O_{10}(OH)_2)$

Si	2.654	2.762	2.749	2.746	2.661	2.659	2.676
Al^{IV}	1.346	1.238	1.251	1.254	1.339	1.341	1.324
Al^{VI}	0.097	0.400	0.516	0.462	0.270	0.224	0.126
Ti	0.236	0.152	0.120	0.123	0.186	0.202	0.234
Fe*	1.327	1.156	1.110	1.163	1.255	1.176	1.329
Mn	0.003	0.007	0.001	0.002	0.007	0.004	0.008
Mg	1.235	1.124	1.078	1.098	1.142	1.282	1.194
Ca	0.016	0.006	0.006	0.006	0.010	0.012	0.010
Na	0.038	0.000	0.000	0.000	0.026	0.011	0.024
K	0.911	0.845	0.834	0.838	0.930	0.904	0.902
Total	7.863	7.690	7.664	7.692	7.826	7.814	7.828
X_{Mg}	0.482	0.493	0.493	0.486	0.476	0.522	0.473
X_{Fe}	0.518	0.507	0.507	0.514	0.524	0.478	0.527

MICROPROBE ANALYSES

BIOTITES

	ID1283	ID1683A	JS2583	JS2983	JS3883A	LS17	LS42
SiO_2	37.55	38.25	36.45	38.00	38.19	37.68	37.41
TiO_2	3.04	5.05	1.30	1.78	2.02	2.11	3.58
Al_2O_3	17.64	16.98	21.78	18.02	18.76	19.74	18.68
FeO	16.19	16.35	21.97	19.81	17.01	20.82	18.51
MnO	0.03	0.03	0.03	0.07	0.11	0.11	0.03
MgO	12.19	12.00	7.06	10.29	11.99	9.36	10.04
CaO	0.06	0.08	0.08	0.08	0.07	0.04	0.03
Na_2O	0.00	0.21	0.10	0.28	0.17	0.07	0.00
K_2O	6.93	8.91	8.45	8.57	8.63	9.00	8.90
Total	93.63	97.86	97.22	96.90	96.95	98.93	97.18

Normalized moles based on $(O_{10}(OH)_2)$

Si	2.808	2.774	2.712	2.818	2.791	2.750	2.754
Al^{IV}	1.192	1.226	1.288	1.182	1.209	1.250	1.246
Al^{VI}	0.363	0.225	0.621	0.393	0.407	0.447	0.375
Ti	0.171	0.275	0.073	0.099	0.111	0.116	0.198
Fe*	1.013	0.992	1.367	1.229	1.040	1.271	1.140
Mn	0.002	0.002	0.002	0.004	0.007	0.007	0.002
Mg	1.359	1.297	0.783	1.138	1.306	1.018	1.102
Ca	0.005	0.006	0.006	0.006	0.005	0.003	0.002
Na	0.000	0.030	0.014	0.040	0.024	0.010	0.000
K	0.661	0.824	0.802	0.811	0.805	0.838	0.836
Total	7.574	7.652	7.669	7.721	7.704	7.710	7.655
X_{Mg}	0.573	0.567	0.364	0.481	0.557	0.445	0.492
X_{Fe}	0.427	0.433	0.636	0.519	0.443	0.555	0.508

MICROPROBE ANALYSES

BIOTITES

	LS51A	LS66A	LS69	LS76A	LS78	LS92B	MN1083B
SiO_2	37.40	38.13	36.81	37.56	37.54	38.87	37.72
TiO_2	3.33	2.83	2.43	2.73	3.05	3.61	2.84
Al_2O_3	17.83	18.47	17.82	17.86	18.87	17.43	18.49
FeO	17.38	17.61	19.42	17.26	18.51	16.39	18.14
MnO	0.01	0.06	0.02	0.03	0.00	0.00	0.08
MgO	10.91	11.72	10.47	11.63	10.02	12.91	11.15
CaO	0.03	0.05	0.04	0.01	0.01	0.05	0.10
Na_2O	0.00	0.03	0.13	0.00	0.00	0.00	0.04
K_2O	8.85	8.89	8.54	9.08	8.89	9.09	8.91
Total	95.74	97.79	95.68	96.16	96.89	98.35	97.47

Normalized moles based on $(O_{10}(OH)_2)$

Si	2.783	2.775	2.768	2.784	2.769	2.798	2.764
Al^{IV}	1.217	1.225	1.232	1.216	1.231	1.202	1.236
Al^{VI}	0.347	0.358	0.348	0.344	0.410	0.277	0.362
Ti	0.186	0.155	0.137	0.152	0.169	0.195	0.157
Fe^*	1.082	1.072	1.221	1.070	1.142	0.987	1.112
Mn	0.001	0.004	0.001	0.002	0.000	0.000	0.005
Mg	1.210	1.271	1.174	1.285	1.102	1.386	1.218
Ca	0.002	0.004	0.003	0.001	0.001	0.004	0.008
Na	0.000	0.004	0.019	0.000	0.000	0.000	0.006
K	0.840	0.825	0.819	0.859	0.837	0.835	0.833
Total	7.669	7.693	7.724	7.713	7.660	7.684	7.700
X_{Mg}	0.528	0.543	0.490	0.546	0.491	0.584	0.523
X_{Fe}	0.472	0.457	0.510	0.454	0.509	0.416	0.477

MICROPROBE ANALYSES

BIOTITES

	MN1883	MN1983	MN2183	RF1283	RF1483	RF1883	RF2183A
SiO_2	38.14	37.11	38.07	38.15	37.32	37.71	38.30
TiO_2	3.59	3.13	2.86	3.62	2.49	3.01	3.29
Al_2O_3	18.85	19.22	19.46	17.56	17.99	17.89	18.02
FeO	16.16	17.30	15.63	16.65	18.07	17.38	16.11
MnO	0.00	0.00	0.05	0.05	0.00	0.07	0.04
MgO	11.93	9.64	11.93	12.15	11.40	11.38	12.49
CaO	0.11	0.06	0.04	0.08	0.02	0.07	0.07
Na_2O	0.11	0.05	0.08	0.04	0.00	0.12	0.11
K_2O	9.09	8.88	9.14	8.99	9.06	9.04	8.93
Total	97.98	95.39	97.26	97.29	96.35	96.67	97.36

Normalized moles based on $(O_{10}(OH)_2)$

Si_{IV}	2.754	2.767	2.761	2.784	2.772	2.782	2.783
Al_{VI}	1.246	1.233	1.239	1.216	1.228	1.218	1.217
Al	0.359	0.456	0.424	0.295	0.347	0.338	0.325
Ti	0.195	0.176	0.156	0.199	0.139	0.167	0.180
Fe*	0.976	1.079	0.948	1.016	1.122	1.072	0.979
Mn	0.000	0.000	0.003	0.003	0.000	0.004	0.002
Mg	1.284	1.072	1.290	1.322	1.262	1.252	1.353
Ca	0.009	0.005	0.003	0.006	0.002	0.006	0.005
Na	0.015	0.007	0.011	0.006	0.000	0.017	0.015
K	0.837	0.845	0.845	0.837	0.858	0.851	0.828
Total	7.675	7.639	7.680	7.683	7.731	7.707	7.688
X_{Mg}	0.568	0.498	0.576	0.565	0.529	0.539	0.580
X_{Fe}	0.432	0.502	0.424	0.435	0.471	0.461	0.420

MICROPROBE ANALYSES

BIOTITES

	RF2283	RF2583A	RW1283B	RW2583	VM1683	VM2183	VM2683A
SiO_2	36.79	37.28	36.08	34.96	37.28	36.23	37.14
TiO_2	2.68	2.94	3.17	3.66	2.02	2.52	2.54
Al_2O_3	18.77	18.60	16.92	16.07	20.63	20.10	19.26
FeO	17.51	17.09	16.35	17.87	19.59	18.42	17.09
MnO	0.02	0.06	0.07	0.00	0.03	0.14	0.00
MgO	10.42	10.86	12.27	12.16	8.63	8.85	10.74
CaO	0.05	0.08	0.12	0.17	0.07	0.10	0.08
Na_2O	0.04	0.00	0.30	0.08	0.00	0.00	0.00
K_2O	8.78	8.78	9.23	9.58	8.87	8.61	9.01
Total	95.06	95.69	94.51	94.55	97.12	94.97	95.86

Normalized moles based on $(O_{10}(OH)_2)$

Si	2.759	2.769	2.734	2.684	2.751	2.728	2.755
Al^{IV}	1.241	1.231	1.266	1.316	1.249	1.272	1.245
Al^{VI}	0.418	0.398	0.245	0.138	0.545	0.511	0.439
Ti	0.151	0.164	0.181	0.211	0.112	0.143	0.142
Fe^*	1.098	1.062	1.036	1.147	1.209	1.160	1.060
Mn	0.001	0.004	0.004	0.000	0.002	0.009	0.000
Mg	1.165	1.203	1.386	1.392	0.949	0.993	1.188
Ca	0.004	0.006	0.010	0.014	0.006	0.008	0.006
Na	0.006	0.000	0.044	0.012	0.000	0.000	0.000
K	0.840	0.832	0.892	0.938	0.835	0.827	0.853
Total	7.683	7.668	7.798	7.853	7.658	7.651	7.688
X_{Mg}	0.515	0.531	0.572	0.548	0.440	0.461	0.528
X_{Fe}	0.485	0.469	0.428	0.452	0.560	0.539	0.472

MICROPROBE ANALYSES

BIOTITES

	VM2783	VM3583B	VM3883B	VM4383	VM4983	VR13A	VR1583
SiO_2	37.75	37.10	37.56	37.46	37.24	37.38	35.61
TiO_2	2.48	3.08	3.96	3.66	2.37	2.55	3.10
Al_2O_3	18.09	17.99	17.07	17.37	18.67	20.23	18.12
FeO	18.16	17.89	17.33	17.56	17.07	17.76	18.87
MnO	0.08	0.05	0.03	0.07	0.00	0.05	0.08
MgO	10.72	10.69	11.41	11.21	11.63	9.41	11.15
CaO	0.08	0.05	0.07	0.07	0.05	0.05	0.11
Na_2O	0.03	0.06	0.00	0.00	0.06	0.03	0.24
K_2O	8.71	8.94	9.04	9.16	8.96	8.85	9.87
Total	96.10	95.85	96.47	96.56	96.05	96.31	97.15

Normalized moles based on $(O_{10}(OH)_2)$

Si	2.804	2.769	2.780	2.775	2.759	2.759	2.664
Al^{IV}	1.196	1.231	1.220	1.225	1.241	1.241	1.336
Al^{VI}	0.387	0.351	0.269	0.291	0.389	0.519	0.262
Ti	0.139	0.173	0.220	0.204	0.132	0.142	0.174
Fe*	1.128	1.117	1.073	1.088	1.058	1.096	1.181
Mn	0.005	0.003	0.002	0.004	0.000	0.003	0.005
Mg	1.187	1.189	1.259	1.238	1.284	1.036	1.244
Ca	0.006	0.004	0.006	0.006	0.004	0.004	0.009
Na	0.004	0.009	0.000	0.000	0.009	0.004	0.035
K	0.825	0.851	0.853	0.866	0.847	0.833	0.942
Total	7.681	7.697	7.682	7.696	7.722	7.638	7.851
X_{Mg}	0.513	0.516	0.540	0.532	0.548	0.486	0.513
X_{Fe}	0.487	0.484	0.460	0.468	0.452	0.514	0.487

APPENDIX C III

CORDIERITE

MICROPROBE ANALYSIS

CORDIERITE

	CH1283A	DS2183B	EB1083A	LS42	LS51A	LS78	RF2283
SiO_2	46.64	47.64	47.93	48.39	47.75	46.79	47.42
TiO_2	0.00	0.00	0.00	0.02	0.00	0.00	0.02
Al_2O_3	35.60	36.62	33.52	36.81	36.31	35.68	36.51
FeO	6.97	8.05	7.31	7.35	6.39	6.91	7.00
MnO	0.00	0.28	0.00	0.05	0.03	0.17	0.00
MgO	8.71	8.34	8.78	8.81	9.15	8.21	8.89
CaO	0.00	0.07	0.03	0.00	0.02	0.05	0.07
Na_2O	0.00	0.18	0.11	0.00	0.00	0.00	0.00
K_2O	0.00	0.01	0.02	0.02	0.00	0.00	0.00
Total	97.92	101.19	97.70	101.45	99.65	97.81	99.91

Normalized moles based on 11 total cations and 18(O)

Si	4.776	4.736	4.932	4.789	4.793	4.808	4.757
Al^{IV}	1.224	1.264	1.068	1.211	1.207	1.192	1.243
Al^{VI}	3.073	3.028	2.996	3.083	3.089	3.128	3.074
Ti	0.000	0.000	0.000	0.001	0.000	0.000	0.002
Fe^{+3}	0.150	0.272	0.096	0.126	0.118	0.064	0.166
Mg	1.330	1.236	1.347	1.300	1.369	1.258	1.330
Fe^{+2}	0.447	0.397	0.533	0.482	0.418	0.530	0.421
Mn	0.000	0.024	0.000	0.004	0.003	0.015	0.000
Na	0.000	0.035	0.022	0.000	0.000	0.000	0.000
Ca	0.000	0.007	0.003	0.000	0.002	0.006	0.008
K	0.000	0.001	0.003	0.003	0.000	0.000	0.000
Total	11.000	11.000	11.000	11.000	11.000	11.000	11.000
X_{Mg}	0.690	0.649	0.682	0.681	0.719	0.679	0.694
X_{Fe}	0.310	0.351	0.318	0.319	0.281	0.321	0.306

MICROPROBE ANALYSES

CORDIERITE

	RF2583A	RW1283B	VM2183	VM2683A	VM3583B	VM3883B	VR13A
SiO_2	47.55	47.45	47.09	47.46	46.98	45.21	46.60
TiO_2	0.00	0.02	0.00	0.02	0.00	0.00	0.00
Al_2O_3	36.21	35.87	35.61	36.28	36.00	34.48	35.65
FeO	7.05	6.31	8.40	7.26	7.24	5.76	7.96
MnO	0.05	0.00	0.28	0.10	0.00	0.10	0.16
MgO	8.80	9.50	7.69	9.00	8.77	9.05	7.97
CaO	0.06	0.03	0.15	0.02	0.02	0.02	0.00
Na_2O	0.00	0.00	0.13	0.10	0.16	0.20	0.00
K_2O	0.03	0.00	0.00	0.02	0.03	0.03	0.00
Total	99.75	99.18	99.35	100.26	99.20	94.85	98.34

Normalized moles based on 11 total cations and 18(O)

Si	4.782	4.779	4.787	4.744	4.745	4.750	4.778
Al^{IV}	1.218	1.221	1.213	1.256	1.255	1.250	1.222
Al^{VI}	3.073	3.037	3.054	3.018	3.031	3.020	3.085
Ti	0.000	0.002	0.000	0.002	0.000	0.000	0.000
Fe^{+3}	0.148	0.180	0.184	0.258	0.260	0.274	0.136
Mg	1.319	1.426	1.166	1.341	1.321	1.418	1.218
Fe^{+2}	0.445	0.352	0.530	0.349	0.352	0.232	0.547
Mn	0.004	0.000	0.024	0.008	0.000	0.009	0.014
Na	0.000	0.000	0.026	0.019	0.031	0.041	0.000
Ca	0.006	0.003	0.016	0.002	0.002	0.002	0.000
K	0.004	0.000	0.000	0.003	0.004	0.004	0.000
Total	11.000	11.000	11.000	11.000	11.000	11.000	11.000
X_{Mg}	0.690	0.729	0.620	0.688	0.683	0.737	0.641
X_{Fe}	0.310	0.271	0.380	0.312	0.317	0.263	0.359

APPENDIX C IV

FELDSPAR

$$X_{an} = Ca/Ca+Na+K$$

$$X_{ab} = Na/Ca+Na+K$$

$$X_{or} = K/Ca+Na+K$$

(all iron assumed trivalent)

MICROPROBE ANALYSES

FELDSPARS

	BL1083E Plag	BL1183A Plag	CH1283A Plag	CL2283A Plag	DS1183 Plag	DS2183B Plag	EB1083A Plag	G1A Plag
SiO_2	57.03	54.62	62.67	59.07	56.08	62.96	62.63	59.49
Al_2O_3	26.19	27.76	24.15	25.14	28.63	24.01	24.31	25.72
Fe_2O_3	0.10	0.17	0.00	0.00	0.16	0.09	0.06	0.07
CaO	8.02	9.68	5.09	6.86	10.66	4.76	5.35	7.47
Na_2O	6.82	5.74	8.69	7.31	5.55	9.05	8.78	7.17
K_2O	0.14	0.30	0.30	0.35	0.09	0.26	0.20	0.31
Total	98.30	98.27	100.90	98.73	101.17	101.13	101.33	100.23

Normalized moles based on 5 total cations

Si	2.593	2.497	2.753	2.669	2.498	2.754	2.739	2.652
Al	1.403	1.496	1.250	1.339	1.503	1.238	1.253	1.351
Fe^{+3}	0.004	0.006	0.000	0.000	0.006	0.003	0.002	0.003
Na	0.601	0.509	0.740	0.640	0.479	0.768	0.744	0.620
Ca	0.391	0.474	0.240	0.332	0.509	0.223	0.251	0.357
K	0.008	0.017	0.017	0.020	0.005	0.015	0.011	0.018
Total	5.000	5.000	5.000	5.000	5.000	5.000	5.000	5.000
O	7.992	7.985	8.000	8.008	8.010	7.983	7.988	8.010
X_{an}	0.391	0.474	0.240	0.335	0.512	0.222	0.249	0.359
X_{ab}	0.601	0.509	0.743	0.645	0.483	0.764	0.740	0.623
X_{or}	0.008	0.017	0.017	0.020	0.005	0.014	0.011	0.018

MICROPROBE ANALYSES

FELDSPARS

	G63B Plag	HS1183C Plag	HS1583C Plag	ID1083A Plag	ID1683A Plag	ID1683B Plag	ID2083A Plag	JS1983B Plag
SiO_2	54.13	57.65	55.26	48.34	61.39	48.85	57.31	45.63
Al_2O_3	29.41	27.05	27.39	34.31	24.72	32.86	27.36	35.43
Fe_2O_3	0.00	0.09	0.11	0.00	0.10	0.08	0.08	0.13
CaO	11.58	8.67	9.35	16.50	5.98	16.04	9.22	18.78
Na_2O	4.85	6.45	5.76	2.45	8.17	2.87	6.13	1.20
K_2O	0.11	0.37	0.08	0.00	0.36	0.00	0.11	0.14
Total	100.08	100.28	97.95	101.60	100.72	100.70	100.21	101.31

Normalized moles based on 5 total cations

Si	2.444	2.577	2.537	2.173	2.709	2.212	2.569	2.072
Al	1.565	1.425	1.482	1.818	1.286	1.754	1.446	1.896
Fe^{+3}	0.000	0.003	0.004	0.000	0.004	0.003	0.003	0.005
Na	0.425	0.559	0.513	0.214	0.699	0.252	0.533	0.106
Ca	0.560	0.415	0.460	0.795	0.283	0.778	0.443	0.914
K	0.006	0.021	0.005	0.000	0.020	0.000	0.006	0.008
Total	5.000	5.000	5.000	5.000	5.000	5.000	5.000	5.000
O	8.011	8.001	8.021	7.976	7.994	7.965	8.024	7.965
X_{an}	0.565	0.417	0.471	0.788	0.282	0.755	0.451	0.889
X_{ab}	0.428	0.562	0.525	0.212	0.698	0.245	0.543	0.103
X_{or}	0.006	0.021	0.005	0.000	0.020	0.000	0.006	0.008

MICROPROBE ANALYSES

FELDSPARS

	JS2583 Plag	JS3283 Plag	JS3483C Plag	LS42 Plag	LS51A Plag	LS78 Plag	MB8A Plag	MN1083 Kspar
SiO_2	60.38	62.81	67.04	61.61	60.55	61.68	62.20	63.60
Al_2O_3	25.32	23.49	19.74	24.02	20.07	24.34	24.64	18.87
Fe_2O_3	0.11	0.16	0.40	0.14	0.15	0.00	0.00	0.00
CaO	6.68	4.89	0.97	5.21	5.49	5.33	6.18	0.55
Na_2O	8.11	8.90	10.73	8.84	8.38	8.79	7.84	1.34
K_2O	0.15	0.17	0.11	0.25	0.27	0.27	0.37	15.47
Total	100.75	100.42	98.99	100.07	94.91	100.41	101.23	99.83

Normalized moles based on 5 total cations

Si	2.663	2.771	2.976	2.724	2.835	2.718	2.739	2.924
Al	1.316	1.221	1.033	1.252	1.107	1.264	1.279	1.022
Fe^{+3}	0.004	0.006	0.015	0.005	0.006	0.000	0.000	0.000
Na	0.693	0.761	0.924	0.758	0.761	0.751	0.669	0.119
Ca	0.316	0.231	0.046	0.247	0.275	0.252	0.292	0.027
K	0.008	0.010	0.006	0.014	0.016	0.015	0.021	0.907
Total	5.000	5.000	5.000	5.000	5.000	5.000	5.000	5.000
O	7.972	7.999	8.035	7.967	8.003	7.967	8.034	7.922
X_{an}	0.310	0.231	0.047	0.242	0.262	0.247	0.297	0.026
X_{ab}	0.682	0.760	0.946	0.744	0.723	0.738	0.682	0.113
X_{or}	0.008	0.010	0.006	0.014	0.015	0.015	0.021	0.861

MICROPROBE ANALYSES

FELDSPARS

	MN1083 Plag	MN1983 Kspar	MN1983 Plag	RF2283 Plag	RF2583A Plag	RW1283B Plag	VM1683 Plag	VM1683 Plag
SiO_2	61.24	63.97	61.69	62.95	62.15	61.47	62.30	63.42
Al_2O_3	24.19	18.90	24.25	24.48	24.16	24.52	23.61	18.64
Fe_2O_3	0.00	0.11	0.05	0.08	0.04	0.00	0.07	0.00
CaO	5.41	0.51	5.07	5.35	5.37	5.92	4.46	0.27
Na_2O	8.46	1.10	8.55	8.68	8.75	8.22	9.08	1.28
K_2O	0.15	15.78	0.25	0.31	0.38	0.27	0.24	15.51
Total	99.45	100.37	99.86	101.85	100.85	100.40	99.76	99.12

Normalized moles based on 5 total cations

Si	2.730	2.930	2.738	2.741	2.729	2.720	2.760	2.938
Al	1.271	1.020	1.269	1.256	1.250	1.279	1.233	1.018
Fe^{+3}	0.000	0.004	0.002	0.003	0.001	0.000	0.003	0.000
Na	0.731	0.098	0.736	0.733	0.745	0.705	0.780	0.115
Ca	0.258	0.025	0.241	0.250	0.253	0.281	0.212	0.013
K	0.009	0.922	0.014	0.017	0.021	0.015	0.014	0.916
Total	5.000	5.000	5.000	5.000	5.000	5.000	5.000	5.000
O	7.996	7.933	7.999	7.996	7.972	7.999	7.981	7.931
X_{an}	0.259	0.024	0.243	0.250	0.248	0.280	0.211	0.013
X_{ab}	0.733	0.094	0.742	0.733	0.731	0.704	0.776	0.110
X_{or}	0.009	0.883	0.014	0.017	0.021	0.015	0.013	0.877

MICROPROBE ANALYSES

FELDSPARS

	VM1683 Plag	VM2183 Plag	VM2683A Plag	VM3583B Plag	VM3883B Plag	VR13A Plag
SiO_2	62.17	62.98	61.66	61.40	60.09	61.91
Al_2O_3	23.13	24.21	24.12	24.09	25.07	24.29
Fe_2O_3	0.00	0.00	0.04	0.13	0.13	0.14
CaO	4.50	5.42	5.52	5.74	6.97	5.34
Na_2O	8.93	8.54	8.59	8.41	7.51	8.82
K_2O	0.25	0.32	0.27	0.35	0.28	0.26
Total	98.98	101.47	100.20	100.12	100.05	100.76

Normalized moles based on 5 total cations

Si	2.778	2.755	2.727	2.722	2.679	2.720
Al	1.218	1.248	1.257	1.258	1.318	1.258
Fe^{+3}	0.000	0.000	0.001	0.005	0.005	0.005
Na	0.774	0.724	0.737	0.723	0.649	0.751
Ca	0.215	0.254	0.262	0.273	0.333	0.251
K	0.014	0.018	0.015	0.020	0.016	0.015
Total	5.000	5.000	5.000	5.000	5.000	5.000
O	7.993	8.008	7.981	7.982	8.008	7.968
X_{an}	0.215	0.255	0.258	0.269	0.334	0.247
X_{ab}	0.771	0.727	0.727	0.712	0.650	0.739
X_{or}	0.014	0.018	0.015	0.019	0.016	0.014

APPENDIX C V

GARNET

X_{py} = Mg/Mg+Fe+Ca+Mn

X_{al} = Fe/Mg+Fe+Ca+Mn

X_{sp} = Mn/Mg+Fe+Ca+Mn

X_{gr} = Ca/Mg+Fe+Ca+Mn

MICROPROBE ANALYSES

GARNETS

	BL1083C	BL1083E	CH1183A	CH1283A	CH1483B	CH1683	CL1183A
SiO_2	37.28	36.34	38.36	38.78	37.41	38.30	37.02
Al_2O_3	21.90	20.98	21.10	21.28	20.53	20.75	21.72
FeO	32.51	34.00	30.23	30.90	31.58	31.45	32.17
MnO	0.74	2.27	7.08	2.05	1.58	4.61	1.16
MgO	7.69	4.47	3.75	6.36	6.03	4.30	7.40
CaO	1.09	2.65	0.88	0.83	0.80	1.03	0.93
Total	101.21	100.71	101.40	100.20	97.93	100.44	100.40

Normalized moles based on 8 total cations

Si	2.880	2.880	3.037	3.047	3.017	3.049	2.888
Al^{IV}	0.120	0.120	0.000	0.000	0.000	0.000	0.112
Al^{VI}	1.875	1.840	1.969	1.971	1.951	1.947	1.886
Mg	0.886	0.528	0.443	0.745	0.725	0.510	0.861
Fe^*	2.101	2.254	2.002	2.031	2.130	2.094	2.099
Mn	0.048	0.152	0.475	0.136	0.108	0.311	0.077
Ca	0.090	0.225	0.075	0.070	0.069	0.088	0.078
Total	8.000	8.000	8.000	8.000	8.000	8.000	8.000
O	11.878	11.860	12.022	12.033	11.993	12.023	11.887

X_{py}	0.283	0.167	0.148	0.250	0.239	0.170	0.276
X_{al}	0.672	0.713	0.669	0.681	0.702	0.697	0.674
X_{sp}	0.015	0.048	0.159	0.046	0.036	0.104	0.025
X_{gr}	0.029	0.071	0.025	0.023	0.023	0.029	0.025

MICROPROBE ANALYSES

GARNETS

	CL2283A	DS1683	DS2183B	DS2483	EB1083A	G1A	G63B
SiO_2	36.70	37.97	37.87	38.22	35.39	38.28	39.16
Al_2O_3	21.26	21.16	21.13	21.01	20.53	20.06	21.31
FeO	31.76	30.70	31.11	30.86	35.13	29.36	28.80
MnO	1.95	4.06	4.03	5.32	1.23	3.91	2.46
MgO	6.00	4.93	4.74	3.58	4.40	4.58	6.67
CaO	1.58	1.16	0.81	1.25	0.96	2.53	2.43
Total	99.25	99.98	99.69	100.24	97.64	98.72	100.83

Normalized moles based on 8 total cations

Si	2.918	3.019	3.025	3.058	2.901	3.083	3.042
Al^{IV}	0.082	0.000	0.000	0.000	0.099	0.000	0.000
Al^{VI}	1.911	1.983	1.990	1.982	1.884	1.904	1.951
Mg_*	0.711	0.584	0.565	0.427	0.538	0.550	0.772
Fe	2.112	2.041	2.079	2.065	2.408	1.978	1.871
Mn	0.131	0.273	0.273	0.361	0.085	0.267	0.162
Ca	0.135	0.099	0.069	0.107	0.084	0.218	0.202
Total	8.000	8.000	8.000	8.000	8.000	8.000	8.000
O	11.915	12.011	12.020	12.049	11.893	12.035	12.017
X_{py}	0.230	0.195	0.189	0.144	0.173	0.183	0.257
X_{al}	0.684	0.681	0.696	0.698	0.773	0.656	0.622
X_{sp}	0.043	0.091	0.091	0.122	0.027	0.089	0.054
X_{gr}	0.044	0.033	0.023	0.036	0.027	0.072	0.067

MICROPROBE ANALYSES

GARNETS

	HS1483C	HS1583C	ID1283	ID1683A	JS2583	JS2983	JS3883A
SiO_2	36.05	38.17	38.53	38.95	37.60	38.31	37.06
Al_2O_3	20.86	21.23	20.80	21.45	20.86	21.25	20.27
FeO	34.04	29.70	30.47	29.02	33.45	30.09	27.46
MnO	0.68	3.17	1.19	1.45	2.11	4.14	7.37
MgO	5.60	4.22	7.05	8.07	2.39	2.96	3.82
CaO	1.19	3.21	0.83	1.03	2.37	3.33	1.86
Total	98.42	99.70	98.87	99.97	98.78	100.08	97.84

Normalized moles based on 8 total cations

Si	2.904	3.040	3.054	3.029	3.068	3.065	3.030
Al^{IV}	0.096	0.000	0.000	0.000	0.000	0.000	0.000
Al^{VI}	1.885	1.993	1.943	1.966	2.006	2.003	1.953
Mg	0.673	0.501	0.833	0.936	0.291	0.353	0.466
Fe*	2.293	1.978	2.020	1.888	2.282	2.013	1.878
Mn	0.046	0.214	0.080	0.096	0.146	0.281	0.510
Ca	0.103	0.274	0.070	0.086	0.207	0.285	0.163
Total	8.000	8.000	8.000	8.000	8.000	8.000	8.000
O	11.895	12.036	12.025	12.012	12.071	12.066	12.007
X_{py}	0.216	0.169	0.277	0.311	0.099	0.120	0.154
X_{al}	0.736	0.667	0.673	0.628	0.780	0.687	0.622
X_{sp}	0.015	0.072	0.027	0.032	0.050	0.096	0.169
X_{gr}	0.033	0.092	0.023	0.029	0.071	0.097	0.054

MICROPROBE ANALYSES

GARNETS

	LS17	LS42	LS51A	LS66A	LS69	LS76A	LS78
SiO_2	39.27	39.35	39.27	39.73	38.93	39.26	38.88
Al_2O_3	21.59	21.47	21.00	21.71	21.26	21.50	20.91
FeO	32.20	32.48	29.51	31.18	31.60	30.54	31.26
MnO	4.42	1.54	0.97	2.30	1.39	2.10	1.59
MgO	4.20	6.22	7.82	6.72	5.97	7.08	5.80
CaO	0.93	0.84	0.79	1.02	1.18	0.89	0.79
Total	102.61	101.90	99.36	102.66	100.33	101.37	99.23

Normalized moles based on 8 total cations

Si	3.061	3.048	3.079	3.043	3.061	3.037	3.095
Al^{IV}	0.000	0.000	0.000	0.000	0.000	0.000	0.000
Al^{VI}	1.983	1.960	1.941	1.960	1.970	1.960	1.962
Mg_*	0.488	0.718	0.914	0.767	0.700	0.816	0.688
Fe^*	2.099	2.104	1.935	1.997	2.078	1.976	2.081
Mn	0.292	0.101	0.064	0.149	0.093	0.138	0.107
Ca	0.078	0.070	0.066	0.084	0.099	0.074	0.067
Total	8.000	8.000	8.000	8.000	8.000	8.000	8.000
O	12.052	12.027	12.050	12.023	12.046	12.017	12.076
X_{py}	0.165	0.240	0.307	0.256	0.236	0.272	0.234
X_{al}	0.710	0.703	0.649	0.666	0.700	0.658	0.707
X_{sp}	0.099	0.034	0.022	0.050	0.031	0.046	0.036
X_{gr}	0.026	0.023	0.022	0.028	0.033	0.025	0.023

MICROPROBE ANALYSES

GARNETS

	LS92B	MB8A	MN1083B	MN1883	MN1983	MN2183	RF1283
SiO_2	39.76	38.86	38.74	39.02	38.35	38.60	39.16
Al_2O_3	21.51	21.19	21.38	21.52	20.68	21.40	21.37
FeO	27.86	28.98	30.27	29.96	31.13	30.45	29.44
MnO	1.11	2.96	1.55	1.19	2.43	1.61	1.00
MgO	9.50	6.77	7.12	8.11	5.62	6.93	8.15
CaO	0.86	1.57	0.98	0.89	0.74	0.93	0.90
Total	100.60	100.33	100.04	100.69	98.95	99.92	100.02

Normalized moles based on 8 total cations

Si	3.046	3.037	3.032	3.016	3.068	3.028	3.044
Al^{IV}	0.000	0.000	0.000	0.000	0.000	0.000	0.000
Al^{VI}	1.942	1.952	1.972	1.961	1.950	1.979	1.958
Mg	1.085	0.789	0.831	0.935	0.670	0.810	0.944
Fe*	1.785	1.894	1.981	1.937	2.083	1.998	1.914
Mn	0.072	0.196	0.103	0.078	0.165	0.107	0.066
Ca	0.071	0.131	0.082	0.074	0.063	0.078	0.075
Total	8.000	8.000	8.000	8.000	8.000	8.000	8.000
O	12.017	12.013	12.018	11.997	12.043	12.017	12.022
X_{py}	0.360	0.262	0.277	0.309	0.225	0.271	0.315
X_{al}	0.593	0.629	0.661	0.641	0.699	0.667	0.638
X_{sp}	0.024	0.065	0.034	0.026	0.055	0.036	0.022
X_{gr}	0.023	0.044	0.027	0.024	0.021	0.026	0.025

MICROPROBE ANALYSES

GARNETS

	RF1483	RF1883	RF2183A	RF2283	RF2583A	RW1283B	RW2583
SiO_2	39.19	38.44	39.11	38.31	37.89	39.13	37.11
Al_2O_3	20.88	21.28	21.50	21.22	20.81	21.01	21.59
FeO	30.13	29.89	29.25	32.21	30.59	28.89	33.35
MnO	2.04	2.19	1.20	1.42	1.68	1.23	1.22
MgO	7.37	6.84	7.81	5.73	6.53	7.88	6.50
CaO	0.98	1.11	1.02	0.83	0.78	1.01	1.24
Total	100.59	99.75	99.89	99.72	98.28	99.15	101.01

Normalized moles based on 8 total cations

Si_{IV}	3.051	3.022	3.048	3.038	3.031	3.071	2.896
Al_{VI}	0.000	0.000	0.000	0.000	0.000	0.000	0.104
Al	1.916	1.972	1.975	1.983	1.962	1.944	1.882
Mg	0.855	0.802	0.907	0.677	0.779	0.922	0.756
Fe	1.962	1.965	1.906	2.136	2.047	1.896	2.177
Mn	0.135	0.146	0.079	0.095	0.114	0.082	0.081
Ca	0.082	0.093	0.085	0.071	0.067	0.085	0.104
Total	8.000	8.000	8.000	8.000	8.000	8.000	8.000
O	12.009	12.008	12.035	12.029	12.013	12.043	11.889
X_{py}	0.282	0.267	0.305	0.227	0.259	0.309	0.243
X_{al}	0.647	0.654	0.640	0.717	0.681	0.635	0.698
X_{sp}	0.044	0.049	0.027	0.032	0.038	0.027	0.026
X_{gr}	0.027	0.031	0.029	0.024	0.022	0.028	0.033

MICROPROBE ANALYSES

GARNETS

	VM1683	VM2183	VM2683A	VM2783	VM3583B	VM3883B	VM4383
SiO_2	37.28	37.43	38.68	38.76	38.59	39.02	39.33
Al_2O_3	20.38	20.88	20.93	21.11	20.96	21.03	21.28
FeO	30.19	30.36	31.85	30.19	31.27	30.43	30.98
MnO	5.71	5.17	1.99	3.57	0.91	1.39	1.55
MgO	3.72	4.10	5.80	5.31	6.99	6.97	7.28
CaO	0.68	0.85	0.88	1.66	0.81	1.06	0.84
Total	97.96	98.79	100.13	100.60	99.53	99.90	101.26

Normalized moles based on 8 total cations

Si	3.054	3.030	3.056	3.052	3.041	3.062	3.043
Al^{IV}	0.000	0.000	0.000	0.000	0.000	0.000	0.000
Al^{VI}	1.968	1.992	1.949	1.959	1.947	1.945	1.941
Mg	0.454	0.495	0.683	0.623	0.821	0.815	0.840
Fe*	2.068	2.055	2.104	1.988	2.061	1.997	2.005
Mn	0.396	0.354	0.133	0.238	0.061	0.092	0.102
Ca	0.060	0.074	0.074	0.140	0.068	0.089	0.070
Total	8.000	8.000	8.000	8.000	8.000	8.000	8.000
O	12.038	12.026	12.030	12.031	12.015	12.034	12.014
X_{py}	0.153	0.166	0.228	0.209	0.273	0.272	0.278
X_{al}	0.694	0.690	0.703	0.665	0.684	0.667	0.665
X_{sp}	0.133	0.119	0.044	0.080	0.020	0.031	0.034
X_{gr}	0.020	0.025	0.025	0.047	0.023	0.030	0.023

MICROPROBE ANALYSES

GARNETS

	VM4983	VR13A	VR1583
SiO_2	38.59	38.11	36.97
Al_2O_3	20.99	20.91	21.80
FeO	31.26	32.11	35.18
MnO	2.38	2.57	1.25
MgO	5.86	4.70	5.86
CaO	0.93	0.81	0.73
Total	100.01	99.21	101.79

Normalized moles based on 8 total cations

Si	3.050	3.059	2.881
Al^{IV}	0.000	0.000	0.119
Al^{VI}	1.955	1.978	1.883
Mg	0.690	0.562	0.681
Fe^*	2.066	2.156	2.293
Mn	0.159	0.175	0.083
Ca	0.079	0.070	0.061
Total	8.000	8.000	8.000
O	12.028	12.048	11.882

X_{py}	0.231	0.190	0.218
X_{al}	0.690	0.728	0.736
X_{sp}	0.053	0.059	0.026
X_{gr}	0.026	0.024	0.020

APPENDIX C VI

PYROXENE

(Normalized in the manner of Wood and Banno, 1973)

MICROPROBE ANALYSES

PYROXENES

	BL1083E Opx	BL1183A Cpx	BL1183A Opx	CL2283A Opx	G1A Opx	G63B Opx	HS1183C Opx	HS1183C Cpx
SiO_2	52.03	51.67	51.45	48.73	49.19	53.19	51.25	51.31
TiO_2	0.00	0.00	0.06	0.03	0.00	0.04	0.00	0.08
Al_2O_3	1.29	1.26	0.41	3.69	1.73	2.15	0.00	0.99
FeO	26.50	12.01	31.00	27.90	31.82	21.84	29.18	10.60
MnO	0.74	0.21	0.70	0.83	1.59	0.84	1.09	0.51
MgO	15.56	12.18	18.23	17.75	15.70	19.57	18.93	12.75
CaO	0.39	21.94	0.50	0.15	0.24	0.22	0.56	22.66
Na_2O	0.17	0.19	0.00	0.13	0.09	0.14	0.00	0.52
Total	96.68	99.46	102.35	99.21	100.36	97.99	101.01	99.42

Normalized moles based on 4 total cations

Si	2.075	1.961	1.938	1.874	1.910	2.038	1.945	1.934
Al^{IV}	0.000	0.039	0.018	0.126	0.079	0.000	0.000	0.044
Al^{VI}	0.061	0.017	0.000	0.041	0.000	0.097	0.000	0.000
Ti	0.000	0.000	0.002	0.001	0.000	0.001	0.000	0.002
Fe^{+3}	0.000	0.036	0.015	0.093	0.086	0.000	0.000	0.077
Mg	0.925	0.689	1.024	1.018	0.909	1.118	1.071	0.716
Fe^{+2}	0.884	0.345	0.962	0.805	0.947	0.700	0.926	0.257
Mn	0.025	0.007	0.022	0.027	0.052	0.027	0.035	0.016
Ca	0.017	0.892	0.020	0.006	0.010	0.009	0.023	0.915
Na	0.013	0.014	0.000	0.010	0.007	0.010	0.000	0.038
Total	4.000	4.000	4.000	4.000	4.000	4.000	4.000	4.000
O	6.099	6.000	5.956	6.000	5.989	6.082	5.945	5.978
X_{Mg}	0.511	0.644	0.512	0.531	0.468	0.615	0.536	0.682
X_{Fe}	0.489	0.356	0.488	0.469	0.532	0.385	0.464	0.318

MICROPROBE ANALYSES

PYROXENES

	HS1583C Opx	ID1683A Opx	ID1683B Opx	MB8A Opx	RW1283B Opx	RW1683B Cpx	RW1683B Opx	RW2483 Cpx
SiO_2	52.68	49.07	53.55	50.31	48.97	50.26	50.50	48.71
TiO_2	0.00	0.00	0.00	0.00	0.02	0.00	0.04	0.07
Al_2O_3	1.54	3.64	0.00	1.36	4.27	1.75	0.72	1.78
FeO	24.74	26.91	21.15	30.07	27.11	11.66	29.20	14.75
MnO	0.66	0.36	0.68	1.03	0.59	0.48	1.26	0.81
MgO	17.55	19.24	24.69	17.83	18.99	12.06	18.13	9.89
CaO	0.16	0.05	0.40	0.08	0.04	21.09	0.56	20.88
Na_2O	0.43	0.08	0.00	0.00	0.11	0.64	0.60	0.29
Total	97.76	99.35	100.47	100.68	100.10	97.94	101.01	97.18

Normalized moles based on 4 total cations

Si	2.048	1.868	1.964	1.924	1.852	1.928	1.912	1.918
Al^{IV}	0.000	0.132	0.000	0.061	0.148	0.072	0.032	0.082
Al^{VI}	0.071	0.032	0.000	0.000	0.043	0.007	0.000	0.001
Ti	0.000	0.000	0.000	0.000	0.001	0.000	0.001	0.002
Fe^{+3}	0.000	0.106	0.000	0.061	0.112	0.113	0.074	0.098
Mg	1.017	1.092	1.350	1.016	1.071	0.690	1.023	0.581
Fe^{+2}	0.804	0.751	0.649	0.900	0.745	0.261	0.851	0.387
Mn	0.022	0.012	0.021	0.033	0.019	0.016	0.040	0.027
Ca	0.007	0.002	0.016	0.003	0.002	0.867	0.023	0.881
Na	0.032	0.006	0.000	0.000	0.008	0.048	0.044	0.022
Total	4.000	4.000	4.000	4.000	4.000	4.000	4.000	4.000
O	6.067	6.000	5.964	5.985	6.000	6.000	5.944	6.000
X_{Mg}	0.558	0.560	0.675	0.514	0.555	0.648	0.525	0.544
X_{Fe}	0.442	0.440	0.325	0.486	0.445	0.352	0.475	0.456

APPENDIX D

TREND SURFACE ANALYSIS

Trend surface analysis is based on the least-squares criterion of fitting polynomial functions to areally distributed data. Taking X-Y coordinates (sample locations), a least-squares regression is performed to formulate an equation that describes the Z surface (temperatures). The polynomial functions for the various degree surfaces are as follows:

First Degree

$$T = C1 + C2*X + C3*Y$$

Second Degree

$$T = C1 + C2*X + C3*Y + C4*X^2 + C5*X*Y + C6*Y^2$$

Third Degree

$$T = C1 + C2*X + C3*Y + C4*X^2 + C5*X*Y + C6*Y^2 + C7*X^3 + C8*X^2*Y + C9*X*Y^2 + C10*Y^3$$

Fourth Degree

$$T = C1 + C2*X + C3*Y + C4*X^2 + C5*X*Y + C6*Y^2 + C7*X^3 + C8*X^2*Y + C9*X*Y^2 + C10*Y^3 + C11*X^4 + C12*X^3*Y + C13*X^2*Y^2 + C14*X*Y^3 + C15*Y^4$$

Fifth Degree

$$T = C1 + C2*X + C3*Y + C4*X^2 + C5*X*Y + C6*Y^2 + C7*X^3 + C8*X^2*Y + C9*X*Y^2 + C10*Y^3 + C11*X^4 + C12*X^3*Y + C13*X^2*Y^2 + C14*X*Y^3 + C15*Y^4 + C16*X^5 + C17*X^4*Y + C18*X^3*Y^2 + C19*X^2*Y^3 + C20*X*Y^4 + C21*Y^5$$

Sixth Degree

$$T = C1 + C2*X + C3*Y + C4*X^2 + C5*X*Y + C6*Y^2 + C7*X^3 + C8*X^2*Y + C9*X*Y^2 + C10*Y^3 + C11*X^4 + C12*X^3*Y + C13*X^2*Y^2 + C14*X*Y^3 + C15*Y^4 + C16*X^5 + C17*X^4*Y + C18*X^3*Y^2 + C19*X^2*Y^3 + C20*X*Y^4 + C21*Y^5 + C22*X^6 + C23*X^5*Y + C24*X^4*Y^2 + C25*X^3*Y^3 + C26*X^2*Y^4 + C27*X*Y^5 + C28*Y^6$$

C's are constants calculated from the least squares regressions

The variations in the Z variables (temperature) can be subdivided into two components; that of the regional nature (the regression), and

that of residuals or deviations from the regression (local variation). The amount of temperature variation that is explained by each degree surface is related to the "goodness of fit" of the regression to the data -- the higher the percent explained, the better the fit. The residuals or deviations from the regional surface may represent "real" local variation, disequilibrium or reequilibrium in the rocks, or imprecision of the geothermometers.

Increasing the order of the polynomial function tends to describe a more complicated surface. To determine if the increased order produces a statistically significant better fit than the previous fit, an analysis of variance is performed using an F-test.

$$F \text{ ratio} = \frac{(SSR_n - SSR_{n-1}) / (DFR_n - DFR_{n-1})}{(SSD_n / DFD_n)}$$

(SSR = Sum of Squares Regression; SSD = Sum of Squares Deviation)
(DFR = Degrees Freedom Regression; DFD = Degrees Freedom Deviation)
(n = Order of Equation)

If the computed F-ratio for a n'th degree polynomial regression exceeds the tabulated F-test value for the significance level desired (Davis, 1973), the extra terms that were added to increase the degree of the polynomial function (and improve the fit) are not statistically significant.

The trend surface analysis used in this thesis was conducted with the aid of an unnamed trend surface program, writen in FORTRAN by R. D. LeFever. The program takes as input data, the X and Y coordinates (location) and up to eight Z variables for each sample.

For each Z variable, the program calculates and prints out:

1) A table of the input coordinates and Z variables for all the samples, and the calculated Z variables for the regression and the resultant residuals (calculated Z variable - the input Z variable) for each of the degree surfaces.
2) The polynomial functions used to fit the trend surfaces. The constants of the polynomial functions are carried out to eight decimal places and are in expodential format.
3) A table composed of all relevant regression statistics involved in the F-test.
   a) Sum of Squares Regression
   b) Sum of Squares Deviation
   c) Total Variation
   d) Percent Variation Explained by the Regression
   e) Degrees Freedom Regression
   f) Degrees Freedom Deviation
   g) F-Ratio
4) A plot of each of the six degree surfaces.

REFERENCES

REFERENCES

Aranovich. L. Ya., and Podlesskii, K. K., 1980, Garnet-plagioclase geobarometer: Acad. Nauk. USSR Dokl., v. 251, p. 1216-1219.

Ashwal, L. D., Morgan, P., and Leslie, W. W., 1983, Thermal constraints on high-pressure granulite metamorphism of supracrustal rocks: Lunar and Planetary Institute Technical Report 83-03, p. 13-19.

Ashworth, J. R., and Chinner, G. A., 1978, Coexisting garnet and cordierite in migmatites from the Scottish Caledonides: Contrib Mineral Petrol., v. 65, p. 379-394.

Baumann, R. M., Chipera, S. J., and Perkins, D., 1984, Archean migmatites from western Ontario: EOS, v. 65, no. 16, p. 291.

Beakhouse, G. P., 1977, A subdivision of the western English River subprovince: Can J Earth Sci., v. 14, p. 1481-1489.

Blackwell, D. D., and Steele, J. L., 1983, A summary of heat flow studies in the Cascade range: Geothermal Resources Council, Transactions, v. 7, p. 233-236.

Bluemel, P., and Schreyer, W., 1977, Phase relations in pelitic and psammitic gneisses of the sillimanite-potash feldspar and cordierite-potash feldspar zones in the Moldanubicum of the Lam-Bodenmais area, Bavaria: J Petrol., v. 18, no. 3, p. 431-459.

Bohlen, S. R., 1983, Retrograde P-T paths for granulites: EOS, v. 64, p. 878.

Bohlen, S. R., Wall, V. J., and Boettcher, A. L., 1983, Experimental investigation and application of garnet granulite equilibria: Contrib Mineral Petrol., v. 83, p. 52-61.

Bohlen, S. R., Essene, E. J., 1980, Evaluation of coexisting garnet-biotite, garnet-clinopyroxene, and other Mg-Fe exchange thermometers in Adirondack granulites: Geol Soc Am Bull., Part II, v. 91, p. 685-719.

Boyd, F. R., and England, J. L., 1964, The system enstatite-pyrope: Carnegie Inst. Washington Year Book, v. 63, p. 157-161.

Breaks, F. W., Bond, W. D., and Stone, D., 1978, Preliminary geological synthesis of the English River subprovince, northwestern Ontario and its bearing upon mineral exploration: Ont Geol Surv Misc Pap 72, 55 p.

Chipera, S. J., Baumann, R. M., Robinson, S. E., Perkins, D., and Gosnold, W. D., 1984a, Archean tectonism: an example from western Ontario: GSA Abstract with Prog, v. 16, no. 6, p. 469-470.

Chipera, S. J., Henke, K. R., and Perkins, D., 1984b, Recalibration of garnet-orthopyroxene barometers and application to granulites of the English River subprovince, western Ontario: EOS v. 65, no. 16, p. 288.

Churkin, M. Jr., Foster, H. L., Chapman, R. M., and Weber, F. R., 1982, Terranes and suture zones in east central Alaska: J Geophys Res., v. 87, no. B5, p. 3718-3730.

Clifford, P. M., 1969, Geology of the western Lake St. Joseph area: Ontario Dept. of Mines; Geol Report 70.

Condie, K. C., 1982, Plate-tectonics model for Proterozoic continental accretion in the southwestern United States: Geology, v. 10, p. 37-42.

Coney, P. J., Jones, D. J., and Monger, J. W. H., 1980, Cordilleran suspect terranes: Nature, v. 288, p. 329-333.

Csejtey, B. Jr., Cox, D. P., Evarts, R. C., Stricker, G. D., Foster, H. L., 1982, The Cenozoic Denali fault system and the Cretaceous accretionary development of southern Alaska: J Geophys Res., v. 87, no. B5, p. 3741-3754.

Davis, J. C., 1973, Statisitics and Data Analysis in Geology: John Wiley and Sons, New York, 550 p.

de Waard, D., 1965, A proposed subdivision of the granulite facies: Am J Sci., v. 263, p. 455-461.

Edwards, R. L., and Essene, E. J., 1981, Zoning patterns and their effect on biotite-garnet K_D thermometry: EOS, v. 62, p. 411-412.

England, P. C., and Richardson, S. W., 1977, The influence of erosion upon the mineral facies of rocks from different metamorphic environments: J Geol Soc Lond., v. 134, p. 201-213.

Ferry, J. M., 1980, A comparative study of geothermometers and geobarometers in pelitic schists from south-central Maine: Am Mineral., v. 65, p. 720-732.

Ferry, J. M., and Spear, F. S., 1978, Experimental calibration of the partitioning of Fe and Mg between biotite and garnet: Contrib Mineral Petrol., v. 66, p. 113-117.

Ganguly, J., and Saxena, S. K., 1984, Mixing properties of aluminosilicate garnets: constraints from natural and experimental data, and applications to geothermometry: Am Mineral., v. 69, p. 88-97.

Ganguly, J., and Kennedy, G. C., 1974, The energetics of natural garnet solid solutions: Mixing of the aluminosilicate end-members: Contrib Mineral Petrol., v. 48, p. 137-148.

Ghent, E. D., 1976, Plagioclase-garnet-Al_2SiO_5-quartz: a potential geobarometer-geothermometer: Am Mineral., v. 61, p. 710-714.

Goldman, D. S., and Albee, A. L., 1977, Correlation of Mg/Fe partitioning between garnet and biotite with O^{18}/O^{16} partitioning between quartz and magnetite: Am J Sci., v. 277, p. 750-767.

Goldsmith, J. S., 1980, The melting and breakdown reactions of anorthite at high pressures and temperatures: Am Mineral., v. 65, p. 272-284.

Goodwin, A. M., 1981, Precambrian perspectives: Science, v. 213, p. 55-61.

Goodwin, A. M., 1965, Geology of Pashkokagan Lake - Eastern Lake St. Joseph area: Ontario Dept. of Mines; Geological report 42, 58 p.

Grant, J. A., 1973, Phase Equilibria in high-grade metamorphism and partial melting of pelitic rocks: Am J Sci., v. 273, p. 289-317.

Gravity and Geodynamics Division, Earth Physics Branch, Energy, Mines and Resources Canada, 1981: Manuscript Map no. 48090 for Gravity Map of Canada 1980, Ottawa, Canada.

Grew, E. S., 1980, Sapphirine + quartz association from Archean rocks in Enderby Land, Antarctica: Am Mineral., v. 65, p. 821-836.

Hall, D. H., and Brisbin, W. C., 1982, Overview of regional geophysical studies in Manitoba and northwestern Ontario: Can J Earth Sci. v. 19, p. 2049-2059.

Hall, D. H., and Hajnal, Z., 1969, Crustal structure of northwestern Ontario: Refraction seismology: Can J Earth Sci., v. 6, p. 81-99.

Harley, S. L., and Green, D. H., 1982, Garnet-orthopyroxene barometry for granulites and peridotites: Nature, v. 300, p. 697-701.

Harris, N. B. W., 1976, The Significance of garnet and cordierite from the Sioux Lookout region of the English River gneiss belt, northern Ontario: Contrib Mineral Petrol., v. 55, p. 91-104.

Harris, N. B. W., and Jayaram, S., 1982, Metamorphism of cordierite gneisses from the Bangalore region of the Indian Archaean: Lithos, v. 15, p. 89-97.

Harris, N. B. W., and Goodwin, A. M., 1976, Archean rocks from the eastern Lac Seul region of the English River gneiss belt, northwestern Ontario, part 1: Petrology, chemistry, and metamorphism: Can J Earth Sci., v. 13, p. 1201-1215.

Haselton, H. T., Hovis, G. L., Hemingway, B. S., and Robie, R. A., 1983, Calorimetric investigations of the excess entropy of mixing in an albite-sanidine solid solutions: lack of evidence for Na, K short-range order and implications for two-feldspar thermometry: Am Mineral., v. 68, p. 398-413.

Haselton, H. T., and Westrum, E. F., 1980, Low-temperature heat capacities of synthetic pyrope, grossular, and $pyrope_{60}grossular_{40}$: Geochim Cosmoshim Acta., v. 44, p. 701-709.

Henke, K. R., 1984, Archean metamorphism in northwestern Ontario and southeastern Manitoba: unpub. M.Sci. thesis, Univ. of North Dakota.

Hess, P. C., 1969, The metamorphic paragenesis of cordierite in pelitic rocks: Contrib Mineral Petrol., v. 24, p. 191-207.

Hodges, K. V., and Spear, F. S. 1982, Geothermometry, geobarometry and the Al_2SiO_5 triple point at Mt. Moosilauke, New Hampshire: Am Mineral., v. 67, p. 1118-1134.

Holdaway, M. J., 1971, Stability of andalusite and the aluminum silicate phase diagram: Am J Sci., v. 271, p. 97-131.

Holdaway, M. J., and Lee, A. M., 1977, Fe-Mg cordierite stability in high-grade pelitic rocks based on experimental, theoretical, and natural observations: Contrib Mineral Petrol., v. 63, p. 175-198.

Holland, T. J. B., 1981, Thermodynamic analysis of simple mineral systems: In Newton, R. C., Navrotsky, V., Wood, B. J., Eds., Thermodynamics of Minerals and Melts, Springer, p. 19-34.

Hollister, L. S., 1977, The reaction forming cordierite from garnet: The Khtada Lake metamorphic complex, British Columbia: Can Mineral., v. 15, p. 217-229.

Hormann, P. K., Raith, M., Raase, P., Ackermank, D., and Seifert, F., 1980, The granulite complex of Finnish Lapland: Petrology and metamorphic conditions in the Ivalojoki-Inarijarvi area: Geol Soc Finland Bull., v. 308, p. 1-95.

Hoschek, G., 1969, The stability of staurolite and chloritoid and their significance in metamorphism of pelitic rocks: Contrib Mineral Petrol., v. 22, p. 298-232.

Hutcheon, I., Froese, E., and Gordon, T. M., 1974, The assemblage quartz-sillimanite-garnet-cordierite as an indicator of metamorphic conditions: Contrib Mineral Petrol., v. 44, p. 29-34.

Hyndman, D. W., 1981, Controls on source and depth of emplacement of granitic magma: Geology, v. 9, p. 244-249.

Indares, A., and Martignole, J., 1985, Biotite-garnet geothermometry in granulite facies: The infuence of Ti and Al in biotite: Am Mineral., (in press).

Jones, D. L., Silberling, N. J., Gilbert, W., and Coney, P., 1982, Character, distribution and tectonic significance of accretionary terranes in the central Alaskan range: J Geophys Res., v. 87, no. B5, p. 3709-3717.

Karlstrom, K. E., 1983, Reinterpretation of Newfoundland gravity data and arguments for an allochthonous Dunnage Zone: Geology, v. 11, p. 263-266.

Kays, M. A., and Medaris, L. G. Jr., 1976, Petrology of the Hara Lake paragneisses, northeastern Saskatchewan, Canada: Contrib Mineral Petrol., v. 59, p. 141-159.

Kretz, R., 1959, Chemical study of garnet, biotite and hornblende from gneisses of southwestern Quebec, with emphasis on distribution of elements in coexisting minerals: J Geology., v. 67, p. 371-403.

Krogh, T. E., Harris, N. B. W., and Davis, G. L., 1976, Archean rocks from the eastern Lac Seul region of the English River gneiss belt, northwestern Ontario, part 2, Geochronology: Can J Earth Sci., v. 13, p. 1212-1215.

Langford, F. F., and Morin, J. A., 1976, The development of the Superior Province of northwestern Ontario by merging island arcs: Am J Sci., v. 276, p. 1023-1034.

Martignole, J. and Sisi, J. C., 1981, Cordierite-garnet-H_2O equilibrium: A geological thermometer, barometer and water fugacity indicator: Contrib Mineral Petrol., v. 77, p. 38-46.

Molnar, P., Chen, W. P., and Padovani, E., 1983, Calculated temperatures in overthrust terrains and possible combinations of heat sources responsible for the Tertiary granites in the greater Himalaya: J Geophys Res., v. 88, no. B8, p. 6415-6429.

Monger, J. W. H., Price, R. A., and Tempelman-Kluit, D. J., 1982, Tectonic accretion and the origin of the two major metamorphic and plutonic welts in the Canadian Cordillera: Geology, v. 10, p. 70-75.

Newton, R. C., 1983, Geobarometry of high-grade metamorphic rocks: Am J Sci., v. 283-A, p. 1-28.

Newton, R. C., and Perkins, D. III, 1982, Thermodynamic calibration of geobarometers based on the assemblages garnet-plagioclase-orthopyroxene(clinopyroxene)-quartz: Am Mineral., v. 67, p. 203-222.

Newton, R. C., and Haselton, H. T., 1981, Thermodynamics of the garnet-plagioclase-Al_2SiO_5-quartz geobarometer: In Newton R. C., Navrotsky A., and Wood B. J., Eds., Thermodynamics of Minerals and Melts, Springer, p. 131-148.

Newton, R. C. and Wood, B. J., 1979, Thermodynamics of water in cordierite and some petrologic consequences of cordierite as a hydrous phase: Contrib Mineral Petrol., v. 68, p. 391-405.

Orville, P. M., 1972, Plagioclase cation exchange equilibria with aqueous chloride solution: Results at 700°C and 2000 bars in the presence of quartz: Am J Sci., v. 272, p. 234-272.

Oxburgh, E. R., 1972, Flake tectonics and continental collision: Nature, v. 239, p. 202-204.

Perchuk, L. L., and Lavrent'eva, I. V., 1983, Experimental investigation of exchange equilibria in the system cordierite-garnet-biotite: In Saxena S. K., Ed., Kinetics and Equilibrium in Mineral Reactions, Springer, p. 199-239.

Perchuk, L. L., Podlesskii, K. K., and Aranovic, L. Ya., 1981, Calculation of thermodynamic properties of end-member minerals from natural parageneses: In Newton R. C., Navrotsky A., and Wood B. J., Eds., Thermodynamics of Minerals and Melts, Springer, p. 111-129.

Percival, J. A., 1983, Preliminary results of geological synthesis in the western Superior Province: Geol Surv Canada Pap 83-1A, p. 125-131.

Perkins, D., and Chipera, S. J., 1985, Garnet-orthhopyroxene-plagioclase-quartz barometry: Refinement and application to the English River subprovince and the Minnesota River Valley: Contrib Mineral Petrol., in press.

Perkins, D., and Chipera, S. J., 1984, Garnet-cordierite-plagioclase-quartz assemblages as indicators of water fugacity: EOS, v. 65, no. 16, p. 292-293.

Perkins, D. III, Essene, E. J., and Marcotty, L. A., 1982, Thermometry and barometry of some amphibolite-granulite facies rocks from the Otter Lake area, southern Quebec: Can J Earth Sci., v. 19-9, p. 1759-1774.

Perkins III, D., and Newton, R.C., 1981, Charnockite geobarometers based on coexisting garnet-pyroxene-plagioclase-quartz: Nature, v. 292, p. 144-146.

Robie, R. A., Hemingway, B. S., and Fisher, J., R., 1978, Thermodynamic properties of minerals and related substances at 298.15 K and 1 Bar (10^5 Pascals) pressure and at higher temperature: US Geol Surv Bull., no. 1452.

Roy, R. F., Blackwell, D. D., and Decker, E. R., 1972, Continental heat flow: In Robertson E. C., Ed., The Nature of the Solid Earth, McGraw-Hill, p. 506-543.

Saito, Y., and Hashimoto, M., 1982, South Kitakami Region: An allochthonous terrane in Japan: J Geophys Res., v. 87, no. B5, p. 3691-3696.

Schmid, R., and Wood, B. J., 1976, Phase reactions in granulitic metapelites from the Ivrea-Verbano Zone (northern Italy): Contrib Mineral Petrol., v. 54, p. 255-279.

Skinner, 1969, Geology of Sioux Lookout map-area, Ontario; A part of the Superior Province of the Precambrian Shield (52J): Can Geol Surv Pap., 68-45.

Smithson, S. B., 1978, Modeling continental crust: Structure and chemical constraints: Geophys Res Lett., v. 5, no. 9, p. 749-752.

Smithson, S. B., and Brown, S. K., 1977, A model for lower continental crust: Earth Planet Sci Lett., v. 35, p. 134-144.

Speed, R. C., and Larue, D. K., 1982, Barbados: Architecture and implications for accretion: J Geophys Res., v. 87, no. B5, p. 3633-3643.

Stormer, J. C. Jr., 1975, A practical two-feldspar geothermometer: Am Mineral., v. 60, p. 667-674.

Swanberg, C. A., and Blackwell, D. D., 1973, Areal distribution and geophysical significance of heat generation in the Idaho batholith and adjacent intrusions in eastern Oregon and western Montana: Geol Soc Am Bull., v. 84, p. 1261-1282.

Thompson, A. B., 1981, The pressure-temperature (P-T) plane viewed by geophysicists and petrologists: Terra Cognita 1, p. 11-20.

Thompson, A. B., 1976, Mineral reactions in pelitic rocks: I. Prediction of P-T-X(Fe-Mg) phase relations: Am J Sci., v. 276, p. 401-454.

Tracy, R. J., Robinson, P., and Thompson, A. B., 1976, Garnet composition and zoning in the determination of temperature and pressure of metamorphism, central Massachusetts: Am Mineral., v. 61, p. 762-775.

Urquhart, W. E. S., 1976, Investigation of the geological significance of linear aeromagnetic anomalies in the English River gneissic belt: unpub. M.Sci. thesis, Univ. of Toronto.

Wells, P. R. A., 1980, Thermal models for the magmatic accretion and subsequent metamorphism of continental crust: Earth Planet Sci Lett., v. 46, p. 253-265.

Wells, P. R. A., 1977, Pyroxene thermometry in simple and complex systems: Contrib Mineral Petrol., v. 62, p. 129-139.

Westbrook, G. K., and Smith, M. J., 1983, Long decollements and mud volcanoes: Evidence from the Barbados Ridge Complex for the role of high pore-fluid pressure in the development of an accretionary complex: Geology, v. 11, p. 279-283.

Williams, H., and Hatcher, R. D. Jr., 1982, Suspect terranes and accretionary history of the Appalachian orogen: Geology, v. 10, p. 530-536.

Wilson, H. D. B., 1971, The Superior Province in the Precambrian of Manitoba: In Geosciences in Manitoba, Edited by A. C. Turnock. Geol Assoc Canada, Special Pap. 16, p. 41-49.

Windley, B. F., 1977, The Evolving Continents: John Wiley and Sons, New York, 385 p.

Winkler, H. G. F., 1979, Petrogenesis of Metamorphic Rocks, (5th ed.): Springer-Verlag, New York, 348 p.

Wood, B. J., and Banno, S., 1973, Garnet-orthopyroxene and orthopyroxene-clinopyroxene relationships in simple and complex systems: Contrib Mineral Petrol., v. 42, p. 109-124.

Woodsworth, G. J., 1977, Homogenization of zoned garnets from pelitic schists: Can Mineral., v. 15, p. 230-242.

Wynne-Edwards, H. R., and Hay, P. W., 1963, Coexisting cordierite and garnet in regionally metamorphosed rocks from the Westport area, Ontario: Can Mineral., v. 7, p. 453-478.